University of Alberta

Characterization of Iron Sulfur Cluster Binding Consensus Sequence Mutants of DmsA – the Active Subunit of an Important E. coli Respiratory Enzyme, DMSO Reductase

by

James Even Voss

A thesis submitted to the Faculty of Graduate Studies and Research in partial fulfillment of the

requirements for the degree of *Master of Science*

Department of *Biochemistry*

Edmonton, Alberta
Spring, 2004

Library and Archives Canada

Published Heritage Branch

395 Wellington Street
Ottawa ON K1A 0N4
Canada

Bibliothèque et Archives Canada

Direction du Patrimoine de l'édition

395, rue Wellington
Ottawa ON K1A 0N4
Canada

Your file Votre référence
ISBN: 0-612-96563-5
Our file Notre référence
ISBN: 0-612-96563-5

The author has granted a non-exclusive license allowing the Library and Archives Canada to reproduce, loan, distribute or sell copies of this thesis in microform, paper or electronic formats.

The author retains ownership of the copyright in this thesis. Neither the thesis nor substantial extracts from it may be printed or otherwise reproduced without the author's permission.

L'auteur a accordé une licence non exclusive permettant à la Bibliothèque et Archives Canada de reproduire, prêter, distribuer ou vendre des copies de cette thèse sous la forme de microfiche/film, de reproduction sur papier ou sur format électronique.

L'auteur conserve la propriété du droit d'auteur qui protège cette thèse. Ni la thèse ni des extraits substantiels de celle-ci ne doivent être imprimés ou aturement reproduits sans son autorisation.

In compliance with the Canadian Privacy Act some supporting forms may have been removed from this thesis.

While these forms may be included in the document page count, their removal does not represent any loss of content from the thesis.

Conformément à la loi canadienne sur la protection de la vie privée, quelques formulaires secondaires ont été enlevés de cette thèse.

Bien que ces formulaires aient inclus dans la pagination, il n'y aura aucun contenu manquant.

Canada

Abstract

Anaerobic growth of *E. coli* on glycerol and dimethylsulfoxide (DMSO), requires the expression of DMSO reductase (DmsABC). DMSO reductase is well characterized at the biochemical, biophysical and molecular levels and is an excellent model system for investigating the structure and mechanism of electron-transfer chain complexes. DmsABC is a complex iron sulfur cluster, molybdopterin cofactor containing enzyme that has four [4Fe-4S] clusters visible by conventional electron paramagnetic resonance (EPR) spectroscopy. It contains four ferredoxin-like Cys motifs in the electron transfer subunit (DmsB), and an additional Cys motif in the catalytic subunit (DmsA). An accumulation of data has shown that the DmsB subunit contains all four of the EPR visible clusters. Site-directed mutagenesis was used to investigate the role of the Cys motif of DmsA. Results suggest that DmsA binds a [4Fe-4S] cluster in a similar way to nitrate reductase from *E. coli* and that this cluster is not visible by conventional EPR spectroscopy.

Acknowledgements

Hooray for Everyone!!

Table of Contents

1.0 ***INTRODUCTION*** 1
- 1.1 ***PMF Through the Redox Loop*** 1
- 1.2 ***E. coli Respiratory Chains*** 2
- 1.3 ***DMSO Reductase is an Important Terminal Electron Acceptor in E. coli*** 9
  - *1.3.1 Organization of the Operon* 10
  - *1.3.2 The DmsC subunit and its Topology in the Inner Membrane* 13
  - *1.3.3 DMSO Reductase Targeting to the Inner Membrane of E. coli* 15
    - *1.3.3.1 the Tat Transport System* 15
    - *1.3.3.2 the Signal Sequence is Important in Tat Directed Protein Translocation* 19
    - *1.3.3.3 Targeting of DMSO Reductase* 20
    - *1.3.3.4 DmsC Quinol Binding, Oxidation and Electron Transport* 22
  - *1.3.4 the DmsB Subunit* 24
  - *1.3.5 the DmsA Subunit* 26
    - *1.3.5.1 the Molybdenum Active Site* 27
    - *1.3.5.2 DmsA Substrate Specificity* 32
  - *1.3.6 Electron Transfer and Structural Characterization of DmsA* 35
- 1.4 ***Experimental Objectives*** 40

2.0 ***MATERIALS AND METHODS*** 42
- 2.1 ***Cell Strains and Plasmids*** 42
- 2.2 ***Synthesis of Oligonucleotides and DNA Sequencing*** 44
- 2.3 ***Mutagenic Primers*** 44
- 2.4 ***Creation of DmsA N-Terminal Cysteine Motif Mutants*** 45
- 2.5 ***Growth Curve Analysis of E. coli Expressing DMSO Reductase*** 46
- 2.6 ***DmsABC and Mutant Expression and Preparation*** 47
- 2.7 ***Protein Quantification*** 48
- 2.8 ***DMSO Reductase Activity Assays*** 49
- 2.9 ***Spectroscopic Analysis of the Quinol Binding Site of DMSO Reductase by Fluorescence Quench Titrations*** 50
- 2.10 ***Spectroscopic Characterization of the Molybdenum Cofactor*** 51
- 2.11 ***EPR Analysis of DMSO Reductase and the N-Terminal Cysteine Cluster Mutants*** 52
  - 2.11.1 *Introduction; EPR Analysis of Redox Proteins* 52
  - 2.11.2 *Solving the EPR Spectra of DMSO Reductase* 52
  - 2.11.3 *EPR Analysis of Mutant Enzymes* 59

3.0 CHARACTERIZATION OF A DmsA C75S BC MUTANT..... 60
3.1 *Introduction*..... 60
3.2 *Results and Discussion*..... 61
3.3 *Conclusions*..... 71

4.0 N-TERMINAL CYSTEINE CLUSTER MUTANTS OF DmsA..... 74
4.1 *Introduction*..... 74
4.2 *Results and Discussion*..... 77
4.3 *Conclusions*..... 88

5.0 CONCLUSIONS AND FUTURE DIRECTIONS..... 91

List of Tables

1.1 Primary Dehydrogenases and Terminal Reductases.....4
1.2 Rates of Reaction of Some S and N-Oxides by DMSO Reductase.....33
2.1 Bacterial Strains Used in Experiments.....43
2.2 Description of Plasmids Used.....44
3.1 DMSO Reductase Activities (DmsA C75S mutant).....66
4.1 DMSO Reductase Activities (Five FeS Cluster Mutants).....82

List of Figures

1.0 Two Mechanisms of Proton Translocation..... 1
1.1 The Nitrate Respiratory Pathway..... 3
1.2 Chemical Structures of Some Quinones..... 5
1.3 The Sec Leader Sequence..... 6
1.4 The Tat Leader Sequence..... 6
1.5 *E. coli* Dehydrogenases..... 7
1.6 *E. coli* Terminal Reductases and Oxidases..... 7
1.7 Quinone Specificity..... 8
1.8 Coincidence of Electron Donor and Acceptor Proteins..... 9
1.9 Reduction of DMSO..... 10
1.10 *E. coli* Chromosome..... 11
1.11 Organization of the DmsABC Operron..... 12
1.12 Location of Fusion Sites in DmsC..... 14
1.13 Electron Micrograph of Membrane Vessicles..... 15
1.14 Sec and TAT Mechanisms..... 16
1.15 Organization of the TAT Operon..... 17
1.16 Green Fluorescent Protein Fusion of DmsA..... 21
1.17 Four Conserved Cysteine Groups of DmsB..... 25
1.18 FeS Cluster Positioning in NarH..... 27
1.19 Mo-bisMGD Cofactor Chemical Structure..... 28
1.20 Mo Active Site (Oxidized Form)..... 29
1.21 Reduced and Oxidized Forms of Mo..... 30
1.22 Mo(V) Oxidation State is Rate Limiting..... 30
1.23 Mo(V) Oxidation State..... 30
1.24 Mo (VII) Oxidation State..... 31
1.25 Catalytic Cycle of the Active Site..... 32
1.26 Tyr114 Positioning in the Active Site..... 34
1.27 Active Site Funnel and Mutated Residues..... 35
1.28 Evolutionary Distance Tree of DMSO Reductase..... 37
1.29 Conserved N-Terminal Cysteine Motif..... 38
1.30 DmsA Mutants Which Have an Effect on the Enzyme..... 39
2.1 Expression Vectors..... 43
2.2 Chemicals Used in Activity Assays..... 50
2.3 Form A Derivative of the Molybdopterin Cofactor..... 51
2.4 EPR Spectra of DMSO Reductase..... 54
2.5 EPR Spectra of Redox Poised Samples..... 56
2.6 Redox Titration Curves of DMSO Reductase..... 57
2.7 EPR Spectra of Purified DMSO Reductase..... 58
2.8 Power Saturation Curves of Mo(V) Signal..... 58
3.1 N-Terminal Region of DmsA..... 60
3.2 Growth Curve of DmsA C75S on GF Media..... 63
3.3 Growth Curve of DmsA C75S on GD Media..... 63
3.4 Western Blot of DmsAC75S from DSS301 cells..... 64
3.5 Western Blot of DmsAC75S from RK5209 cells..... 64

3.6 Fluorescence Spectra on DmsAC75S Membranes..... 67
3.7 Fluorescence Quench Titrations on C75S Mutant..... 68
3.8 EPR Spectra of C75S Mutant..... 70
3.9 Cysteine and Serine..... 72
3.10 Proximity of C75 to Mo-bisMGD Cofactor..... 73
4.1 N-Terminal Region of DmsA..... 74
4.2 Five Mutants in the N-Terminal Cys Region..... 76
4.3 Growth Curves of FeS Cluster Mutnats in DSS301 on GF Media..... 78
4.4 Growth Curves of FeS Cluster Mutants in HB101 on GF Media..... 78
4.5 Growth Curves of FeS Cluster Mutants in DSS301 on GD Media..... 79
4.6 Growth Curves of FeS Cluster Mutants in DSS301 on GD Media..... 79
4.7 Western Blot of FeS Cluster Mutants..... 81
4.8 Fluorescence Spectra of FeS Cluster Mutants..... 84
4.9 Redox Titration Data For The CS1 Mutant of DmsABC..... 86
4.10 Oxidized and Reduced Spectra of FeS Cluster Mutant..... 87
4.11 Model of FeS cluster in Active Subunits..... 90

List of Appendices

App. A (BV Activity Assays)..... 104
App. B (EPR Analysis of Enzymes)..... 105
App. C (Form A Fluorescence)..... 106
App. D (HOQNO Fluorescence Quench Titrations)..... 107
App. E (Lapachol Activity Assays)..... 108
App. F (Electrocompetent Cell Prep and Plasmid Transformation)..... 109
App. G (Gel Electrophoresis)..... 110
App. H (Growth Media)..... 115
App. I (Membrane Preparation)..... 118
App. J (Lowery Protein Assay)..... 119

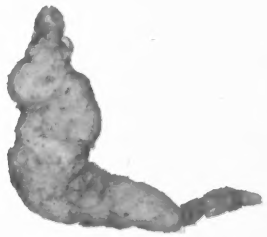

List of Abbreviations Used

ATP……..…..Adenosine triphosphate
BlaM……..….β-lactamase
DMK/H2..……..Demethylmenaquinone (oxidized/reduced)
DMS…..……..Dimethylsulfide
DmsABC…..……..Dimethylsulfoxide reductase
DMSO……....Dimethylsulfoxide
EPR……..……....Electron Paramagnetic Resonance
ER……..Endoplasmic reticulum
FAD……....Flavin Dinucleotide
Fdh……....Formate Dehydrogenase
FeS…….Iron Sulfur clusters
FMN……..…...Flavin Mononucleotide
GFP……..……..Green Fluorescent Protein
HOQNO…..…..2-n-heptyl-4-hydroxyquinoline-N-oxide
Lep……....Periplasmic signal peptidase-I
LPCH2…….Lapachol
MGD……....Molybdopterin Guanine dinucleotide
MK/H2…..……...Menaquinone (oxidized/reduced)
Mo……Molybdenum
MTT……Membrane targeting and Translocation
NAD……..…..Nicotinamide Adenine Dinucleotide
Nar……Nitrate reductase
Ni……...Nickel
PBH2……....Plumbagin
PhoA……..…Alkaline phosphotase
PMF……..…..Protonmotive force
Sec……General Secretory Pathway
Tat……Twin arginine translocase
TMAO…….Trimethylamine oxide
UQ…..…….. Ubiquinone
W……...Tungstate

1.0 INTRODUCTION

The bacteria *Escherichia coli* is capable of respiration under a variety of environmental growth conditions. When grown anaerobically on glycerol and dimethylsulfoxide (DMSO), the cell expresses DMSO reductase (DmsABC). This enzyme reduces DMSO to dimethylsulfide (DMS) in order to complete a respiratory chain which creates an electrochemical gradient across the inner membrane utilizing the energy stored as chemical potential from glycerol. DMSO reductase is well characterized at the biochemical, biophysical, and molecular levels, and is proving to be an excellent model system for investigating the structure and mechanism of electron-transfer chain complexes.

If the crystal structure of a protein has been solved, important structural and functional properties of the enzyme can be easily elucidated. When the structure of an enzyme is unavailable, as is the case with DMSO reductase from *E. coli* and other integral membrane proteins, site-directed mutagenesis has proven to be a useful way of characterizing some of the structural and functional properties of an enzyme. The following presents the results of site-directed mutagenesis experiments aimed at better understanding the structure and electron transfer pathway of the catalytic subunit (DmsA) of DMSO reductase.

1.1 Proton Motive Force Through the Redox Loop

In order to carry out important cellular functions, bacteria convert the energy stored as chemical potential in carbon compounds such as glucose into usable forms of energy. It has been over 30 years since a mechanism for this energy conversion was proposed. The mechanism was called the chemiosmotic model of energy coupling [22]. In this model, inner membrane proteins couple electron flow from low-redox potential electron donors (carbon compounds such as succinate), to high potential electron acceptors (such as O_2). This process results in the generation of a transmembrane proton electrochemical gradient or proton motive force (pmf) [23]. The energy stored

in this electrochemical gradient works directly to power important cellular processes such as motility and active membrane transport, or it is used to synthesize ATP (using ATP synthase) which can be used to energize a wide variety of important cellular processes [23].

Early formulations of the theory proposed that proton translocation was accomplished in one of two ways. The first involves the direct pumping of protons across the membrane by means of a proton pump. The other mechanism utilizes a redox loop to transport protons across the membrane. Here, two electrons are transferred by means of an integral membrane protein, from the positive (periplasmic) side of the membrane, to the negative (cytoplasmic) side. Then in combination with two protons, they reduce a membrane soluble quinone to a quinol. The quinol then diffuses back across the membrane lipid bilayer and is enzymatically reoxidized on the periplasmic side of the membrane releasing the protons [24] [25]. The full proton motive redox loop requires the participation of two catalytically distinct enzyme complexes. This loop has been found on the inner membrane of bacteria and can be well illustrated by the nitrate respiratory pathway consisting of the formate dehydrogenase-N (Fdh-N) and nitrate reductase (Nar) enzymes [26].

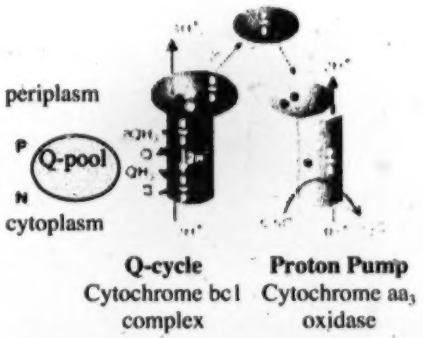

Fig 1.0 Depiction of the Q-cycle and proton pump as mechanisms for the creation of a proton gradient across the membrane [24].

1.2 E. coli Respiratory Chains

E. coli is a versatile bacterium capable of respiration under a variety of environmental conditions. It is able to utilize a variety of carbon sources and reduce a number of different electron acceptors depending on what is available to the cell. This requires significant diversity and variability in the respiratory chains [23]. This complexity hampered investigation of *E. coli* respiratory chain enzymes for a long time. At

present, the nucleotide and protein sequences of all the respiratory enzymes are known and many have been isolated and characterized [23]. Respiratory chains of the bacteria *E. coli* consist of primary dehydrogenases and of terminal reductases or oxidases which are functionally linked through membrane soluble quinones [4]. The characterized respiratory chains of *E. coli* consist of 15 primary dehydrogenases and of 10 terminal reductases. These numbers include isoenzymes for some of the electron donors.

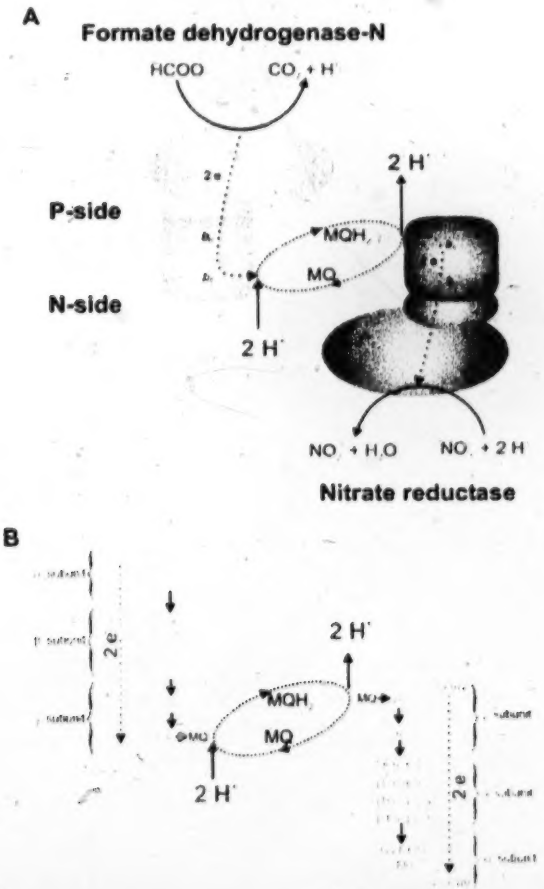

Fig 1.1 The nitrate respiratory pathway **A** Fdh-N is illustrated in red and Nar in blue. The substrate and menaquinone binding sites of the enzymes are situated on opposite sides of the membrane, enabling PMF generation via the redox loop mechanism. Electrons are transferred from the formate oxidation site in the periplasm to the nitrate reduction site situated in the cytoplasmic space of Nar. Menaquinones couple these two reactions by random diffusion through the membrane and translocates two protons from the N-side to the P-side, generating a PMF. **B** The redox centers and potential of the system are illustrated. The highly exergonic reaction allows electrons to be transferred against the membrane potential [18].

Enzyme	*redox couple*		Genes	Map position (min)
	Pair	Emf(V)		
Primary Dehydrogenases :				
Formate DHN	HCO_3^- / HCO_2^-	- 0.43	*fdnGHI*	*33.0*
Formate DHO	HCO_3^- / HCO_2^-	- 0.43	*fdoGHI*	*88.03*
Formate hydrogen-lyase			*fdhF, hycA-H*	*92.6;61.35*
Hydrogenase 1	H^+ / H_2	- 0.42	*hyaABCDEF*	*22.26*
Hydrogenase 2	H^+ / H_2	- 0.42	*hybA-G*	*68.53*
NADH DH I	NAD^+ / NADH	- 0.32	*nuoA-N*	*51.64*
NADH DH II	NAD^+ / NADH	- 0.42	*ndh*	*25.17*
Glycerol-3-P DHO	DHAP / Gly-3-P	- 0.19	*glpD*	*76.89*
Glycerol-3-P DHN	DHAP / Gly-3-P	- 0.19	*glpACB*	*50.76*
Pyruvate oxidase	acetate + CO2 / Pyruvate		*PoxB*	*19.42*
D-lactate DH	pyruvate / D-lactate	- 0.19	*dld*	*47.80*
L-Lactate DH	pyruvate / L-lactate	- 0.19	*lctD*	*81.55*
D- Amino acid DH	2-Oxoacid + NH_4^+ / a.a.	+ 0.03	*dadA*	*26.64*
Glucose dehydrogenase	glucose / gluconate	- 0.14	*gcd*	*2.97*
Succinate DH	fumarate / succinate	+ 0.03	*sdhCDAB*	*16.37*
Terminal reductases :				
Quinol oxidase bo_3	O_2 / H_2O	+ 0.82	*cyoABCDE*	*9.78*
Quinol oxidase bd	O_2 / H_2O	+ 0.82	*cydAB*	*16.67*
Quinol oxidase III (Cyx)	O_2 / H_2O	+ 0.82	*appBC/cyxAB*	*22.42*
Nitrate reductase A	NO_3^- / NO_2^-	+ 0.42	*narGHJI*	*27.53*
Nitrate reductase Z	NO_3^- / NO_2^-	+ 0.42	*nuoA-N*	*51.64*
Nitrate reductase, periplasm	NO_3^- / NO_2^-	+ 0.42	*napFDAGHBC*	*49.5*
Nitrite reductase	NO_2^- / NO^-	+ 0.36	*nrfA-G*	*92.42*
DMSO reductase	DMSO/ DMS	+ 0.16	*dmsABC*	*20.32*
TMAO reductase	TMAO/TMA	+ 0.13	*torCAD*	*21.61*
Fumarate reductase	fumarate / succinate	+ 0.03	*frdABCD*	*94.4*

Table 1.1 A list of primary hydrogenases and terminal reductases describing the reaction catalyzed by each, the midpoint potential for each reaction, the gene name and location on the *E. coli* chromosome. Midpoint potential is the redox potential required to have a balanced half reaction with the molar concentration of reactant is equal to the molar concentration of product [4].

(H_2, formate, NADH and glycerol-3-P) and acceptors (nitrate and O_2) [23]. The isozymes generally have completely different physical and biochemical properties. The electron donors or acceptors for the enzymes have largely differing midpoint potentials in the range of -0.43V (formate) to +0.03V (succinate) for electron donors and from +0.03V (fumarate) to +0.82V (O_2) for the electron acceptors. Three different quinone types can act as mediators between electron donor enzymes (primary

dehydrogenases) and acceptor enzymes (terminal reductases or oxidases); ubiquinone (UQ), menaquinone (MQ) and demethylmenaquinone (DMQ) [27] [28].

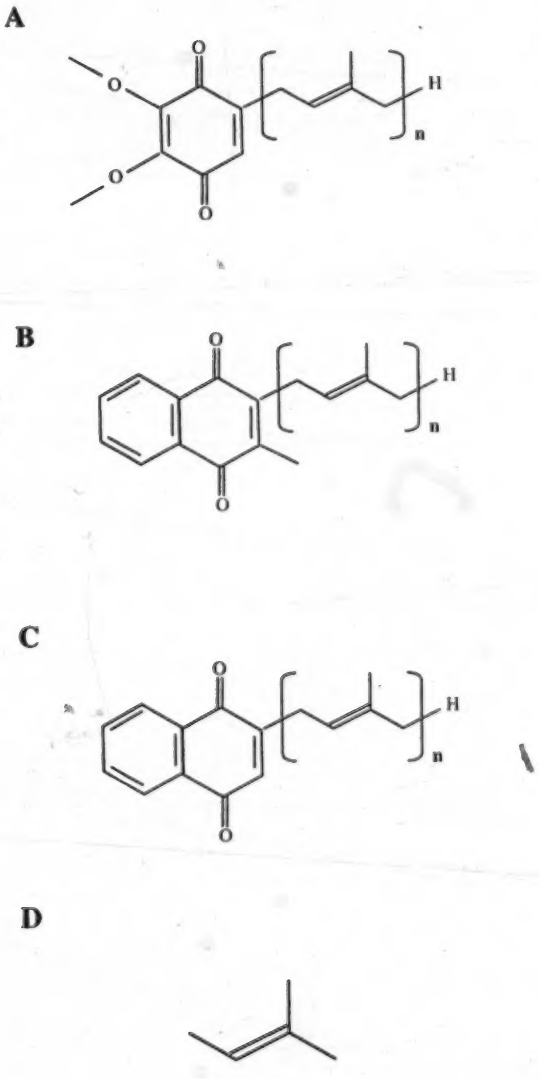

Fig 1.2 Chemical structures for some quinones synthesized by *E. coli* **A** Ubiquinone (UQ) **B.** Menaquinone (MQ) **C.** Demethylmenaquinone (DMQ). There is variability in the length of the isoprenoid chain **(D)** and in the reduced forms of the molecules the carbonyl group is replaced by hydroxyl groups.

These enzymes often contain amino terminal signal peptides. The sequences direct the targeting of the protein subunits to the periplasm. Some leaders are characteristic substrates of the general secretory pathway (Sec). They consist of an N-terminal hydrophilic region with a net positive charge followed by the hydrophobic domain and the Ala-Thr-Ala signal peptidase cleavage site [8]. Other enzymes that assemble redox cofactors in the cytoplasm contain a double arginine signal sequence (**Thr/Ser-Arg-Arg-Xxx-Phe-Xxx-Lys**) and are exported by the alternative Tat pathway which sends fully folded, cofactor containing proteins to or across the plasma membrane [4].

Fig 1.3 The N terminal leader sequence of maltose binding protein from *E. coli*. The N-terminal region has a net positive charge as indicated. The hydrophobic domain is in large bold font. The signal peptidase cleavage site is in italics [8].

Fig 1.4 The leader sequence of DmsA from *E. coli*, a Tat targeted protein. The twin arginine consensus sequence is in large bold font. The cleavage site consensus is italicized [8].

Enzymes differ largely with respect to the orientation of the active sites to the periplasm or cytoplasm and the relative portion of hydrophilic and hydrophobic subunits or transmembrane helices [4]. The interactions which occur between respiratory dehydrogenases and terminal reductases or oxidases is further restricted by the differential expression of these enzymes. Expression of respiratory enzymes is

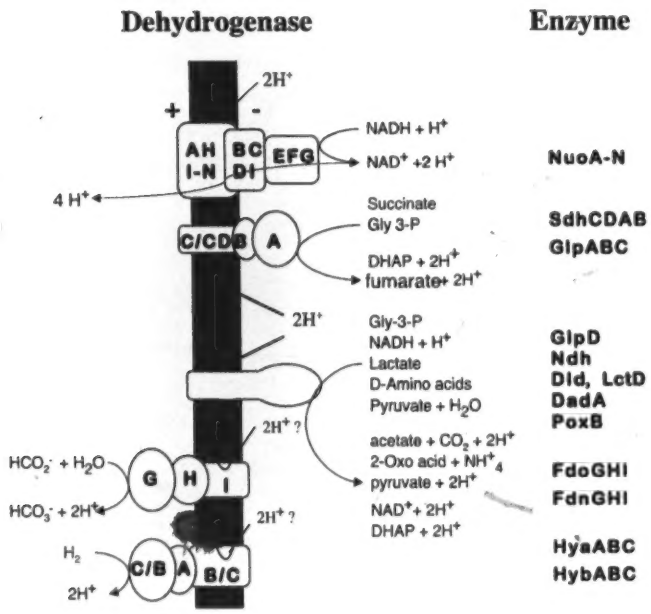

Fig 1.5 Some dehydrogenases of *E. coli* illustrating the diversity in subunit composition and membrane topology [4].

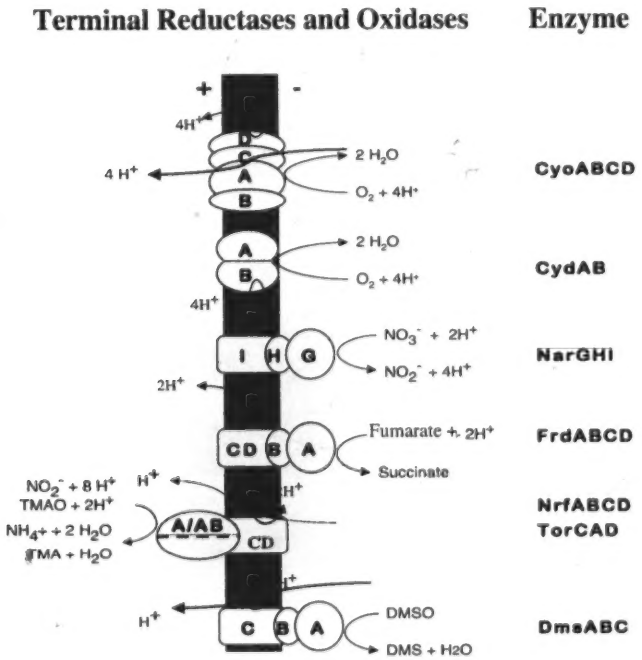

Fig 1.6 Some terminal reductases and oxidases of *E. coli* illustrating the diversity in composition and membrane topology [4] [19].

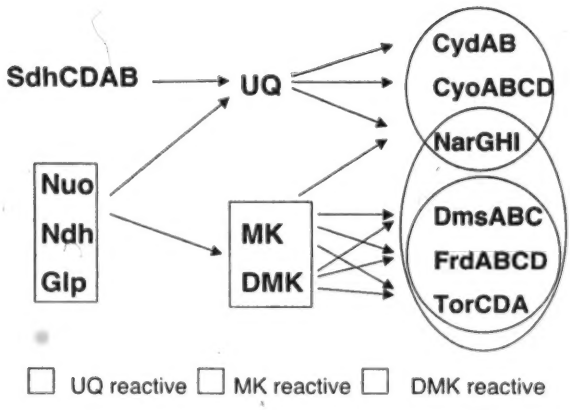

Fig 1.7 Illustration showing the specificity of quinones for electron donor and acceptor proteins [4].

transcriptionally regulated by electron acceptors like O_2 and nitrate resulting in the coexpression of only certain sets of dehydrogenases and terminal reductases [29]. In anaerobic respiration with fumarate and DMSO a unique set of dehydrogenases is expressed. As a result, most dehydrogenases donate electrons preferentially to selected terminal reductases, H_2 to fumarate and formate to nitrate, for example [4].

In facultatively anaerobic bacteria, electron acceptors are usually used in a specific hierarchy. In *E. coli*, O_2 represses all anaerobic respiratory pathways and fermentation. Nitrate is the preferred acceptor under anaerobic conditions and represses other anaerobic pathways [20] [29] [30] [31]. The hierarchy is affected by transcriptional regulation of the corresponding terminal reductases by O_2 and nitrate [32]. With different acceptors, not only respiratory chains but also the overall catabolism including the central pathways can be changed [32]. The use of the acceptors should be related to the ATP yields of the corresponding pathways [20]. The correlation between the energy derived from the pathway with the sequence by which the acceptors are used supports the regulatory significance of the energy yields for the bacteria. In *E. coli*, the growth rates correlate with the hierarchical use of the acceptors and are likely of similar significance for ATP yields [20] [32]. Electron acceptors regulate the expression of the dehydrogenases as well and most of them

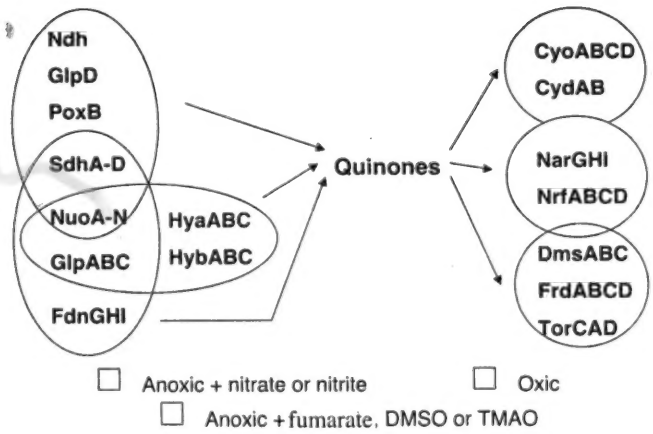

Fig 1.8 Illustration of the coincidence of electron donor and acceptor proteins based on conditions required for expression of these proteins [4].

are expressed preferentially in the presence of specific acceptors. Often the expression of dehydrogenases in aerobic respiration is not always for the maximization of energy production. Other requirements such as high metabolic fluxes or high growth rates due to low coupling coefficients or accelerated NAD regeneration could take priority over maximal energy conservation in aerobic metabolism [33]. Preference of high metabolic fluxes or growth rates is in agreement with the presumption that bacteria are optimized for high growth rates rather than for maximal energy yields [34] [4].

1.3.0 DMSO Reductase is an Important Terminal Electron Acceptor in E. coli

The ability to reduce dimethylsulfoxide (DMSO) to dimethylsufide (DMS), a major intermediate in the global sulfur cycle, is widespread in both prokaryotes and eukaryotes [35] [36]. It is believed that DMS accounts for 50% of the biologically synthesized reduced sulfur in the environment and plays an important role in global climate control [37] [38] [39].

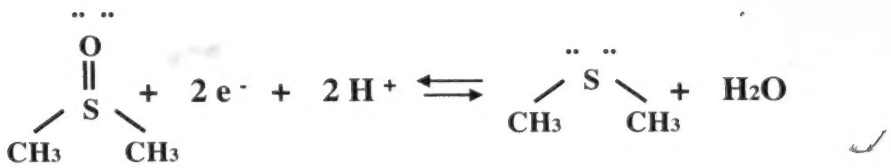

Fig 1.9 Dimethylsulfoxide (DMSO) reacts with two electrons and two protons to form dimethylsulfide (DMS) and H_20.

DMSO Reductase of *E. coli* is a complex membrane-bound [Fe-S] molybdoenzyme, which catalyzes the reduction of DMSO to DMS and reduces a number of other S and N-oxide compounds. It is a well characterized enzyme and an excellent model system for understanding the structure and mechanism of electron-transfer chain complexes [14].

As mentioned earlier, DMSO reductase functions in concert with glycerol-3-P dehydrogenase to create an electrochemical potential gradient across the inner membrane using energy derived from glycerol-3-P [40]. Electrons released in the process are accepted by DMSO reductase and used to reduce DMSO to DMS and H_2O. This respiratory chain functions when cells are restricted to anaerobic respiration when glycerol and DMSO are present. The exact mechanism for the generation of a proton gradient by this cycle is unclear as the orientation of these enzymes in the membrane (both cytoplasmic) make conventional proton translocation by quinones unlikely [14].

1.3.1 Organization of the Operon

There are three open reading frames in the DMSO reductase operon located at 20 minutes on the *E. coli* chromosome. They encode polypeptides with molecular weight

values of 87 350/85 800, 23 070 and 30 789 KDa, (for the DmsA preprotein/mature, B and C subunits respectively) [14]. Organization of the operon closely parallels that seen for fumarate reductase and formate dehydrogenase of *E. coli*. The 5' proximal gene encodes the molybdenum cofactor containing catalytic subunit followed by an electron transfer subunit and this subunit has groups of cysteine residues, which coordinate [4Fe-4S] clusters. The 5' distal gene encodes the membrane anchor and quinol binding subunit, DmsC [14].

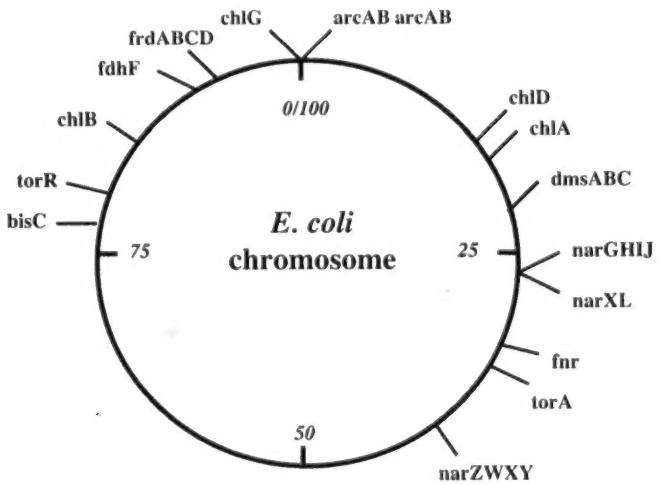

Fig 1.10 The chromosome of *E. coli* with the relevant genes marked. BisC, biotin sulfoxide reductase; chlA,B,D and G steps in molybdopterin cofactor biosynthesis; dmsABC, DMSO reductase; fdhF; formate dehydrogenase; fnr, positive gene activator; fnrABCD, fumarate reductase; narGHIJ, nitrate reductase; narXL, regulator of nitrate repression of DMSO reductase; TorA, TMAO reductase [14].

As mentioned earlier, facultatively anaerobic bacteria utilize electron acceptors in a specific hierarchy. In *E. coli* O_2 represses all anaerobic respiratory pathways as well as fermentation. Under anaerobic conditions nitrate is the preferred electron acceptor and it represses other anaerobic pathways. Different electron acceptors allow for variation not only in respiratory chains, but also in overall catabolism including the

central metabolic pathways. The use of the acceptors is related to the energy yields from the entire pathway. Anaerobic respiration under conditions of low nitrate with different N-oxides or S-sulfoxides such as DMSO or TMAO for use as electron acceptors requires the expression of the broad substrate enzyme encoded by the DmsABC operon [14]. The global regulator Fnr protein controls the 100-fold activation of this operon in response to anaerobic conditions. The transcriptional start site is approximately 220 nucleotides upstream of the translational start of *dmsA* [41]. The presence of nitrate, a preferred alternative electron acceptor, elicits a 10-fold repression of *dmsABC* expression using the NarXLQP two-component regulatory system. Nitrate is detected by NarX or NarQ, which then activates the DNA binding response-regulatory protein NarL by phosphorylating it. This P-protein then negatively regulates *dmsABC* operon expression, probably by interfering with Fnr and/or RNA polymerase interactions at the regulatory region [4].

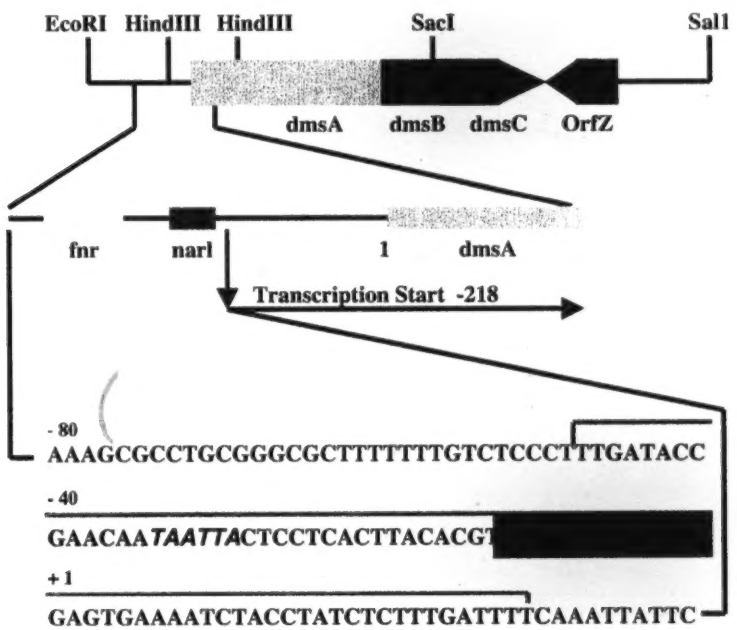

Fig 1.11 Organization of the DmsABC operon. The open reading frames from 5' to 3' are DmsA, B, and C respectively. The promoter region contains Fnr and NarL binding sites. The DNA sequence is numbered relative to the start of transcription. The RNA polymerase recognition sequences in the –35 and –10 regions are in bold italics. The consensus NarL and FNR are binding sites are represented by the blue and purple boxes respectively [14] [20].

1.3.2 The DmsC Subunit and its Topology in the Inner Membrane

Additional regulators of *dmsABC* expression have also been described that involve molybdenum dependent gene expression by means of the ModE transcription factor, and integration host factor (IHF) that interacts with DNA at a downstream site called P2 [42] [43]. It appears that the presence of the substrate molecules DMSO and TMAO do not have an effect on DmsABC expression as is commonly found with other enzymes [44] [45]. DmsC of *E. coli* is the 23 070 kDa plasma membrane anchor subunit of DMSO reductase. It is able to accept electrons from the membrane soluble menaquinol pool and transfer them to the DmsAB catalytic dimer, which reduces DMSO to DMS and H_2O. The topology of DmsC has been considered using amino acid sequence algorithms and hydropathy scales [46].

Experiments using alkaline phosphatase (*phoA)* and β-lactamase (*blaM)* gene fusions have also been carried out to investigate the membrane anchor subunit DmsC. The location of the *phoA* or *blaM* gene product can be assayed for which side of the membrane it is on. The sidedness will be different depending on where the fusion is located within the *dmsC* gene yielding information about the topology of DmsC. The results of these experiments suggest a structure with 8 transmembrane helices [19].

Both the amino and carboxy termini are exposed to the periplasm. The subunit has three relatively large periplasmic loops, P1-P3, and four small cytoplasmic loops C1-C4. In this model the overall distribution of Arg and Lys residues is three on the periplasmic side and eight on the cytoplasmic side in agreement with the positive inside rule for membrane proteins [19]. Cytoplasmic loops C1 and C2 each have 3 Arg or Lys residues, however loops C3 and C4 have only one each. The model also predicts that helix 7 and helix 8 each have 1 Arg residue [19]. The charges of these amino acids in the hydrophobic membrane could be accomadated by the formation of a salt bridge between them.

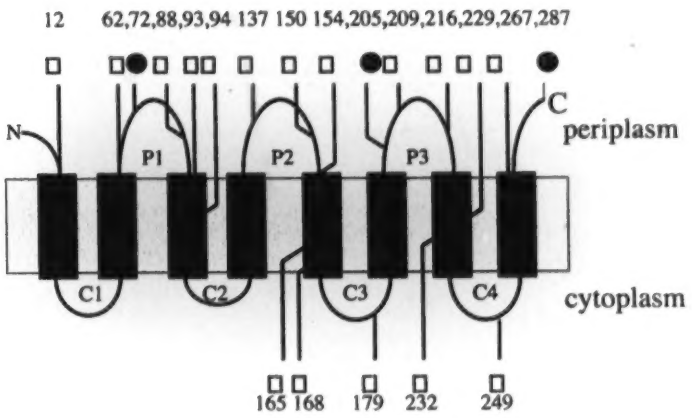

Fig 1.12 Location of the fusion sites within the proposed transmembrane structure of DmsC. This model identifies the location of each fusion given as a DmsC residue number. □ are Amp fusions ● are chimeras with active alkaline phosphatase. P1-P3 and C1-C4 identify periplasmic and cytoplasmic loops respectively. N and C are the amino and carboxyl termini located in the periplasm. [19]

It was also shown that the entire DmsC polypeptide was required for membrane attachment of the DmsAB catalytic dimer [19]. Much investigation into the topology of DMSO reductase in the inner membrane has been carried out. Inverted vesicles isolated from bacteria over-expressing DMSO reductase revealed dumb-bell type structures which were randomly arranged over the membrane, and were shown to be the DmsAB subunits by immunogold electron microscopy using anti-DmsA and anti-DmsB antibodies [47]. These studies suggest that DmsA and B form a side-by-side dimer on the cytoplasmic side of the membrane anchored by DmsC. The cytoplasmic location has been confirmed by a combination of thin section immunogold electron microscopy, antibody labeling, proteolytic digestion, and substrate accessibility assays [47] [48]. Electron paramagnetic resonance (EPR) studies using the paramagnetic broadening reagent, dysprosium (III) [49], have confirmed the cytoplasmic location of the molybdenum center and [Fe-S] clusters [47]. If the DmsAB catalytic dimer is cytoplasmic, then it must somehow associate with the four smaller cytoplasmic loops of DmsC. Because it is understood that DmsC transfers electrons to the FeS cluster containing DmsB subunit, then these must be the loops that make contact.

Fig 1.13 Electron micrograph of *E. coli* inverted inner membrane vesicles stained using immunogold. The catalytic dimer of DMSO reductase coating the surface suggesting a cytoplasmic localization in the cell. It appears that DmsA lies adjacent to DmsB by the dumbbell shape visible by immunogold staining [14].

The important residues for these contacts are as of yet unknown but site directed mutagenesis experiments may yield more information about how DmsC contacts DmsB.

1.3.3 DMSO Reductase Targeting to the Inner Membrane of E. coli

1.3.3.1 The Tat Transport System

The most common pathway of protein transport across the inner membrane of *E. coli* is through the Sec apparatus which threads the proteins through the membrane in an energy dependent fashion. This translocation requires that the substrate proteins remain in an unfolded state and extensive information exists for this system [12]. A more recently discovered alternative translocation system termed membrane targeting

and translocation (Mtt), also termed the twin arginine translocase (Tat), has been shown to transport fully folded proteins to or across the membrane. Most of these proteins require the cytoplasmic assembly of a redox cofactor which induces protein folding. These substrates cannot be translocated by the Sec apparatus [12].

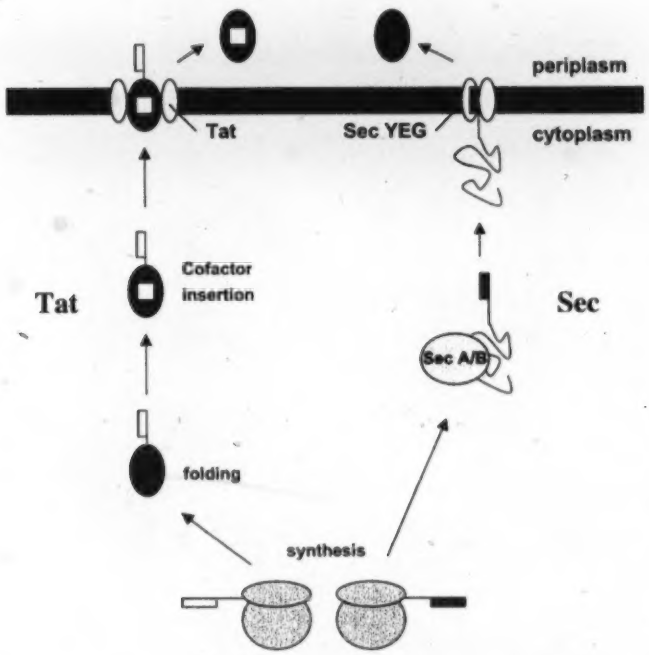

Fig. 1.14 Illustration of the two mechanisms bacteria use to export proteins across the inner membrane. The Sec apparatus transports unfolded proteins and the tat apparatus transports fully folded proteins which usually contain redox cofactors [11].

The known Tat genes are organized into a constitutively expressed *tatABCD* operon as shown in ***fig 1.17.*** The *tatABC* genes encode important (TatA) or essential (TatB and C) membrane bound components, whereas the *tatD* gene encodes a cytoplasmic protein whose activity does not seem to be important for tat-dependant export. The monocistronic *tatE* gene encodes a TatA homologue, but this gene is expressed at very low levels and the function of the encoded protein is largely dispensable [50] [11].

TatA, B, and E are predicted to contain very short periplasmic amino-terminal domains and single membrane spanning regions followed by short amphipathic regions. TatA and E contain a small cytoplasmic domain. TatB has a larger cytoplasmic domain. TatC is predicted to contain six transmembrane helices with short interconnecting loop regions and with the amino and carboxy termini located in the cytoplasm [12] [11].

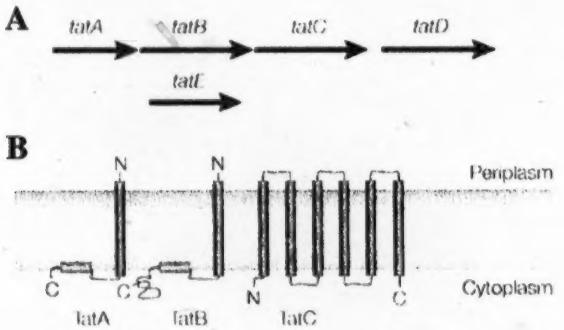

Fig 1.15 **A** Organization of the Tat operon. TatA,B,C and D are constitutively expressed from the same operon whereas TatE is monocistronic and expressed at very low levels **B** Topology of the various Tat integral membrane proteins components. TatE is most closely homologous to TatA [12] [11].

Tat A, B and C exist in a molar ratio of approximately 40:2:1 respectively [12]. The integral membrane complex has a molecular weight of 600-700KDa and is thus much larger than the combined molecular weights of the monomeric proteins. This suggests that multiple copies of some or all of the tat components are required to make up a functional translocon [12]. Transport of proteins using Tat has been extensively studied and has been shown to be rather complicated. Several models have been proposed for the operation of the Tat translocase.

The first step of the process would have to be substrate signal sequence recognition by the translocase [12] [51]. Most of the Tat components have been suggested to play a role in this for different reasons. For example, TatB and TatA because they have a receptor like topology and TatC because of its high degree of conservation among different organisms. (The Tat signal sequence is also highly conserved among

different organisms) [11] [12]. Experimental data point to the B and C subunits acting in the early stages of the translocation process. One model has suggested that membrane integration of substrate protein could precede Tat-dependent translocation. This idea is mainly supported by observations of Tat-independent membrane insertion of Tat substrates in vivo and in vitro. Membrane insertion may allow a quality control of the folded state by membrane bound proteases. The membrane spanning signal peptide could then be recognized by the signal sequence recognition protein of the translocase. Whether guided to the translocase through an initial membrane integration step or directly, it is likely that chaperone proteins aid in the process by binding the signal sequence and guiding it to the translocase signal sequence recognition protein [12] [11].

The second step in translocation by Tat (at least for most of its substrate proteins) would be protein transport. Here, the unique situation exists that large folded proteins are passed through the membrane bilayer. Some of the largest proteins utilizing the Tat system would require a pore 60 Å in diameter [12] [51]. The TatABC complexes observed experimentally often vary in size and the largest often appear too small to be able to form a proteinaceous pore capable of transporting fully folded proteins. It is possible that the channel could increase in size as required by either the recruitment of additional TatA subunits or the operation of several TatABC complexes in concert. TatA subunits have been shown to form large homo-oligomeric complexes and recent studies suggest an average size of around 460 KDa. Conceivably, the addition of such a complex could generate the required channel [12] [51] [11]. This implies a very dynamic structure for the Tat translocase. In any case the mechanism for protein transport is a complicated one. For example an ionic seal must be maintained around the protein throughout transport that is difficult to model especially considering many of the substrate proteins are large enough to simultaneously be exposed to both the cytoplasm and periplasm during transport. Perhaps the amphipathic helices of TatA, B and E are somehow able to assist in this function by associating with the protein as it slides through the pore. The flexibility in the loop region connecting the transmembrane helix with the amphipathic helix would allow for flexibility ensuring

the maintenance of an ionic seal around the protein at all stages of transport. In the case of some membrane bound redox proteins targeted by Tat, it has been observed that the catalytic subunits are not even transported across the membrane but remain in the cytoplasm peripherally associated with their membrane anchor subunits [11] [12]. DmsABC is such an enzyme. Much about how these proteins are targeted by the Tat apparatus is being learned by mutagenic and fusion protein studies [11] [12].

Structural analysis of the Tat system suggests that the third step would likely be the proton anti-transport step, which uses the proton gradient of the membrane to energize the transport process [51] [52]. It is known that Tat transport is energized solely by the transmembrane proton electrochemical gradient and that it requires no nucleotides or other soluble factors. The mechanism of energy transduction during protein export by the Tat apparatus remains unclear however sequence analysis points to Tat as the component likely to perform this function [12],[51].

The fourth and final step of tat translocation would be signal-peptide cleavage. It has been shown using enzyme specific inhibitors that Tat signal-peptide cleavage is accomplished by the periplasmic signal peptidase-I (Lep) [11].

1.3.3.2 The Signal Sequence is Important in Tat Directed Protein Translocation

Features such as protein leader sequences, as well as structural information contribute to the differential targeting to either the Tat or Sec apparatus. Other features are important in determining whether Tat will translocate a protein right across the plasma membrane or to either the periplasmic or cytoplasmic face of the membrane.

The ER and bacterial Sec systems recognize amino terminal targeting signals that comprise three distinct domains, an amino terminal domain containing on average one or two basic residues, a hydrophobic core and a more polar carboxy terminal domain that ends with a short chain residues at the –3 and –1 positions [11] [53].

Tat leader sequences have a similar tripartite organization but are particularly long, usually between 30 and 60 amino acids and contain a conserved twin argenine motif **(S/T)-R-R-X-F-(X/L)-K**. Most have one or two positively charged residues just upstream of the cleavage site. This leader has been found associated with a large number of periplasmic redox proteins and a few cytoplasmic inner membrane peripheral proteins including TMAO reductase and DMSO reductase [11] [12].

Mutagenic studies have established a vital role for the twin arginine signal sequence in targeting proteins for transport by Tat. The Tat leader has successfully targeted normally Sec dependent proteins to the Tat apparatus for example [12].

1.3.3.3 Targeting of DMSO Reductase

DMSO reductase is the archetype of a subclass of Tat substrates for which the Tat apparatus is involved solely in membrane targeting and not in protein translocation.

The mature form of DmsA begins with Val-Asp-Ser and the second upstream methionine (46 residues upstream of the Val) appears to be the initiating methionine. This 45 amino acid leader encodes a twin arginine motif and has Ala-His-Ala immediately upstream of the cleavage site in accord with other proteins containing this type of leader [11]. It is not known what peptidase is used to cleave the leader but experimental evidence shows that the Tat apparatus is required for this to occur.

The deletion of the leader sequence of some Tat translocated proteins such as TMAO reductase and DMSO reductase results in the cytoplasmic localization of the proteins consistent with a predicted role for the leader peptide in targeting to the membrane. These leaderless enzymes were stable and incorporated molybdenum cofactor. This was not the case for DMSO reductase and implies a dual role in targeting and stability in this enzyme [11].

Deletion of the leader of DmsA resulted in a protein that was not only impaired in membrane targeting by tat but was also unstable. This leads to the notion that the Tat leader peptide, at least for DmsA, could have two distinct functions: targeting and stability [11]. Twin arginine leaders may play specific roles in the assembly of redox enzymes and may not be interchangeable.

A study was done in which DmsAB was expressed in the absence of the anchor subunit DmsC. In the absence of DmsC one might expect that DmsAB should be translocated to the periplasm directed by the twin arginine leader. This is in fact not observed. Could the leader contain stop transfer information? This is unlikely because the DmsA leader in fusion with GFP targets the protein to the periplasm. It seems as though DmsAB contains information in the mature polypeptide that prevents its translocation to the periplasm [11].

Fig 1.16 Fluorescence microscope images of *E. coli* cells expressing GFP fused to to the DmsA leader sequence. The green halo observed is the GFP that has been targeted to the periplasmic space in these cells [11].

It appears that Tat catalyzes the targeting of DmsAB to the cytoplasmic face of the membrane but not its translocation and that a functional Tat system is required for processing of DmsA to its mature form and for the stability of the dimer [11].

1.3.3.4. DmsC Quinol Binding, Oxidation and Electron Transport

DmsC, the membrane anchor subunit of DMSO reductase, is the subunit involved in menaquinol binding, oxidation and the initial phase of electron transport to the active site [49]. This subunit interacts with 2-n-heptyl-4-hydroxyquinoline-N-oxide (HOQNO), a membrane quinol analog. This molecule associates with the quinol binding cleft in the same way as menaquinol and its higher binding affinity results in a blockage of electron transfer [54]. The fluorescence properties of HOQNO have provided a convenient means of studying its binding and inhibition reactions. When bound to the DmsC quinol binding site, the molecule has no spectroscopic properties. When these sites are saturated and the molecule must exist in solution, it has characteristic emission and excitation spectra. This feature has been used to assay properties of quinol binding in respiratory chain enzymes [54].

Steady state and rapid reaction methodologies [54] have been utilized to show that HOQNO interacts with very high affinity and with a 1:1 stoichiometry at a site within the DmsC subunit [54]. A mutation of His 65 to Arg in DmsC blocks quinol activity and eliminates all HOQNO binding. These findings suggest there is only one exchangeable binding site in DmsC, differing from fumarate reductase and nitrate reductase where two quinol binding sites have been proposed [55] [56]. Stopped-flow studies suggest that binding of HOQNO takes place in a two-step mechanism. It is suggested that initially HOQNO (E) exists loosely-bound to the binding site (L) of DmsC, in the form 'EL'. This initial binding step occurs rapidly by a bimolecular association and then it is converted to a more tightly and specifically bound complex EL*, by a slow unimolecular process (an isomerization step). The isomerzation may take place through several possible pathways, such as a rearrangement of EL without any conformational change in E or L, or, conformational changes in both E and L [54]. This description of HOQNO binding is also a likely scenario for the binding of the natural substrate electron donor menaquinol. Other menaquinol like molecules have been shown to be oxidized by the DmsC subunit. Two hydroxylated napthoquinol menaquinol analogues, reduced plumbagin (PBH_2), 5-hydroxy-2-methyl-1,4-

naphtoquinol and reduced lapachol ($LPCH_2$), 2-hydroxy-2-methyl-1,4-naphthoquinol have been shown to be substrates for *Escherichia coli* anaerobic reductases. These compounds have optical, solubility and redox properties that make them suitable for use in studies of the enzymology of menaquinol oxidation [57].

DmsC differs from the membrane anchor subunits of a number of different membrane bound respiratory chain enzymes whose crystal structures have been solved in that it does not appear to ligate any redox cofactors to aid in electron transport through this subunit. Other enzymes often utilize hemes for electron transport functionally connecting the quinol binding site and FeS clusters of the electron transfer subunit. Examples of these enzymes include the *E. coli* nitrate reductase, fumarate reductase, and succinate dehydrogenase [56] [55] [58]. It appears that DmsC shuttles electrons from the quinol binding site directly to the Em,7 (midpoint redox potential @ pH 7.0) = –50mV iron sulfur cluster (see *fig 1.17*) of DmsB. The interaction between the quinol binding site of DmsC and the closest iron sulfur cluster was studied using electron paramagnetic resonance spectroscopy (EPR) [58]. Mutants of DmsB were created so that the enzyme assembled a 3Fe-4S cluster rather than a 4Fe-4S cluster in this position. This was accomplished by substituting cysteine 102 with serine or tryptophan. The effect of assembling a 3Fe-4S cluster in these mutants on electron transfer from the MQH_2 site was investigated using the Q-pool coupling assay [58].

It was confirmed by EPR studies of the MQH_2 oxidoreductase activities of the $DmsAB^{C102S}C$ and $DmsAB^{C102W}C$ mutants as well as by observing the effect of HOQNO on these mutant enzymes, that the 3Fe-4S cluster is functionally and conformationally linked to a MQH_2 binding site of DmsC [58]. By extrapolation, it was concluded that the –50 mV cluster of the wild type enzyme is also functionally and conformationally linked to this MQH_2 binding site and is an important component of the electron transfer pathway through DmsB to the molybdenum cofactor of DmsA [58]. This is further supported by the thermodynamic competency of the -50 mV cluster of DmsABC to accept electrons from MQH_2 (-70mV) [59]. These conclusions are also consistent with topological data that suggests that the

DmsB-C102S [3Fe-4S] cluster is located approximately 21Å from the cytoplasmic surface of DmsAB^{C102S}C close to the quinol-binding site of DmsC. This information comes from experiments utilizing the exogenous paramagnetic probe dysprosium (III) complexed with EDTA as mentioned earlier. Here, magnetic interactions between the probe surrounding the protein and its interaction with redox centers within the protein can be analyzed and the spatial positioning of these redox centers understood [49].

1.3.5 The DmsB Subunit

DmsB from *E. coli* is the 23.1 kDa electron transfer subunit of DMSO reductase. It connects the membrane anchor and menaquinol oxidizing subunit (DmsC) to the TMAO/DMSO reducing subunit (DmsA) in both a structural and functional sense.

The amino acid sequence of DmsB shows sixteen cysteine residues organized into four sequence clusters bearing homology to the iron-sulfur center binding clusters of the eight iron ferredoxins. The cysteine groups are similar to those found in proteins known to contain 4Fe-4S clusters specifically. In the case of the bacterial eight-iron ferredoxins, it was found that the first three cysteine residues of each group ligate one [4Fe-4S] cluster, while the fourth cysteine provides the fourth ligand to the other cluster in the protein. Consideration of the spacing found in the bacterial ferredoxins as well as sequence similarities to homologous subunits whose crystal structure has been elucidated allows a model to be proposed for the interaction of the cysteine residues of DmsB with four 4Fe-4S clusters [14].

The EPR spectrum of the reduced form of both membrane bound and purified DMSO reductase can best be interpreted to suggest the protein does indeed contain four 4Fe-4S cluster centers. The very complex EPR spectrum of the protein has features which closely resemble the spectra of other proteins containing multiple 4Fe-4S clusters such as *Clostridium pasteurianum* ferredoxin and *Micrococcus lactilyticus* ferredoxin [14]. Because the magnetic interactions between the reduced clusters make the spectrum so

complex, it is not possible to assign the features of the fully reduced spectrum to individual clusters of the enzyme, however the spectrum can be loosely interpreted as two pairs of interacting 4Fe-4S clusters with each pair having spectroscopic similarities to the bacterial eight-iron ferredoxins [14]. DMSO Reductase titrates with four mid-point potentials at pH 7 of –50, -120, -240, and –330mV [59]. Spin quantifications indicate that the enzyme contains a total of four 4Fe-4S clusters in addition to the single molybdopterin cofactor in the catalytic subunit. The enzyme catalyzes electron transfer from menaquinol at a midpoint potential of approximately –74mV and reduces DMSO at a midpoint potential of about +160mV [59].

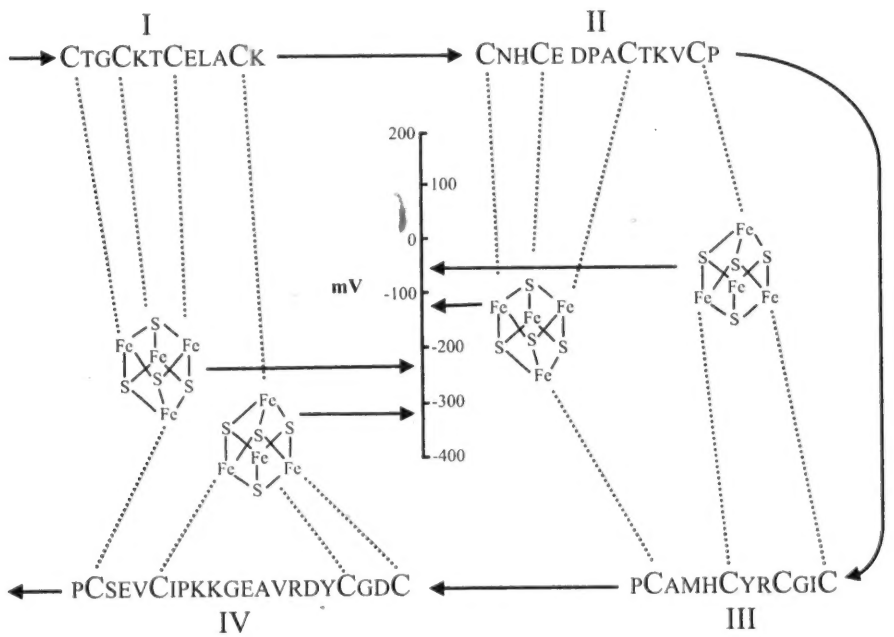

Fig 1.17 The four ferredoxin like conserved cysteine groups of DmsB that bind 4Fe-4S clusters.

Interactions between the –50 mV and –120 mV iron-sulfur clusters and between the –330 mV cluster and some of the other clusters were observed as changes in the EPR

line shape during progressive reduction of the protein [3]. The two higher midpoint potential clusters are well placed to accept electrons from the intermediate carrier menaquinol. The potentials of the lower potential clusters seem too negative to be a part of the electron transfer pathway. This feature is also reminiscent of a typical 4Fe-4S bacterial ferredoxin [3]. Crystal structures of closely homologous subunits such as fumarate reductase, succinate dehydrogenase and nitrate reductase from *E. coli* clearly place all iron sulfur clusters of these subunits in a way that very strongly suggests that they all participate in the electron pathway through the subunit and are all utilized in electron transfer. This means that likely all clusters are used in DMSO reductase and that kinetics rather than thermodynamics are more realistic in terms of understanding electron transfer through a protein.

The midpoint potentials of the Mo(VI)/(V) and Mo(V)/(IV) transitions lie between the potential of the iron-sulfur clusters and that of the DMSO/dimethylsulfide couple. The observed spin-spin interactions between molybdenum and at least one of the iron-sulfur clusters show that the redox centers are in fairly close proximity even though they are on different subunits, DmsA and B respectively. The distance between the molybdenum and closest iron sulfur cluster is believed to be approximately 12 Å.

1.3.6 The DmsA Subunit

DmsA is the largest subunit component of DMSO reductase. It is a 87.4 kDa protein that binds a molybdenum-molybdopterin guanine dinucleotide cofactor, Mo-MGD. This protein is the catalytic subunit of the enzyme. The molybdenum in this subunit accepts electrons from DmsB and reduces the substrate molecule DMSO as well as a number of other S and N-oxides [48]. Much has been discovered about how DmsA works to catalyze the reduction of substrate molecules. A fairly good understanding of DmsA has come from amino acid sequence comparisons with homologous proteins

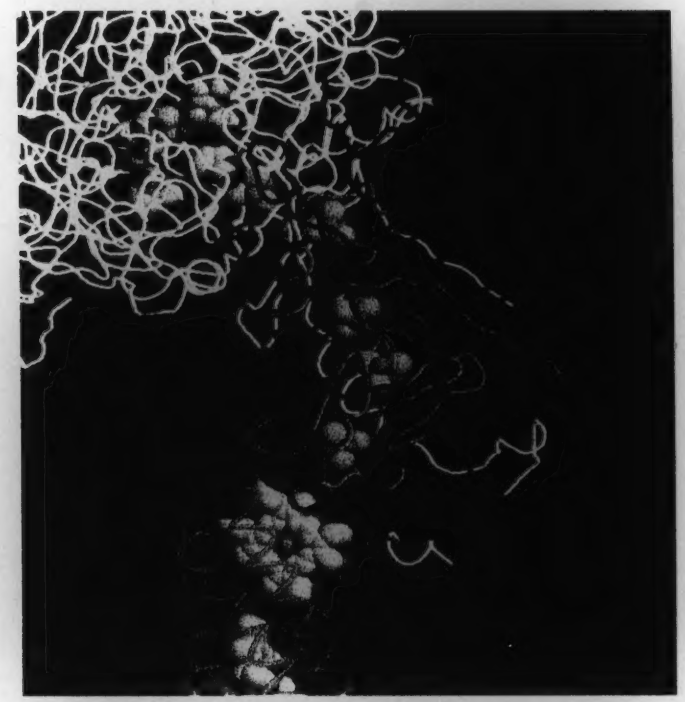

Fig 1.18 Ras mol depiction based on the crystal structure, of the electron transfer pathway of NarGHI of *E. coli*. The NarH subunit is the electron transfer subunit which binds 4Fe-4S clusters in a similar way to DmsB. The illustration shows all four clusters are aligned in an obvious pathway for electron transfer. All clusters seem to be utilized in this pathway.

whose crystal structures have been elucidated. These studies have been complemented with mutagenesis experiments to identify important residues involved in active site function, substrate specificity, cofactor coordination, structural integrity and even electron transfer from the redox centers of DmsB to the active site molybdenum. Spectroscopic studies have revealed important information about the mechanism of the catalytic cycle of substrate reduction.

1.3.6.1 The Molybdenum Active Site

DmsA binds a molybdenum containing cofactor which is utilized in substrate reduction. Molybdenum and tungsten are the only second row transition metals that have a known biological function [1]. Most enzymes that contain molybdenum

catalyze hydroxylations and net oxygen transfer reactions to and from a variety of biologically relevant substrates [1]. In the case of *E. coli* DMSO reductase, the molybdenum is coordinated by two unique ene-dithiolate ligands derived from the sidechain of a nonprotein pterin heterocycle [17]. The coordination of the Mo to these cofactors is required for the reactions [60].

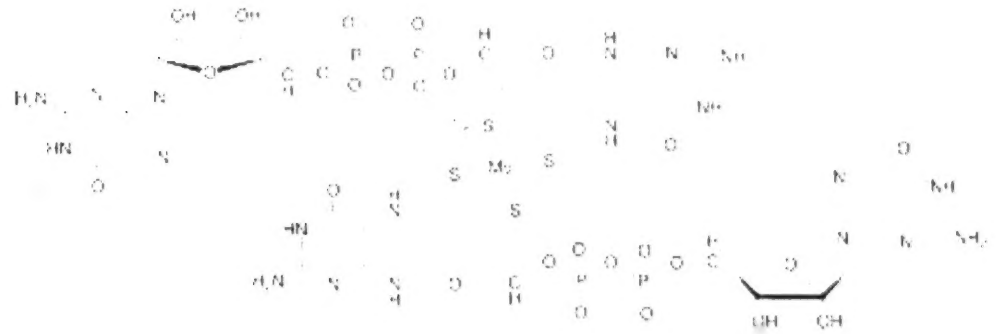

Fig. 1.19 The Mo-bisMGD cofactor. The molybdenum is coordinated by two sulfurs from each of two MGDs, (molybdopterin guanine dinucleotides), this coordination is required for catalytic activity [9] [17].

The catalytic mechanism of DMSO reductase explained in greater detail later, is proposed to involve the coordination of water to the metal atom to give Mo-OH_2, Mo-OH or Mo=O where the molybdenum cycles between the Mo(IV) and Mo(VI) oxidation states. Two consecutive one-electron reduction processes involving the prosthetic groups that accompany the cofactor regenerate the resting state of the enzyme [13] [1]. The crystal structures of several molybdenum containing enzymes have formed the basis for the classification of the active sites on the basis of three structural prototypes. Of interest to us is the DMSO reductase family. This family includes dissimilatory nitrate reductases, formate dehydrogenases, trimethylamine-N-oxide reductase and biotin sulfoxide reductase [1]. X-ray crystallography on the oxidized form from *R. sphaeroides* reveals a molybdopterin(2)MoO(O-ser) active site.

In the crystal, the four ene-dithiolate S atoms from the two molybdopterins coordinate the Mo atom [61].

DMSO reductases have been investigated by Extended X-Ray Absorption Fine Structure (EXAFS) Spectroscopy, Raman spectroscopy, EPR, and X-ray Crystallography. Crystallographic investigation on DMSO reductase isolated from *R. sphaeroides* was carried out on the oxidized form as well as on the dithionite reduced form. On the basis of these results a novel mechanism was proposed involving an oxygen transfer reaction. The reduced and catalytically competent molybdenum center is desoxo-Mo(IV) while the fully oxidized state is a monooxo-Mo(VI) center in this mechanism [61] [1]. The step during which the metal loses an oxo group and is in the Mo(V) redox state is considered to be the rate determining step of the catalytic cycle [13]. Electron spin echo envelope modulation (ESEEM) spectroscopy has been used to determine the interaction of the exchangeable proton at the Mo(V) active site of DMSO reductase from *Rhodobacter sphaeroides*. These studies complemented by analysis using X-ray absorption fine structure spectroscopy, resonance Raman

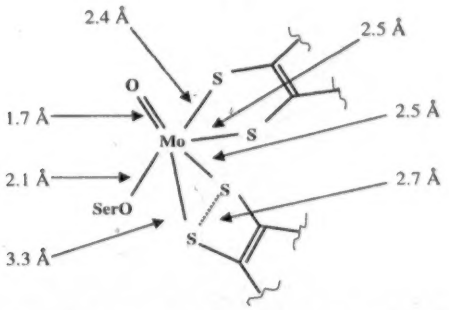

Fig 1.20 The crystal structure of the oxidized form of DMSO reductase from *R. sphaeroides* shows that the active site of this family of molybdoenzymes is unique in that it coordinates four sulfurs from two molybdopterin cofactors and bonds the oxygen of a serine residue from the protein in its resting state [1].

spectroscopy, UV visible spectroscopy and magnetic circular dichroism suggest that the Mo(V) center remains coordinated by two dithiolene moieties and the oxygen atom from ser147 however a hydroxyl group replaces the terminal oxo group. An interesting feature of the active site molybdenum is that

Fig 1.21 The reduced and oxidized forms of molybdenum found in the active site of DMSO reductase [1] [9].

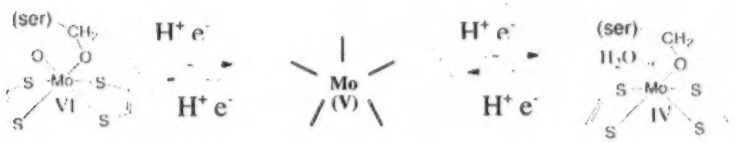

Fig 1.22 The stage of the reaction where molybdenum enters the Mo(V) state is thought to be the limiting step in the catalytic cycle [13].

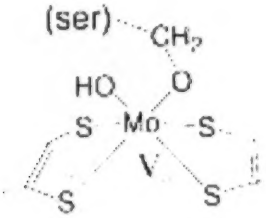

Fig 1.23 The proposed Mo(V) oxidation state in the catalytic cycle of DMSO reductase [5] [9].

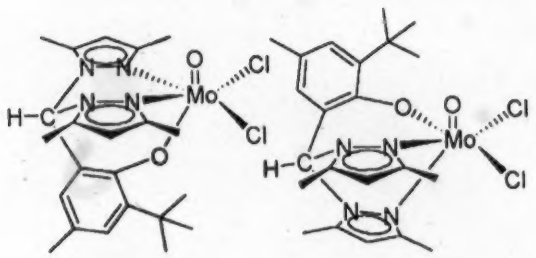

Fig 1.24 Cis and trans isomers of the Mo(VII) [10].

there appears to be a wide variation in the reported O-Mo-O angles ranging from 77-146 degrees in different enzymes [5]. Two geometric isomers have been synthesized to model the physiochemical significance of such variation on the properties of the enzyme. Both of these isomers exhibit well-defined reversible oxidation and reduction couples. Reduction of the cis isomer is more difficult than the reduction of the trans isomer. Dependence of the reduction potential on geometry is an important observation, demonstrating that the position of an oxygen donor relative to the terminal oxo functions to modulate the reduction potential of the metal center [10]. The position of the serine oxygen relative to the terminal oxo may play a critical role in gating the electron transfer process in the regeneration step. In fact substrate bound forms of DMSO reductase exhibit different O-Mo-O angles compared to the structure with no bound substrate. Data suggests that the smaller the angle the easier it is to oxidize Mo(V), while the concomitant reduction becomes more difficult. It appears geometric flexibility ensures that electron transfer is gated as a function of active-site conformation [10]. In the *E. coli* DMSO reductase, the molybdenum binding serine residue Ser176 was mutated to a His or Ala. Loss of Mo ligation by DmsA-ser176 causes major changes in the redox and EPR properties of the enzyme and the molybdenum center. The S176A mutant is unable to cycle through the Mo(V) to Mo(VI) oxidation states [62].

In summary, studies on DMSO reductase from *Rhodobacter capsulatus* and *Rhodobacter sphaeroides* have indicated that the active site undergoes complex structural transformations. Spectroscopy shows that both pairs of dithiolenes remain attached to Mo throughout the catalytic cycle. The Mo site exists in multiple structural states that are not equally active. Protein film voltammetry has confirmed other studies that suggest crucial steps in the mechanism such as the rearrangement of atoms/groups in the active site are facilitated in the Mo(V) oxidation state [13] [5] [60]. A reasonable catalytic mechanism for DMSO reductase is as follows,

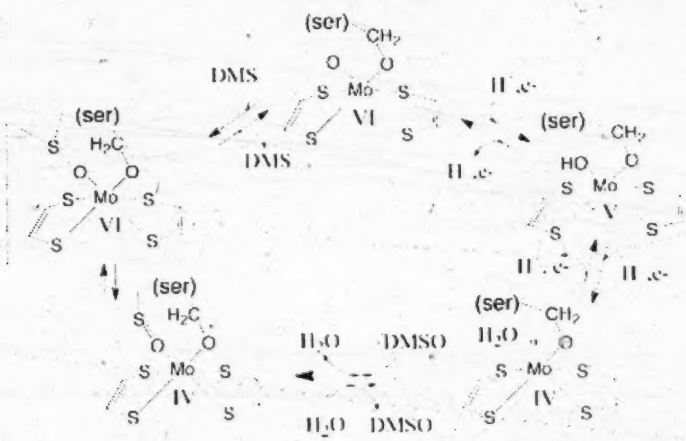

Fig 1.25 Catalytic cycle the active site Mo of DMSO reductase [9].

1.3.6.2 DmsA Substrate Specificity

What other features about the active site of DMSO reductase have been discovered? The enzyme can catalyze the reduction of both DMSO and TMAO as well as a variety of other S and N-oxides.

The presence of a tyrosine residue in the active site of DMSO reductase of *R. sphaeroides* that is missing in TMAO reductase has been implicated in the inability of TMAO reductase, (unlike DMSOR) to utilize S-oxides. This was studied using site

directed mutagenesis changing tyrosine to alanine and phenylalanine in the *Rhodobacter sphaeroides* enzyme and inserting a tyrosine residue into the equivalent position in TMAO reductase of *E. coli*. When tyrosine is absent there does seem to be an increase in the specificity for N-oxides and a decrease in the specificity for S-oxides [9]. The way Tyr114 modulates the substrate specificity of this class of enzymes cannot be answered without more complete mechanistic studies. It is possible that one of the ways in which Tyr114 has an effect upon substrate specificity is by changing the redox potential of the enzyme (because of its proximity to the molybdenum). In all Tyr114 mutants examined, a change in specificity is matched by a change in redox potential. Detailed spectroscopic studies on the mutants generated should provide greater understanding of how alterations in the vicinity of the molybdenum atom affect the catalytic properties of the enzyme. X-ray crystallography of DMSO reductase from *R. sphaeroides* shows that in the catalytically active hexavalently-coordinated molybdenum site,

Substrate	Enzyme Activity		
	Substrate conc. (mM)	Relative Rate (%)	Km (mM)
TMAO	10	100	0.6
Nicotinic acid N-oxide	10	109	N.D.
Nicotinamide N-oxide	3.4	134	0.5
2-Picoline N-oxide	10	84	N.D.
3-Picoline N-oxide	10	124	N.D.
4- Picoline N-oxide	10	134	0.5
Adenosine N-oxide	3.4	9	N.D.
3-Hydroxypyridine N-oxide	10	99	N.D.
Pyradine N-oxide	10	64	N.D.
Hydroxylamine hydrochloride	10	25	N.D.
DMSO	10	30	0.18
L-Methionine sulfoxide	10	28	0.47
Tetramethylene sulfoxide	10	34	N.D.
Methyl phenyl sulfoxide	10	41	N.D.
Sodium chlorate	10	78	7.75

100% activity corresponds to 151.7U of reductase activity per ml with TMAO as a substrate; N.D. is not determined, ususally due to solubility issues; Enzyme displayed simple Michaelis -Menton kinetics with all substrates examined except nicotinamide N-oxide which displayed substrate inhibition at high concentrations.

Table 1.2 The relative rates of reaction for the reduction of some S and N oxides given with respect to the rate for TMAO. In many situations the k_m value for the substrate could not be obtained usually because of low solubility of the substrate listed. Results are from purified enzyme specified in [2].

the single oxo group is coordinated by Trp-116 whereas in the pentavalently-coordinated molybdenum environment Tyr-114 is hydrogen bonded to one of the two oxo groups involved in determining the substrate specificity for the enzyme [9]. X-ray crystallographic studies of the *Rhodobacter sphaeroides* dimethyl sulfoxide reductase indicated that the active site is at the botton of a 25 Å funnel [15]. Substrates must travel to the bottom of the funnel in order to be reduced by the enzyme.

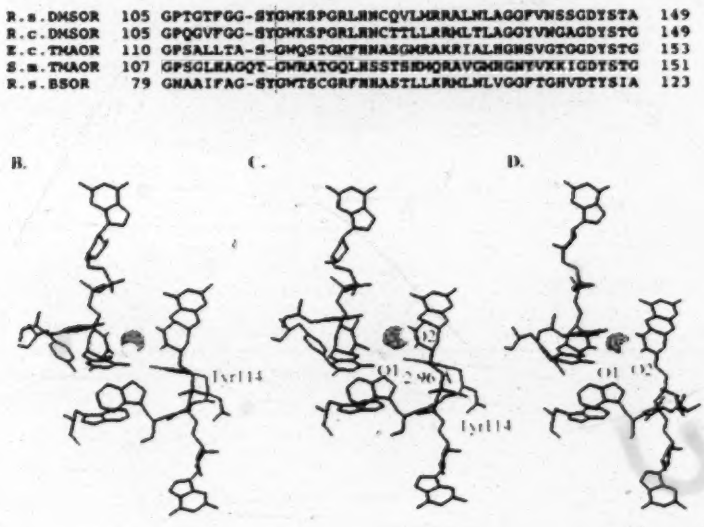

Fig 1.26 **A.** A sequence alignment of *R sphaeroides* DMSO reductase, *R. capsulatus* DMSO reductase, *E. coli* TMAO reductase, *S. massila* TMAO reductase and *R. sphaeroides* BSO reductase. The locations equivalent to Tyr-114 are shown in the box. **B.** Hexa-coordinate active site of *R. sphaeroides* DMSO Reductase from 1.3A structure showing four sulfur dithiolene ligands, one oxo group and one serine oxygen ligand to the molybdenum. The molybdenum atom is in green, the MGD cofactor in blue, and Tyr114 is in red. The serine and dithiolene sulfur ligands to the molybdenum are in yellow. **C.** Penta-coordinated molybdenum environments of *R. sphaeroides* DMSO Reductase showing two oxo ligands to the molybdenum. **D.** Active site structures of S. massila TMAO Reductase. [9]

The DmsA subunit of the *Escherichia coli* enzyme was subjected to site-directed mutagenesis targeting residues potentially lining the bottom of the funnel based on sequence alignment of the *E. coli* and *Rhodobacter* enzymes. Mutants G167N, A178Q, Q179I and R217Q showed functional impairment in activity [63]. The kinetic parameters of the mutant enzymes were examined, mutants A178Q and R217Q

showed dramatic alterations of their electron-acceptor Km, with values at least 35-fold less or greater then wild-type values respectively, for DMSO and pyridine N-oxide. T148S showed altered kinetic parameters for pyridine N-oxide and DMSO, with K_m and $k_{(cat)}$ decreasing and increasing approximately fourfold, respectively. Other mutants showed less drastic alterations in kinetic parameters [63].

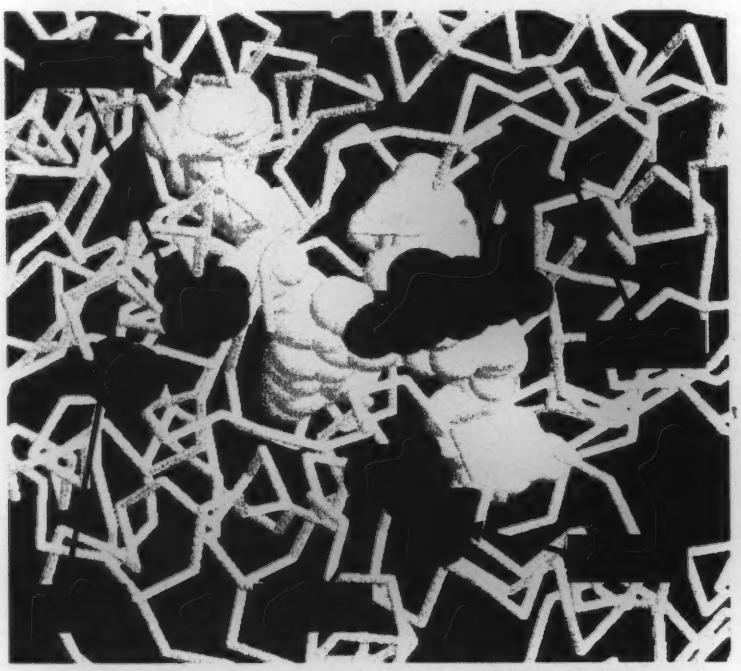

Fig 1.27 Rasmol depiction of the active site funnel from the crystal structure of the *Rhodobacter Sphaeroides* DMSO reductase enzyme. 16 residues in this funnel were mutated in the *E. coli* homologue and characterized. Mutated residues in the active site funnel that altered the activity of the enzyme are listed as the *E. coli* amino acid residue. The red molecule is representative of DMSO binding in the active site funnel [15].

1.3.7 Electron Transfer and Structural Characterization of DmsA

We have looked at the catalytic activity and substrate specificity of DmsA, but what are some of the other important features of the enzyme? What residues make important contacts with the molybdenum cofactor or are necessary for transferring

electrons to the active site for example? The most obvious way of understanding some of the structural features of an unknown protein is by understanding closely homologous proteins whose structures have been solved by X-ray crystallography or which have been characterized by some other means.

DmsA is part of a superfamily of oxidoreductase enzymes with highly conserved organization and sequence. They are prokaryotic enzymes that reduce DMSO, nitrate, biotin sulfoxide and polysulfide or enzymes which oxidize formate [59]. Alignment of these proteins show extensive blocks of homology throughout the length of the polypeptide [59]. To date there are several of these homologous proteins whose 3 dimensional structures have been solved including; DMSO reductase from *Rhodobacter sphaeroides [15],* DMSO reductase from *Rhodobacter capsulatus* [61], dissimilatory nitrate reductase from *Desulfofibrio desulfuricans* [64], formate dehydrogenase from *E. coli* [65]; and most recently nitrate reductase (NarGHI) from *E. coli* [66]. A good understanding of the structural characteristics of the DmsA protein can be inferred from these structures. Of particular interest is the conserved amino terminal ferredoxin like iron sulfur cluster binding motif which is closely conserved in most of these proteins (*fig 1.29*) [59]. Because the sequence resembles an iron sulfur cluster binding region, it could be that electron transfer is mediated by a 4Fe-4S cluster coordinated by this region. The structures of some of the enzymes solved by X-ray crystallography show that this is indeed the case for at least some enzymes. Further comparison of the region pointed out subtle differences in the sequence which suggested the division of these homologs into three distinct types [16]. The **Type I** enzymes contain three Cys residues spaced similar to a bacterial ferredoxin Cys group and one other conserved downstream Cys. Here, two amino acid residues separate the first two conserved Cys residues. Crystal structures from

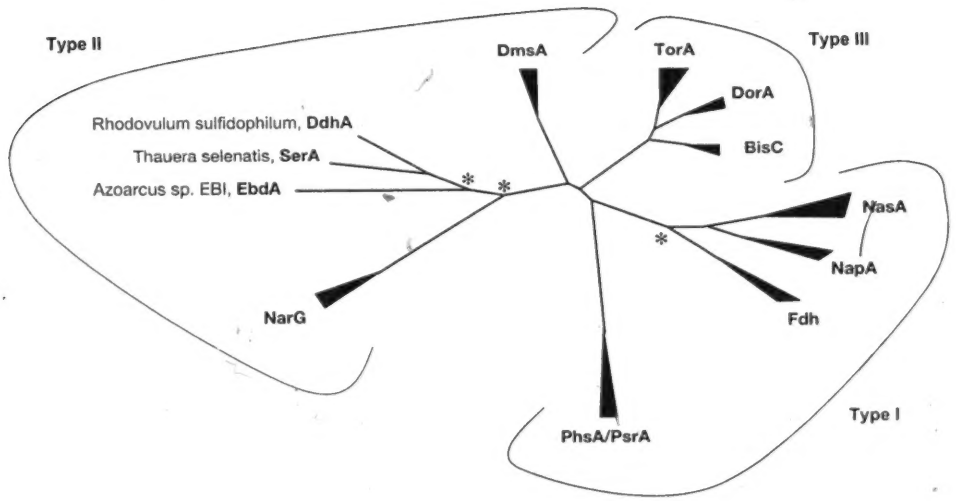

Fig 1.28 Evolutionary distance tree of amino acid sequences of enzymes in the DMSO reductase family. Characterized enzyme families are indicated as wedges that represent the phylogenic span of the sequences that comprise the family. Groups of genes that are reproducibly monophylogenetic are indicated by * on the nodes. "Relatedness distances" were calculated using the Dayhoff model and neighbour joining was used to construct the tree from the distance information. Abbreviations for molybdenum-containing subunits of proteins: **dorA**, dimethyl sulphoxide reductase. **torA**, trimethylamine-N-oxide reductase. **bisC**, biotin sulphoxide reductase. **NasA**, assimilatory nitrate reductase (consisting of NasA and NarB). **NapA**, periplasmic nitrate reductase. **Fdh**, formate dehydrogenase (consisting of FdhA, FdnG and FdoG) [21].

enzymes of this type were shown to form 4Fe-4S clusters using this motif. The **Type II** enzymes shared the feature of having three amino acids between the first two cysteines instead of two. As well, the first cysteine is replaced with a histidine in the *E. coli* nitrate reductases. DmsA belongs to this type. Originally no crystal structures of any Type II enzymes had been solved and it was believed that these enzymes did not coordinate 4Fe-4S clusters, the spacing between the Cys residues likely being critical for cluster assembly. The **Type III** enzymes include biotin sulfoxide reductase (BisC), and TMAO reductase (TorA), which share sequence identity with the other molybdoenzymes but lack the conserved N-terminal Cys motif altogether [16].

Type I

```
S7NarB:  IDTAKTLCPY CGVGCGLEAV PPAQPGRATV RDREGTPIWQ IRGDRQHPSS QGMVCVKG  73
KpNasA:  MTETRTTCPY CGVGCGVIAS RAPHGQVS· ·········· VRGDEQHPAN FGRLCVKG  46
EcFdhF:  MKKVVTVCPY CASGCKINLV VDNGKIVRA·· ········· ··EAAQGKTN QGTLCLKG  45
MfFdhA:  SKKVKTICTY CSVGCGIT· ····AEVV· ····· DGVWVR QEVAQDHPIS QGGHCVKG  98
WsFdhA:  SKKVKTICTY CSVGCGIT· ····AEVV· ····· DGVWVR QEVAQDHPIS QGGHCCKG  98
EcFdnG:  AKEIRNTCTY CSVGCGLLMY SLGDGAKNA· ···· REAIYH IEGDPDHPVS RGALCPKG  98
EcFdoG:  TRETRNTCTY CSVGCGLLMY SLGDGAKNA· ····· KASIFH IEGDPDHPVN RGALCPKG  98
AeNapA:  LKWSKAPCRF CGTGCGVT·· ····· VAVK· ····· KASIFH IEGDPDHPVN RGALCPKG  90
TpNapA:  ITWSKAPCRF CGTGCGVM·· ····· VAVK· ····· EGRVVA THGDLLAEVN RGLNCVKG  87
WsPsrA:  AKFVPSICEM CTSSCTIE··· ····· ARVE· ····· GDKGVF IRGNPKDKSR GGKVCARG  93
```

Type II

```
EcDmsA:  KVIWSACTVN CGSRCPLRMH VVDGEIKYV· ··· ETD····· N TGDDNTDGLH QVRACLRG  75
EcNarG:  KIVRST HGVN CTGSCSWKIY VKNGLVT··· ··· WETQQTDY PRTRPDLPNH EPRGCPRG  99
ECNarZ:  KIVRSTHGVN CTGSCSWKIY VKNGLVT··· ··· WEIQQTDY PRTRPDLPNH EPRGCPRG  99
```

Type III

```
EcTorA:  PSLLTPRRAT AAQAATDAVI SKEGILTGSH WGAIRATVKD GRFVAAKPFE LDKYPSK·  86
RsBisC:                  M ITTRVPHCSH WGAYTLLVDE GRIVGVEPFA HDPAPSEL  39
EcBisC:                                                        ME  99
```

Fig 1.29 Sequence alignment showing the three types of amino-terminal Cys regions present in this family of bacterial molybdoenzymes. The enzymes are *Synechococcus* **NarB**, *Klebsiella pneumoniae* **NasA**, *E. coli* **FdhF**, *Methanobacterium formicicum* **FdhA**, *Wolinella succinogenes* **FdhA**, *E. coli* **FdnG**, *E. coli* **FdoG**, *Alcaligenes eutrophus* **NapA**, *E. coli* **DmsA**, *E. coli* **NarG**, *E. coli* **NarZ**, *T. pantrotropha* **NapA**, *W. succinogenes* **PsrA**, *E. coli* **TorA**, *Rhodobacter sphaeroides* **BisC**, and *E. coli* **BisC.** **[16]**

Site-directed mutagenesis was used to investigate the roles of some of these residues. Cys34 was mutated to His and there was no effect on the properties of the enzyme. Mutagenesis of Arg90 to Ser did not alter any measurable activity of DMSO reductase [59]. Additional conserved residues including Gly78 and Pro94 were not mutated due to their potentially important structural roles [59]. Lys28, Cys38, Cys42, Cys75 and Arg77 in DMSO reductase were examined by site-directed mutagenesis. When Lys28 was mutated to the neutral amino acids Ser or Ala, there was no alteration in enzyme activity. Mutation of Cys38 to Ser resulted in a stable but inactive enzyme as did mutation of Cys42 to Ser. Mutation of Cys75 to Ser yielded a functional enzyme. Arg77-Ser yielded a mutant with impaired growth and activity in a physiologically

relevant activity assay [16] [59]. When the conserved sequence was mutated so that it was unlikely to coordinate an FeS cluster, the EPR spectra did not differ from that of the wild type enzyme suggesting that all the EPR visible clusters in the wild type are contained within the DmsB subunit [16]. It also appeared that when Cys38 was mutated to Ser or Ala, the resulting enzyme assembled a novel 3Fe-4S cluster by EPR spectroscopy. When this mutant was used to make a double mutant changing residue N37C to create a cysteine spacing resembling that of a Type I enzyme, a 3Fe-4S cluster was assembled by EPR analysis [16]. It could be that the lack of activity in these mutant enzymes is a result of the 3Fe-4S cluster having unfavourable midpoint potentials and therefore acting as an "insulating" cluster. This cluster would prevent electron transfer to the molybdenum active site [16]. The magnetic interaction between the Em,7 = -120mV cluster of the DmsB subunit and the molybdenum center of DmsA is seriously altered in these mutants [67].

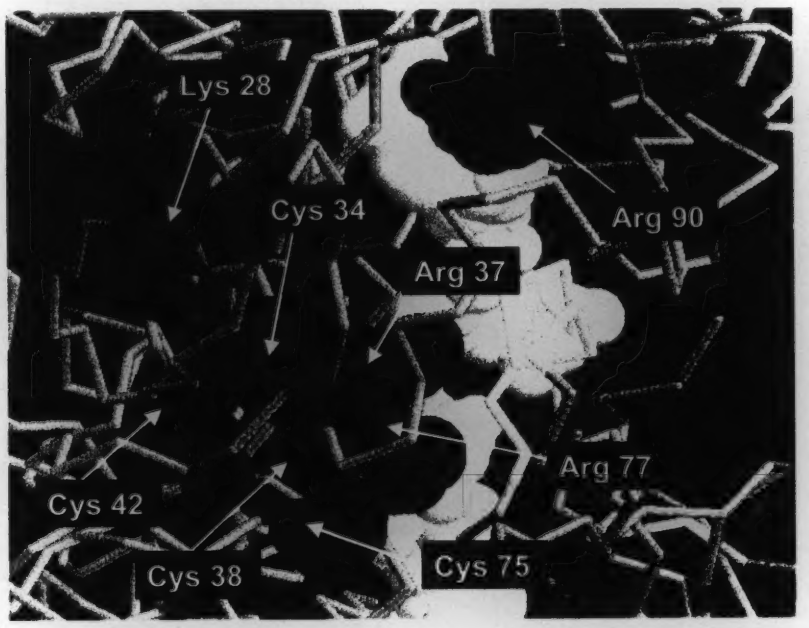

Fig 1.30 Some noteworthy amino acid residues which have an effect on the enzyme when mutated. Ras mol depiction of Dms A homolog FdhA. The residues are labeled as though the enzyme was DmsA from *E. coli*.

In any case, analysis of redox centers by EPR is a complicated ordeal and results from these experiments must be looked at in the context of all of the relevant data contributing to the characterization of an enzyme.

Thus far, site directed mutagenesis studies suggest that in *E. coli* DmsA, the residual FeS cluster binding region does not coordinate a 4Fe-4S cluster but is important in electron transfer between the DmsB subunit and molybdenum cofactor. This makes sense as its position in homologous proteins whose structures have been solved places the sequence between the Em,7 = -120mV cluster of DmsB and in close contact with the Mo-bisMGD cofactor. Perhaps the conserved cysteine residues act directly in this process or perhaps they are used to coordinate some small redox factor such as an iron ion that could be used in the electron transfer pathway. It should also be noted that the recently solved X-ray crystal structure of NarGHI revealed that the catalytic subunit of this enzyme does coordinate a 4Fe-4S cluster by its n-terminal cysteine motif contrary to what was originally thought about type II enzymes. This has led to confusion regarding the understanding of the DmsA subunit.

1.4 Experimental Objectives

The following describes two different experiments done to further our understanding of some of the structural features of the DmsA subunit of DMSO reductase as well as discovering information about the electron pathway through the enzyme. A mutant, C75S, was observed to disrupt the assembly of the enzyme when expressed under conditions that eliminate the assembly of molybdenum cofactor. The wild-type enzyme undergoes normal folding and targeting to the membrane even without cofactor. The following chapter describes the characterization of this mutant and shows that this cysteine is important for the structural integrity of the enzyme and must be closely associated with the molybdenum cofactor. Further investigation of the N-terminal conserved cysteine motif was also attempted. Previous experiments had made alterations in this region to make it more like a type I enzyme and therefore

more likely to bind an iron sulfur cluster. In my experiments more alterations in this region were made by site directed mutagenesis. Five mutants were characterized using a variety of spectroscopic methods and activity assays. Conclusions from these experiments show that altering the sequence has the effect of eliminating the assembly of molybdenum cofactor into the enzyme in all mutants except for a simple R77K mutant.

2.0 MATERIALS AND METHODS

2.1 Cell Strains and Plasmids

Four different strains of *E.coli* were used. **TG-1** is wild-type *E. coli,* grows rapidly and is more "durable" than other lab strains. This strain was used for routine DNA manipulation because of the ease by which it is transformed by electroporation and its speed of growth. **HB101** requires the amino acids proline and leucine be added to the growth media because of other mutations inhibiting synthesis of these amino acids. It is a slow growing strain and requires 48 hours to achieve maximum cell density and protein expression. This strain has been traditionally used in studies of inner membrane proteins. EPR spectra of the inner membranes of this strain have been well characterized and the low levels of fumarate reductase make it possible to analyze DMSO reductase and its mutants by EPR. **DSS301** is similar to TG-1 with a kanamycin resistance cassette inserted into the *dmsABC* operon knocking it out. It is a good strain for studying the effects of mutations of various *dmsABC* mutants expressed from vectors as results are not complicated by expression of the chromosomal copy. **RK5209** is unable to transport molybdenum from the growth media. This results in a deficiency in molybdopterin cofactor and this strain was used in studies designed to observe the effect of the lack of Mo-bisMGD on various DMSO reductase mutants. Preliminary growth studies of the strain showed that this impaired cofactor assembly could be overcome by including excess molybdenum in the growth media. Expression vectors based on the vector pBR322 were used to express dmsABC or mutants of this enzyme in the above cell strains. These plasmids were transformed into cells by electroporation. The plasmid pDMS160 encodes the wild-type enzyme and was constituted by cloning a HindIII-SalI fragment into HindIII-SalI cut pBR322.

E. Coli Strain	Genotype
DSS301	➢ As TG1; Km^r ΔdmsABC
HB101	➢ F$^-$ hsdR hsdM pro leu
RK5209	➢ F- araD139 ΔlacU169 gyrA thi rpsL mod::Mucts
TG-1	➢ Δ(lac-pro) supE thi hsdD5| F' traD36 proA$^+$B$^+$ laclq lacZΔM15

Table 2.1 Table of strains used in these experiments and the genotypes of these strains [6] [16]

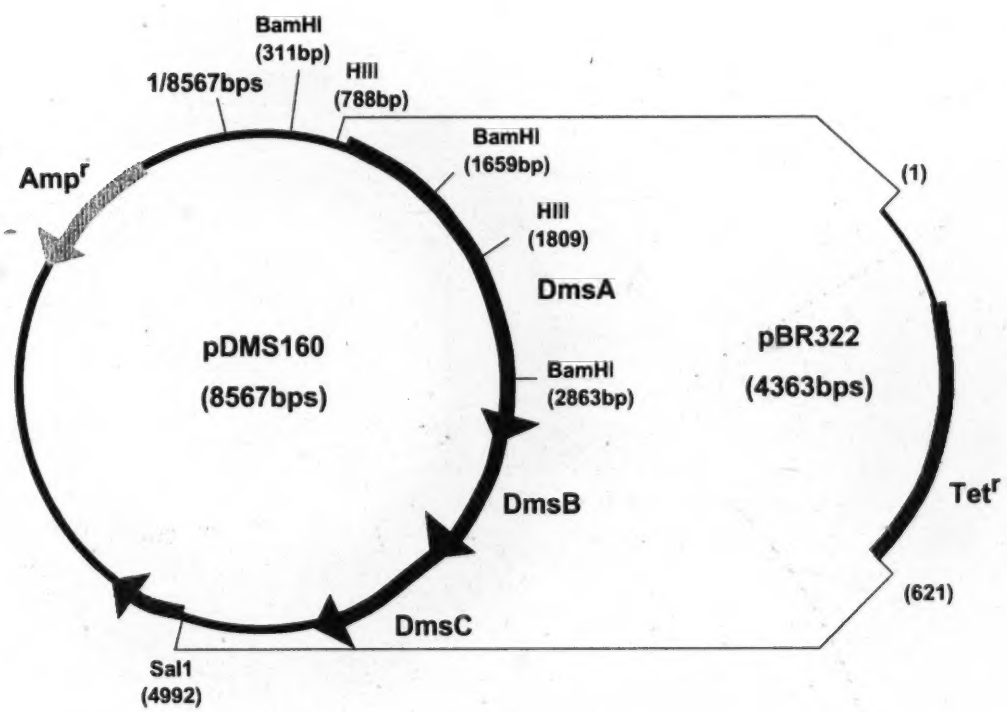

Fig 2.1 Expression vectors pBR322 and italics. pBR322 was obtained from Pharmacia Biotech and is a 4363bp plasmid containing *amp^r* and *tet^r* resistance markers. To obtain pDMS160, pBR322 was cut with HindIII and Sal1 removing a 621 bp fragment from this vector and disrupting the *tet* resistance gene. The HIII, SalI fragment from the *dmsABC* operon was ligated back into the vector creating the 8567bp pDMS160 *(Created from Sequence using Mac Vector 5.0).*

Plasmid	Description
ptz121	1,ooo bp vector wi HindIII site, used in PCR reactions
pBR322	As shown in *fig 2.2*
pDMS160	Contains the *dmsABC* operon cloned into pBR322 as shown in fig 2.2
pDMS160A	pDMS160 with mutations in *dmsA*; V36Y, N37C. *del*C38, S40V, R41G, P43G
pDMS160B	pDMS160 with mutations in *dmsA*; V36Y, *del*N37
pDMS160C	pDMS160 with a mutation in *dmsA*; R77K
pDMS160D	pDMS160 with mutations in *dmsA*; V36Y, N37C. *del*C38, S40V, R41G, P43G, R77K
pDMS160E	pDMS160 with mutations in *dmsA*; V36Y, *del*N37, R77K
pDMS160F	pDMS160 with a *dmsAC75S* mutation

Table 2.2 Table of plasmids used and descriptions of the differences between them. pBR322 was obtained from Pharmacia Biotech and wild-type or mutant DMSO reductase enzymes are expressed from variations of pDMS160.

2.2 Synthesis of Oligonucleotides and DNA Sequencing

The mutant enzymes were expressed from plasmid pDMS160 containing mutations in the *dmsA* gene and are shown in *table 2.2*. Synthesis of oligonucleotides and DNA sequencing was carried out in the Department of Biochemistry DNA core facility at the University of Alberta using an Applied Biosystems model 392 DNA synthesizer and a model 373A DNA sequencer (Perkin Elmer).

Restriction endonucleases and DNA modifying enzymes were obtained from Life Technologies Inc. All other materials were of reagent grade and were obtained from commercial sources.

2.3 *Mutagenic Primers*

Mutant A (pDMS160A): was generated through PCR mutagenesis using the following mutagenic primers: 5′ CTG GAG CGC CTG TAC ATA TTG TGG TGT TGG CTG

CGG GCT ACG TAT GCA CGT CG 3′ and 5′ CGA CGT GCA TAC GTA GCC CGC AGC CAA CAC CAC AAT ATG TAC AGG CGC TCC AG 3′ Length 53 nucleotide basepairs; T_m 76.1°C, 58.5% GC. ***Mutant B (pDMS160B)***: was generated through PCR mutagenesis using the following mutagenic primers: 5′ CTG GAG CGC CTG TAC ATA TTG TGG TAG TCG CTG CCC GCT ACG TAT GCA CGT CG 3′ and 5′ CGA CGT GCA TAC GTA GCG GGC AGC GAC TAC CAC AAT ATG TAC AGG CGC TCC AG 3′ length 53 nucleotide base pairs; T_m: 76.1°C ***Mutant C (pDMS160C)***: was generated through PCR mutagenesis using the following mutagenic primers: 5′ GGC CTG CAC CAG GTT CGC GCC TGT CTG AAA GGT CGT TCC ATG CGT CGC CGT GTC TAC AAT CCG GAC CGC C 3′ and 5′ GGC GGT CCG GAT TGT AGA CAC GGC GAC GCA TGG AAC GAC CTT TCA GAC AGG CGC GAA CCT GGT GCA GGC C ′3 length 70 nucleotide base pairs; T_m 82°C.

2.4 Creation of DmsA N-Terminal Cysteine Motif Mutants

The vector pDMS160, was digested with HindIII restriction enzyme to obtain a small fragment of *dmsA* sequence containing the DNA region of interest for mutagenesis in this experiment. This HindIII fragment was purified by running the digest on a 10% agarose gel. The band corresponding to the ≈ 1000 bp fragment was cut out and the DNA purified from the gel. The fragment was ligated into a HindIII digested pTZ vector and this reaction product was transformed into TG-1 cells. To minimize the amount of vector that ligated without the insert, the vector was first treated with alkaline phosphatase which was removed (after incubation for 1 hour at 30°C) by heat killing the enzyme (10 minutes at 60°C) followed by a phenol extraction. Cells were plated on LB + amp plates and incubated at 37°C. Colonies were picked and cultures grown for DNA isolation using a Qiagen DNA miniprep kit. A sample was digested with HindIII to confirm that the *dmsA* fragment was successfully ligated into pTZ. The entire vector was used as a template for the polymerase chain reaction (PCR) using mutagenic primers previously described. The PCR product was transformed directly into TG-1 cells and plated onto LB + amp plates. DNA from several colonies

was isolated and this DNA was sequenced by the University of Alberta's Department of Biochemistry DNA Core Facility. Correctly mutagenized DNA was then cut with HindIII and the insert purified by running the DNA on an agarose gel. The fragment was recovered from the gel and ligated back into HindIII digested alkaline phosphotase treated pDMS160. This DNA was grown in TG-1 cells and isolated. The plasmids were checked to select for ligation products which contained the mutagenized HindIII fragments ligated in the proper orientation. This was done by restriction analysis using BamHI and HindIII as the orientation of the HindIII fragment in pDMS160 gives distinctive restriction digest products using these enzymes (*fig 2.1*). Mutagenized pDMS160 vectors were grown in TG-1 cells, and the DNA was isolated by maxiprep and stored at -20°C. Mutants containing the mutations introduced by primers A or B in combination with the mutation introduced by primer C were created by using the ptz PCR product containing the primer C mutation in a second round of PCR using either primer A or primer B. These "double mutants" were named D (pDMS160D) and E (pDMS160E) giving a total of five mutants A-E.

2.5 Growth Curve Analysis of E. coli Cells Expressing DMSO Reductase

Initial characterization of DMSO reductase was done by analyzing the growth of DSS301 or HB101 cells transformed with an expression vector encoding either wild-type or a mutant enzyme. Transformation of plasmids into cells was done by electroporation of competent cells (*App. F*).

A small overnight culture of the transformed cells (1.5mls) was grown in LB broth with appropriate antibiotics for cell/plasmid selection, and used to innoculate 160ml Klett flasks (glass flask with a side arm for ease of measuring cell density) containing either glycerol-DMSO or glycerol-fumarate minimal media (*App. H*) and a small stir bar. Lids were wrapped with parafilm to ensure anaerobic environments. In the case of experiments outlined in chapter 3, the media also contained either 15uM Mo or

100uM W. The flasks were then placed in a 37° water bath/magnetic stir plate and grown for 48hrs. with stirring. OD (optical density) readings were taken intermittently using a Klett reader. The Klett flasks were thoroughly mixed with gentle shaking before each reading was taken. Growth curves were then plotted as Klett units (increased Klett units is increased optical density due to cell growth) vs. time (hours since the experiment was initialized).

The growth curves of each of the mutants was then compared with each other as well as with positive and negative controls. That is, cells transformed with pDMS160 (wild type DmsABC) or pBR322 (empty vector).

2.6 DmsABC and Mutant Expression and Preparation

Large 19l carboys of cells expressing the DmsABC variants were grown as a source of protein for mutant characterization experiments (App H). DMSO stocks of HB101 cells or DSS301 cells transformed with the *dmsABC* expression vectors were used to inoculate 250 ml of rich growth media (TB) containing phosphate salts and the appropriate antibiotics (*App. H*). These cells were grown overnight and used to inoculate 19l carboys containing glycerol-fumarate minimal media. In the case of experiments in chapter 3, the media also contained either 15uM Mo or 100uM W. The carboys also contained appropriate antibiotics for cell and plasmid selection and were grown anaerobically at 37°C for 24hrs (for DSS301) or for 48 hrs (for HB101) with constant stirring.

Cells were concentrated by use of a Millipore Pelicon system. This apparatus passes growth media over a cell impermeable membrane and in this way cells are continually concentrated as growth media is filtered off. When the 19l had been concentrated to a reasonable volume, the cells were pelleted in 1L centrifuge tubes by low speed centrifugation (6K for 15 minutes). Pelleted cells were weighed, resuspended in buffer and respun in 250ml centrifuge tubes (8K for 15 minutes) to get rid of

remaining growth media. Cells were then flash frozen in liquid nitrogen and stored overnight in a -70°C freezer.

Cell pellets were resuspended in buffer (approx. 50mls/30g cells) and 0.2mM PMSF, phenyl methyl sulfonyl fluoride, (a protease inhibitor) was added. The cell solution was kept on ice at all times and centrifugation was done at 4°C to prevent protein degradation. Cells were lysed by the French pressure method (*App. I*).

The cell solution was then subjected to low speed centrifugation to pellet unlysed cells as well as any cell debris (8K for 15 minutes). The supernatant was poured into 25ml ultracentrifuge tubes and subjected to a high speed spin to separate membrane and soluble protein fractions (40K for 1.5hrs). The supernatant, containing soluble proteins was poured off and stored on ice. The pellet containing the membrane fractions from cells was scraped out of the tubes and resuspended in buffer using a Teflon homogenizer. Membrane colour was noted as dark brown membranes are indicative of highly expressed DmsABC enzyme while light brown membranes mean expression was poor. Some of this solution was stored on ice as a crude membrane preparation. The remainder was exposed to a further round of centrifugation to isolate the membrane fraction enriched in inner membrane (*App. I*). Soluble, crude, and enriched membrane fractions were then flash frozen using liquid nitrogen and stored in the -70°C freezer.

2.7 Protein Quantification

Protein quantification was done using the Lowry method. (In this analysis the protein preparation reacts with the Lowry solutions.) The amount of protein can then be quantified spectrophotometrically using a BSA protein standard to translate absorbance of the protein solution into protein concentration (*App. J*).

Commassie blue stained polyacrylamide gels of different cell fractions also give an indication of the levels and location of expressed protein relative to other cellular proteins. Soluble, crude, or enriched membrane fractions are mixed into SDS page loading buffer and loaded onto a 10-12% SDS page gel (*App. G*). Electrophoresis is used to separate proteins by molecular weight. Once separated on the gel, it is stained using Comassie blue and destained leaving only protein bands a blue colour. The different bands can be compared with each other and with a DMSO reductase standard also run on the gel to get an idea of where and how much of the enzyme was expressed.

Immunoblot analysis can also be done where proteins separated by electrophoresis on an SDS page gel are transferred to nitrocellulose paper and incubated with a primary antibodies against the DmsA or DmsB subunits (*App. G*). The paper is then incubated with a secondary antibody which binds the primary antibody and has luminescent properties which can be captured on photographic paper. Exposed photographic paper can then be analyzed for a more detailed understanding of DmsABC expression in various cell fractions.

2.8 DMSO Reductase Activity Assays

There are two kinds of activity assays which were used to analyze the DMSO reductase activity in cellular membranes. The first was the benzyl viologen TMAO/DMSO activity assay (*App. A*). Here dithionite was used as a reducing agent. In a cuvette with enzyme and substrate in TMAO buffer (either DMSO or TMAO), this molecule will reduce benzyl viologen which will in turn reduce the enyme and substrate molecule. Benzyl viologen acts as a redox indicator. The molecule is purple when reduced (before substrate reduction) and colourless when oxidized (after substrate reduction). In this way the reduction of substrate can be quantified spectrophotometrically as the rate of decrease in absorbance of benzyl viologen which can be recorded and the slope converted into a numerical value for enzyme activity. There is some confusion as to where benzyl viologen reduces the enzyme. It is a fairly

powerful reducing agent and has been shown to donate electrons directly to the DmsA subunit of DMSO reductase [59]. In the lapachol activity assay on the other hand, electrons are donated to DMSO reductase in a more physiologically relevant way (*App. E*). In a lapachol assay, instead of using dithionite to reduce the membrane solution, a quinol-like molecule with reducing properties "lapachol" is used. It donates electrons directly and soley to the quinol binding site of DmsC. Electrons must pass through the enzyme, passing through the FeS clusters of DmsB and through to DmsA.

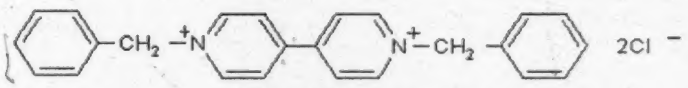

Benzyl Viologen

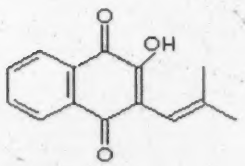

Lapachol

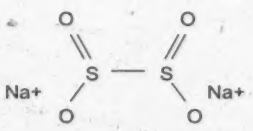

Dithionite

Fig 2.2 The molecular structures of some of the important chemicals used in the activity assays (Sigma website).

2.9 Spectroscopic Analysis of the Quinol Binding Site of DMSO Reductase by Fluorescence Quench Titrations

HOQNO is a structural analog of MQH_2 and it is known to be a classical inhibitor of the mitochondrial cytochrome c reductase [54]. This molecule was shown to bind the DmsC quinol binding site of DMSO reductase and experiments using this molecule established the fact that there is only one quinol binding site in this subunit. The spectroscopic properties of HOQNO have provided a convenient means for studying the binding site as it is quenched when bound to DmsC and fluoresces in solution. This feature is useful for not only studying characteristics of the quinol binding site but also for quantifying levels of DmsC in the membrane. HOQNO titrations were

done on the membrane fractions of cells expressing DMSO reductase (*App. D*). The concentration of HOQNO added at the point where any further addition of HOQNO causes the solution to fluoresce is the concentration which saturates all of the DmsC quinol binding sites and is therefore also equal to the concentration of this enzyme. This concept was applied to complement expression analysis of DmsABC mutants by western blot analysis.

2.10 Spectroscopic Characterization of the Molybdenum Cofactor

All molybdenum containing enzymes examined to date, with the exception of nitrogenase, bind the metal in a complex with a molybdopterin. In vitro, the cofactor can be converted by oxidation into two stable, fluorescent species which have been characterized in detail. For preparation of the fluorescent Form A pterin derivative, samples of enriched HB101 membranes containing DmsABC enzyme were acidified and boiled with iodine [7]. This form of the pterin has characteristic excitation and emission spectra which can be observed spectroscopically and used to quantify the amount of cofactor in a sample (*App. C*).

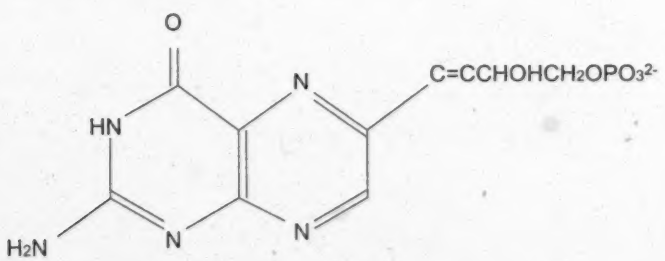

Fig 2.3 Chemical structure of the Form A derivative of the molybdopterin cofactor [7].

2.11 EPR Analysis of DMSO Reductase and the N-terminal Cysteine Cluster Mutants

2.11.1 Introduction; EPR Analysis of Redox Proteins

Electron Paramagnetic resonance (EPR), also known as electron spin resonance (ESR) and electron magnetic resonance (EMR), is the name given to the process of resonant absorption of microwave radiation by paramagnetic ions or molecules, with at least one unpaired electron spin, and in the presence of a static magnetic field. EPR was discovered in 1944 and has been successfully used to analyze the metal centers of a variety of redox proteins. The analysis of proteins by EPR is difficult and the EPR spectra are very complicated. Ultimately, spectra for different proteins can be thought of as a unique fingerprint and changes that occur in this spectra as a function of temperature or redox potential, for example, are also unique for different proteins. The effect of a mutation on the redox center of a protein can be analyzed by comparing the spectra with that of the wild-type protein. If a particular mutation eliminates an iron sulfur cluster from the protein, then the EPR spectra or fingerprint will be altered. In the simplest senario the characteristic spectra for that type of iron sulfur cluster will not be observed. In more complicated situations not only will the spectra for this cluster disappear but also the spectra of any other redox centers of the proteins which are electrically or magnetically linked to this cluster in the wildtype protein will be altered (Rothery RA, personal communication).

2.11.2 Solving the EPR Spectra of DMSO Reductase

The EPR spectra of DMSO Reductase was first obtained and analyzed in 1989 [68]. The following describes the experimental conditions and interpretation of the data from this original paper to provide a context for understanding how the mutants presented herein were analyzed by EPR.

EPR Signals from Iron-Sulfur Clusters in the Membrane-Bound State Enriched membranes of HB101 cells expressing DMSO reductase were used in EPR studies. The only other iron-sufur protein known to be present in the membranes is fumarate reductase, traces of which are shown as a signal with an upward feature at g=2.03, crossing the base line at g=2.01 [69]. This signal, observed in the oxidized state at temperatures below 30K, is characteristic of a 3Fe-4S cluster and can be observed in *(fig 2.4A)* Also visible in *(fig 2.4A)* is a minor signal due to molybdenum, which is saturated with microwave power under the conditions of measurement. The iron-sulfur clusters in the membranes were reduced by dithionite. The EPR spectrum of the reduced membranes, measured at temperatures above 40K, showed a minor signal at g=1.94, which was attributed to fumarate reductase. At temps below 40K a broad and complex feature around g=1.94 was observed. In the membranes from *E. coli* strain HB101/pDMS160, this spectrum was much more intense than that of fumarate reductase and therefore must be attributed to DMSO reductase. All of the spectra of the iron-sulfur clusters in DMSO reductase were most clearly resolved at temperatures around 12K and completely broadened out at 40K. This temperature dependence is characteristic of reduced 4Fe-4S clusters (*fig 2.4B*) [3]. Addition of the DMSO reductase substrates DMSO (*fig 2.4C*) or TMAO (*fig 2.4D*) to the dithionite reduced membranes caused the signal to disappear to the signal of the oxidized membranes further suggesting that the signal in 2.4B must be from the reduced DMSO reductase [3]. Only a small rhombic EPR signal from one reduced iron-sulfur cluster remained in both 2.4C and D. This result suggests that all of the other FeS clusters of the protein must have lower midpoint potentials than either of these two substrate molecules 160mV/130mV DMSO/TMAO respectively) [3].

Redox Potentials of the Iron Sulfur Centers In a titration of the purified protein at controlled redox potentials, at pH 7, reduction of the iron-sulfur clusters could be observed by EPR spectroscopy. Several types of iron-sulfur signals could be resolved as the enzyme was progressively reduced. First, a rhombic EPR signal was observed, at g=2.01, 1.93 and 1.866. A rhombic signal is a peak trough that dips below the sinal

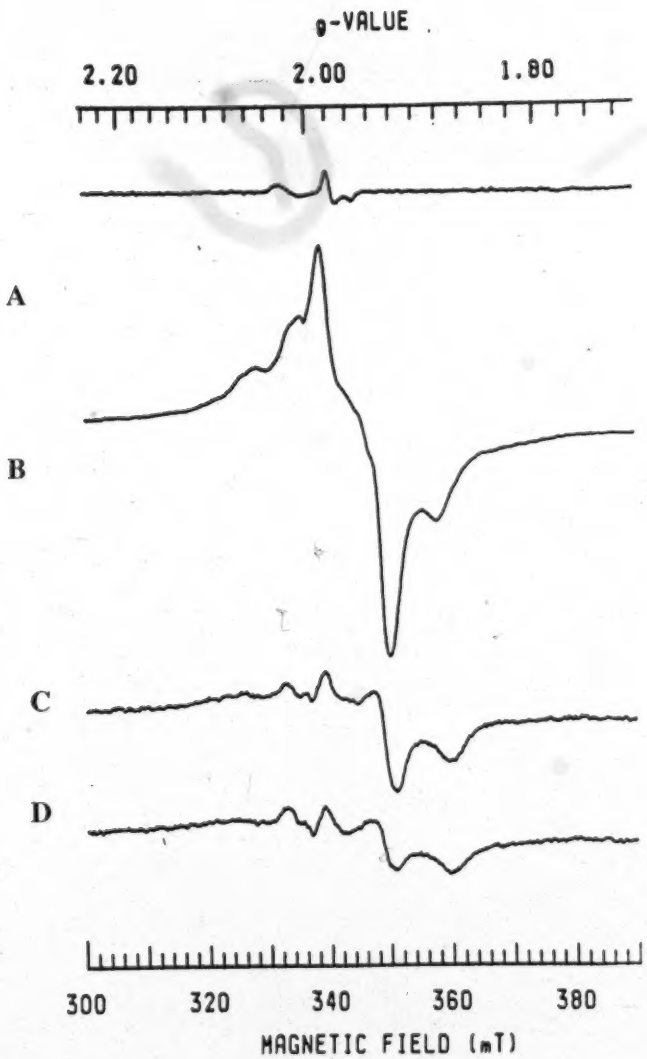

Figure 2.4 Spectra of pDMS159 membranes, measured at 12 K, showing the signals of reduced iron-sulfur clusters. Conditions of measurement were the following: microwave power, 20 mW; frequency, 9.42 GHz; modulation amplitude, 1 mT; modulation frequency, 100 KHz receiver gain, 10^5. **A** Oxidized innermembrane preparation **B** Treated with 2.5 mM dithionite **C** Treated with 2.5 mM dithionite plus 25mM TMAO; **D** Treated with 2.5 mM dithionite plus 25 mM DMSO. Samples were treated for 1 minute at 20°C prior to freezing [3].

baseline before returning to the baseline. This is similar to the spectrum of the DMSO-reoxidized sample of DMSO reductase (compare *fig 2.5A* with *2.4D*). This signal is assigned to the cluster with the most positive midpoint potential. A more complex signal appeared with a feature around g=2, indicating the reduction of another

cluster. At this point the amplitude of the extreme high-field feature of cluster 1 at g=1.866 decreased (fig 2.5B). This behaviour is similar to that observed in the

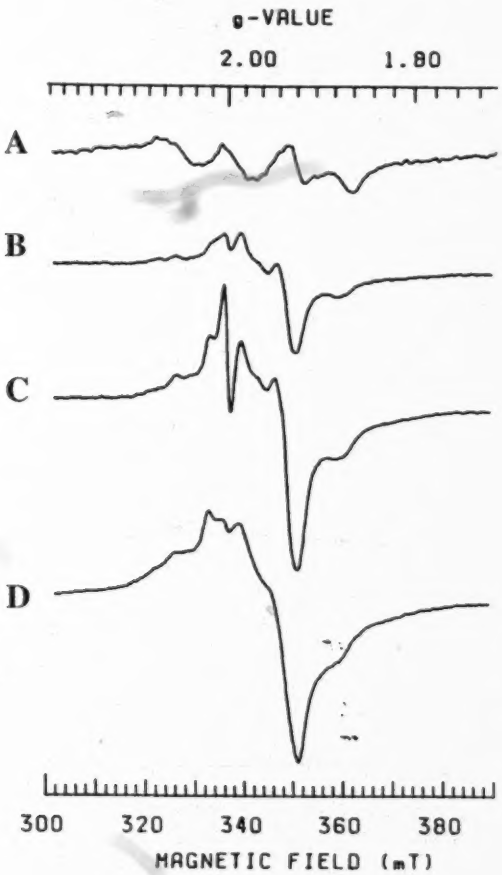

Fig 2.5 EPR spectra from membranes of E. coli F-36, showing the signals due to iron-sulfur clusters. The samples were poised at **A** –51, **B** -157, and **C** -359mV; **D** is a sample without mediators, reduced with dithionite. Spectra were recorded at 12K with a microwave power of 20mW, a frequency of 9.2 Ghz, and a modulation amplitude of 0.2 mT [3].

2[4Fe-4S] ferredoxins and arises because of the spin-spin interactions between two iron-sulfur clusters in the protein. The spectrum of the interacting pair of clusters is different from some of the features of the spectra of the individual clusters [3]. During the final reduction, (-200 to –400mV), the spectrum continued to increase; further spectra appeared around g=1.94, with additional features to low field at g=2.06 and in

the center of the spectrum at g=2.02 and g=1.98 (*Fig 2.5D*). At the lowest potentials, broad outer lines appeared. The broadness is likely due to spin-spin interactions between adjacent iron-sulfur clusters. An indication of the increase in iron-sulfur cluster signal intensity on reduction is provided by the amplitude of the g=1.94 signal [3]. The derivative amplitude of the g=1.94 signal can be plotted as a function of applied redox potential (*Fig 2.6A*) to give a graph whose points of inflection are representative of the midpoint potential of the Fe-S clusters of the protein (*Fig 2.6B*). The graph could best be fitted by a line containing 4 inflection points representative of the enzyme containing 4 4Fe-4S clusters. Different protein preparations showed slightly different midpoint potentials. The differences could have been due to the conversion of a 4Fe-4S cluster to a 3Fe-4S cluster during the purification of the enzyme for example. Midpoint potentials were also pH dependant. When the membranes were extracted with TritonX-100, the EPR signals of the soluble extracts were similar to those of the membrane-bound DMSO reductase [3]. Solubilization did not appear to affect the spectroscopic properties of the iron-sulfur clusters in the protein significantly. The same was found to be true of the EPR signals due to molybdenum. In the membranes isolated from the DMSO reductase enriched cells, an EPR signal was observed with rhombic symmetry at g=1.987, 1.976 and 1.960, at temperatures higher than those required for the iron-sulfur cluster signals (120K). (*fig 2.7*) This is due to Mo(V) in *E. coli* nitrate reductase and it was observed at a range of pHs (5.0-9.0). The signal was stable in oxidized membranes and two midpoint potentials were observed which corresponded to the Mo(VI/V) and Mo(V/IV) redox transitions. (*fig 2.6B*). Microwave power saturation curves of the molybdenum EPR spectrum at 30K show that the power for half-saturation of the normal Mo(V) signal, in a sample where the iron-sulfur clusters were mostly oxidized, was less than 1mW [3].

A

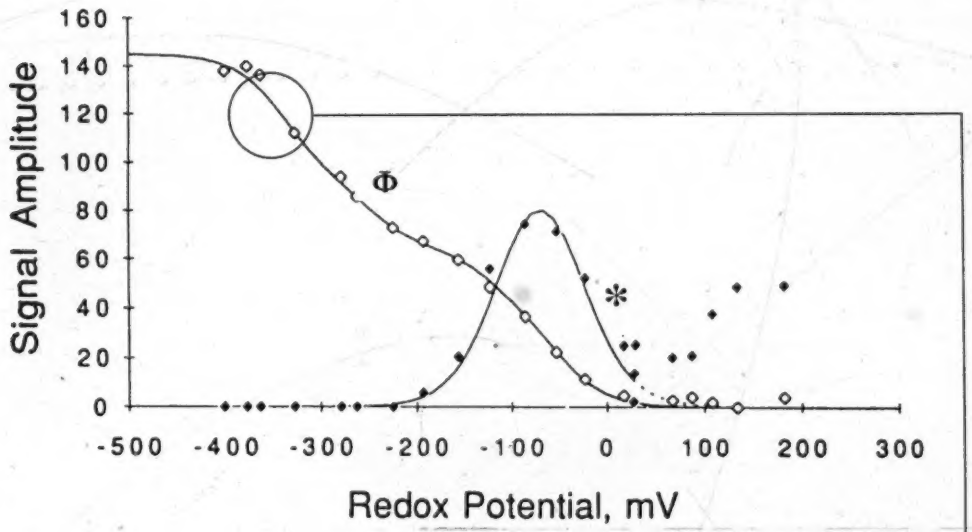

B

		Mo			Fe-S			
Preparation	**pH**	**VI/V**	**V/IV**	**mid**	**1**	**2**	**3**	**4**
pDMS159 membranes	7.0	-75	-90	-83	-50	-120	-240	-330
pDMS159 membranes	9.0	--125	-120	-123	-90	-250	-330	-400
Triton X-100 extract	7.0	15	-100	-43	-25	-130	-250	-340
Triton X-100 extract	5.5	65	35	50	20	-60	-170	-265
F-36 membranes	6.8				-60	-130	-240	-340
Purified "sephacryl"	7.0	45	-150	-53	-50	-120	-230	-330
DmsA	7.0	50	-100	-25				

Fig 2.6 **A** Redox titration curves showing the changes in the amplitude of the g=1.94 signal due to iron-sulfur clusters, recorded at 12 K Φ and the g= 1.98 signal due to molybdenum , recorded at 120 K. * **B** Table listing the midpoint potentials derived from the inflection points of the redox titration curves.

In a sample where a substantial amount of the Fe-S clusters was reduced, a significant proportion of the Mo(V) signal was very rapidly relaxing at this temperature (*fig 2.8*). The pronounced effect the redox state of the Fe-S clusters has on the relaxation times for molybdenum suggests that they are in very close proximity even though they are

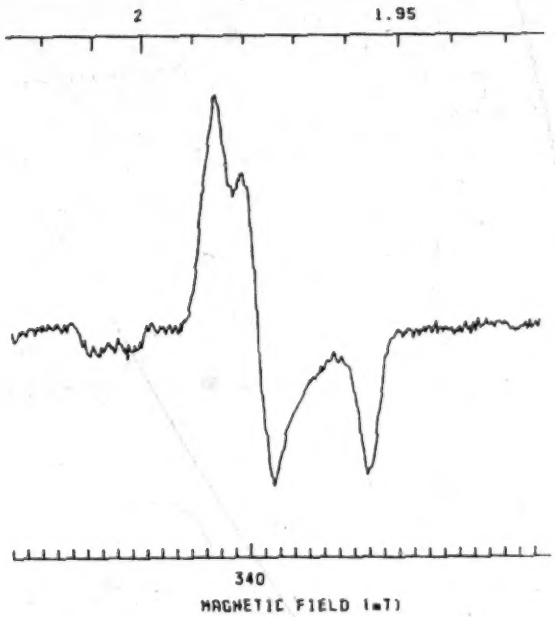

Fig 2.7 EPR spectrum of molybdenum in purified DMSO reductase "Sephacryl form", poised at a potential of –51mV. The spectrum was recorded at 120K, with a microwave power of 20mW, a frequency of 9.42 Ghz, and a modulation amplitude of 0.2mT.

on different enzyme subunits [3]. To summarize the findings of EPR analysis on DMSO reductase; Based on the initial sequence analysis of the inferred DNA sequence of DMSO reductase, it was suggested that the enzyme contained two ferredoxin like 4Fe-4S clusters. EPR data show this to be the case in the redox titration experiments. The midpoint potentials of these clusters at pH 7.0 are –50, -120, -240 and –330 mVs [3]. The midpoint potentials of the molybdenum (VI)/(V) and (V)/(IV) transitions were estimated to be between +220 and +180mV [3]. The observed spin-spin interactions between molybdenum and at least one of the iron-sufur clusters show that the redox centers are in proximity and are likely separated by a distance of approximately 8Å [3].

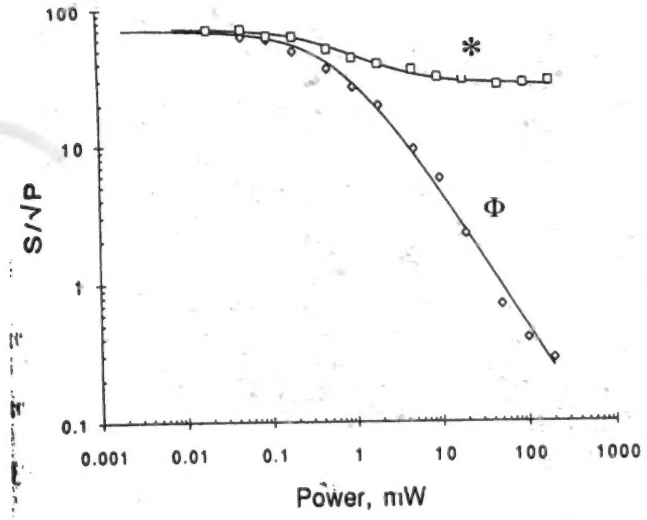

Fig 2.8 Power saturation curves of Mo(V) signals, measured at 3K. Sample poised at –20 (Φ) and –155 mV [3].

2.11.3 EPR Analysis of Mutant Enzymes

Redox poised titrations of enriched membranes containing mutant enzymes expressed in HB101 were performed as with the wild type enzyme just described. Redox titration curves showing the changes in the amplitude of the g=1.94 signal due to iron-sulfur clusters, recorded at 12 K were obtained. The oxidized and reduced spectra were compared with membranes containing wild type DMSO reductase or negative control membranes to see whether or not the N-terminal cysteine cluster mutants were altered in their ability to coordinate FeS clusters by this sequence.

3.0 CHARACTERIZATION OF A DmsA^{C75S}BC MUTANT

3.1 Introduction

Site-directed mutagenesis based on sequence alignment and identification of conserved residues in homologous proteins is an effective way of elucidating structural and functional features of an enzyme without having any structural data for the protein. A highly conserved cysteine residue (C75), found in a conserved region of the N-terminus of DmsA was mutated to a serine and the resulting enzyme was characterized by a number of methods. This conserved region closely resembles a ferredoxin FeS cluster-binding motif and several lines of evidence have suggested that this sequence plays an important role in the transfer of electrons from the DmsB subunit to the Mo-bisMGD catalytic active site in DmsA, in addition to potentially being important to the structural integrity of the subunit [16] [59].

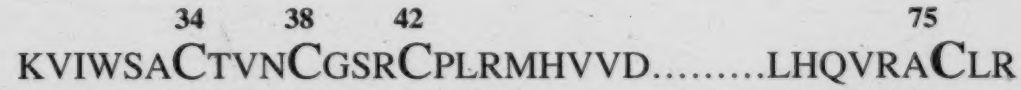

Fig 3.1 The N-terminal region of DmsA. This region is very similar to a ferredoxin 4Fe-4S cluster binding motif and has four highly conserved cysteine residues one of which has been mutated to a serine in this experiment (C75S).

The C75S mutant was characterized using spectroscopic methods after being expressed in different cell types and under different growth conditions. Experiments which eliminated the availability of molybdenum cofactor from the cell and the effect that this had on the mutant enzyme was analyzed. Molybdenum cofactor was eliminated from the cells in two different ways. In the first method, the enzyme was expressed in either HB101 or DSS301 cells and grown in media containing no molybdenum and excess tungstate. This blocks cofactor assembly into the DMSO

reductase enzyme [70]. .The second was by expressing the C75S mutant in a strain of *E. coli* defective in molybdenum uptake, eliminating the need for tungstate in the growth medium yet still blocking cofactor assembly [6]. The following results suggest an important role for this cysteine residue in the structural integrity of the enzyme. In addition, it is likely involved in binding an iron sulfur cluster as substitution of this residue with a closely related one (serine), disrupts enzyme stability when the cofactor is not present.

3.2 *Results and Discussion*

DmsA^{C75S}BC supports the growth of DSS301 cells on GD minimal media when molybdenum cofactor is present in the growth media

Growth experiments were carried out in order to observe the in vivo activity of the mutant enzyme. pDMS160 containing the gene encoding wild-type DMSO reductase, a pDMS160 derivative containing the DmsA Cys75Ser mutant and pBR322, a negative control expression vector were transformed into DSS301 cells and grown anaerobically in klett flasks containing either glycerol-fumarate (GF) minimal media or glycerol-DMSO (GD) minimal media. Growth on GF does not require a functional DMSO reductase enzyme but still allows this enzyme to be expressed under the control of its natural promoter. This experiment was done to observe cell growth when the enzyme is overexpressed in these cells and to make sure the glycerol-fumatate respiratory chain is functional under these conditions as this is the method used for large scale protein preparations for use in enzyme assays to follow. Growth of DSS301 cells on glycerol-DMSO media requires the expression of a functional DMSO reductase enzyme in order to complete the respiratory chain and is done as a preliminary experiment testing the stability and function of the enzyme in the innermembrane. Experiments were also carried out with either 15μM Mo or 100μM W in the growth media. Excess W prevents the assembly of the molybdopterin cofactor and allows the stability of the enzyme without this cofactor to be analyzed.

In ***fig. 3.2*** there appears to be no significant difference in the growth rates between DSS301 cells transformed with plasmids expressing either the wild-type, DmsA C75S mutant, or empty vector when grown on GF minimal media. There is no difference when the media contains either 15μM Mo or 100μM W. In this experiment all cells reach maximum density approximately 25 hours into the growth experiment and shows that transformation of the cells does not negatively affect the required respiratory chain. In ***fig. 3.3*** there appears to be no significant difference in the growth rates of DSS301 cells which have been transformed with either pDMS160, or the DmsA C75S BC mutant vector when grown on glycerol-DMSO minimal media containing 15μM molybdenum. Here, cells reach maximum density approximately 40 hours into growth and there is no growth of cells transformed with empty vector. When the cells are grown on GD minimal media containing 100μM W, there is no growth of any cells. This makes sense, as a functional DMSO reductase is required for growth of DSS301 cells on GD minimal media, and the presence of W impairs Mo-bisMGD cofactor assembly resulting in a non-functional enzyme. This study shows that the C75S mutant is expressed and functional when Mo is present in the growth media. Similar results were observed in growth experiments using HB101 cells which express wild-type DMSO reductase from its chromosome. This is because the over-expressed enzyme competes out the chromosomal copies for targeting to the membrane. In this case however, pBR322 transformed cells are still able to grow as the chromosomal enzyme is still targeted to the membrane.

Western blots show that DmsABC and DmsA^{C75S}BC are both stably expressed in the inner membrane of DSS301 and HB101 cells but when grown in media with excess tungstate the mutant is unstable

Crude membrane fractions from DSS301 or HB101 cells expressing either DmsABC or DmsA^{C75S}BC grown either in the presence of molybdenum or in the presence of excess tungstate on GF mediaas described in the methods section were compared by

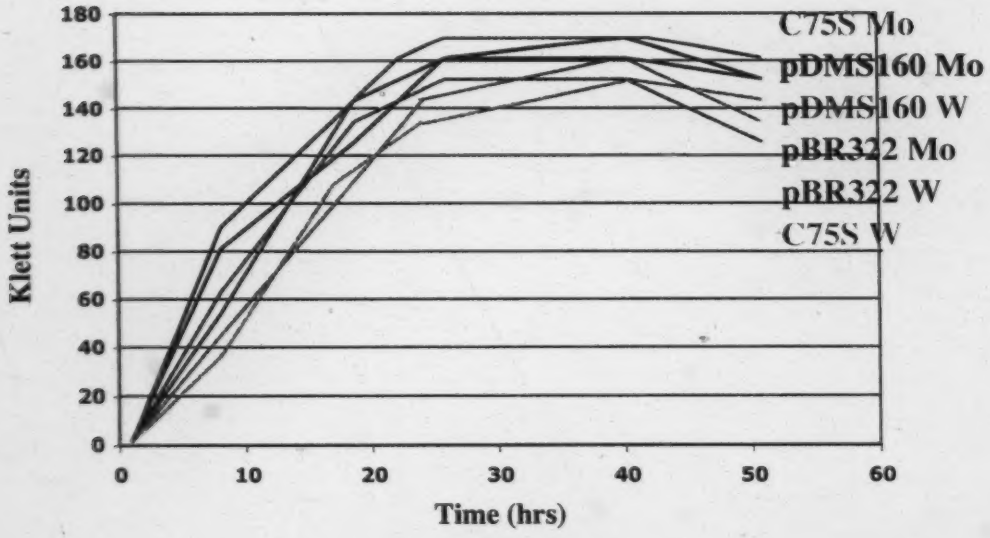

Fig 3.2 DmsAC75S BC grown in DSS301 cells with either 15 μM or 100 μM of molybdenum or tungstate respectively on minimal Glycerol-Fumarate media. Data includes a wild-type control (expressed from pDMS160) and a negative control (from pBR322). Data is an average of three trials and is representative of three sets of experiments.

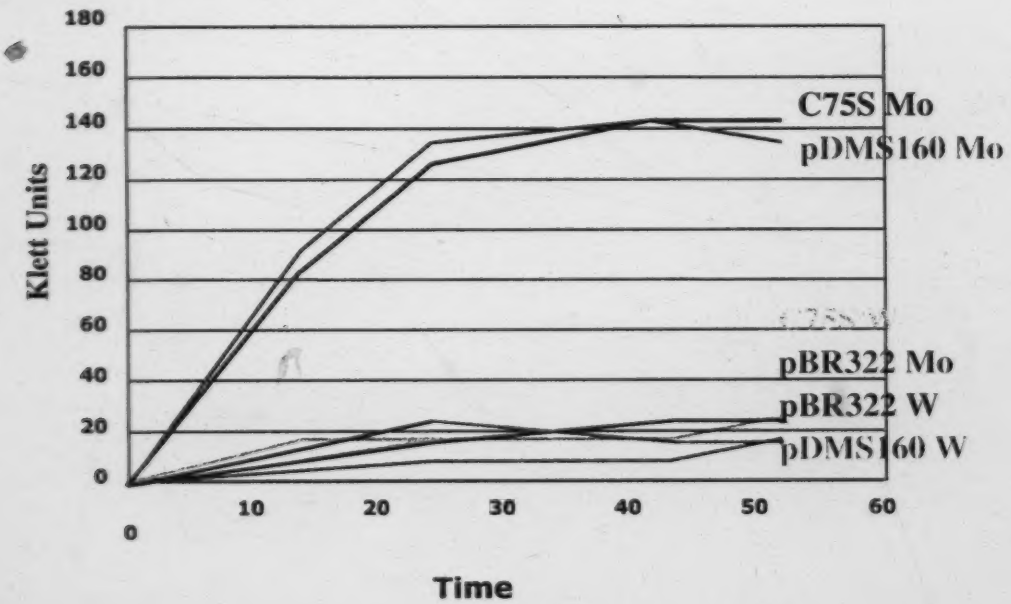

Fig 3.3 DmsAC75S BC grown in DSS301 cells with either 15 μM or 100 μM of excess molybdenum or tungstate respectively on minimal Glycerol-DMSO media. Data includes a wild-type control (expressed from pDMS160) and a negative control (pBR322). Data is an average of three trials and is representative of three sets of experiments.

immunoblotting. There appeared to be little difference in the levels of wild-type DmsABC enzyme in the membrane when grown under the different conditions suggesting that the presence or absence of molybdopterin cofactor has no significant effect on the assembly of the enzyme or its subsequent stability in the inner membrane. There was, however, a significant decrease in the levels of enzyme in crude membranes from cells expressing the DmsA^{C75S}BC mutant when these cells were grown in the presence of excess tungstate. Comparable results were seen in HB101 cells (not shown). This suggests that in the case of the DmsA^{C75S}BC enzyme, the proper assembly of the molybdopterin cofactor is required for protein stability, and suggests

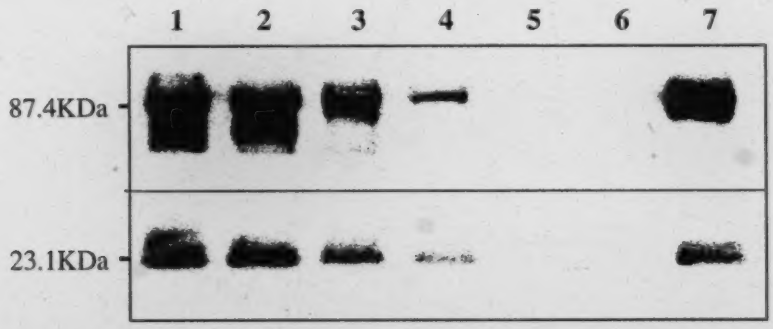

Fig 3.4 Western blot using anti-DmsA or anti-DmsB antibodies on crude membranes from DSS301 cells expressing: DmsABC (lanes 1 and 2); mutant DmsA^{C75S}BC (lanes 3 and 4); or pBR322 (lanes 5 and 6). GF growth media contained either 15μM Na_2MoO_4 (lanes 1, 3, and 5) or 100μM Na_2WO_4 (lanes 2, 4 and 6). Lane 7 contains a DMSO reductase standard. 10μg of protein from crude membrane preparations was loaded/lane (lanes 1-6) as determined by Lowery assays. Blot is representative of three independent gels.

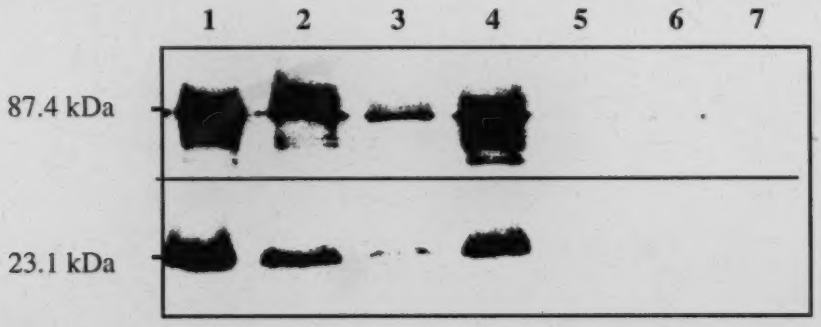

Fig 3.5 Western blot using anti-DmsA or anti-DmsB antibodies on crude membrane preparations from RK5209 cells grown on GF minimal media. Lane 1 is a DMSO reductase standard; DmsABC expressed in cells grown with 100μM Mo (lane 2) or in 0μM Mo (lane 3); DmsA^{C75S}BC grown with 100μM Mo (lane 4); or in 0μM Mo (lane 5) and; crude membranes from RK5209 containing pBR322 and grown in either 100 or 0 μM Mo (lanes 6 and 7 respectively) Blot is representative of three independent gels.

C75 makes important contacts for maintaining this stability. In the X-ray crystal structure of proteins like FdhN, the homologous cysteine residue lies only 6Å from the molybdopterin cofactor. Another possibility is that the cysteine plays a role in the coordination of an FeS cluster and when this coordination is disrupted there are structural alterations that make the enzyme unstable without Mo-bisMGD cofactor. It is unlikely that attenuation of mutant enzyme levels results from down regulation of expression of the enzyme due to a lack of cofactor, as this would have also been observed in the wild-type enzyme because both constructs are regulated by the same promoters. This result suggests that cysteine 75 is important for the structural integrity of the subunit or that it is critical for the proper folding of the enzyme and that it likely in close proximity to the molybdenum cofactor. Western blots of crude membranes of the DmsA^{C75S}BC mutant grown in RK5209 cells confirm these findings. RK5209 is a strain of *E. coli* defective in molybdenum uptake from the growth media and is subsequently impaired in Mo-MGD cofactor assembly. Preliminary experiments showed that this strain was able to take up enough molybdenum for cofactor assembly when grown in media containing greater than 10mM Mo but was impaired in this ability for concentrations of Mo lower than 10mM because of its defective molybdenum transport system. When DmsA^{C75S}BC is expressed in this strain grown with 0mM Mo in the growth media. Almost no enzyme is observed in crude membrane preparations compared with wild-type enzyme grown with 0 mM Mo in the growth media. This is in accordance with the result observed in DSS301 cells expressed with excess tungstate. This experiment eliminates a possible artifact resulting from excess tungstate in the growth medium. Interestingly, when the wild-type enzyme was grown in RK5209 cells with 100mM of Mo, the expression level of DmsABC in the inner membrane was much higher than when the cells were grown with 0mM Mo. This was unexpected, as the wild-type enzyme showed similar levels of expression and assembly to the inner membrane with or without cofactor in DSS301 cells. This is likely the result of a strain specific reduction of enzyme expression levels under the condition of reduced Mo in the growth media. Here we focus on the observation that when expressed in growth media lacking Mo, wild-type DMSO

reductase accumulated in the inner membrane whereas mutant DmsA^{C75S}BC expression was completely attenuated.

Activity assays on the DmsA^{C75S}BC enzyme show that it is active when expressed in cells with normal molybdenum cofactor levels

The activity of DmsABC and DmsA^{C75S}BC in enriched membranes from DSS301 cells was assayed using TMAO benzyl viologen assays as described in the Materials and Methods section. Wild-type enzyme in the membrane fraction of cells grown with molybdenum showed a fairly high activity, comparable to the activities reported previously [16]. A comparable activity was reported for the mutant grown in the Presence of molybdenum, suggesting that the mutation of cysteine 75 to serine does not have a significant affect on the catalytic activity of the enzyme. This result suggests that electron transfer through DmsA to the active site is unaffected by the mutation. (Previous experiments show that reduction of the enzyme by benzyl viologen requires the conserved n-terminal cys motif) [16].

DSS301 sample	Growth Conditions	Activity (U/mg)
pDMS160	15μM Mo	134
pDMS160	100μM W	0
DmsA^{C75S}BC	15μM Mo	98
DmsA^{C75S}BC	100μM W	0
pBR322	15μM Mo	0
pBR322	100μM W	0

Table 3.1 Enzyme activities of the enriched membranes from DSS301 cells expressing protein from either pDMS160 (wild-type), pDMS160-C75S, or pBR322. TMAO benzyl viologen activities were performed and the rate of product formation measured by spectroscopy. Results are based on calculations described in the methods section and are an average of three trials. The data presented are the results of an experiment with results representative of three separate experiments.

Form A fluorescence spectra show that membrane bound DmsA^{C75S}BC assembles a Mo-bisMGD cofactor when it is available

Membrane samples from HB101 cells were prepared and analyzed for molybdopterin

cofactor levels using the Form A fluorescence spectroscopy assay as described in the Materials and Methods section. This was done as an assay for assembly of molybdopterin cofactor into the mutant enzyme. The result from this experiment is consistent with the western blot analysis and shows that both wild-type and mutant enzymes assemble the Mo-bisMGD cofactor in similar amounts in the membrane fraction when grown in the presence of Mo. There is no cofactor in the membrane fraction of cells grown in excess tungstate even though there is still wild-type protein in these membranes as determined by immunoblot analysis.

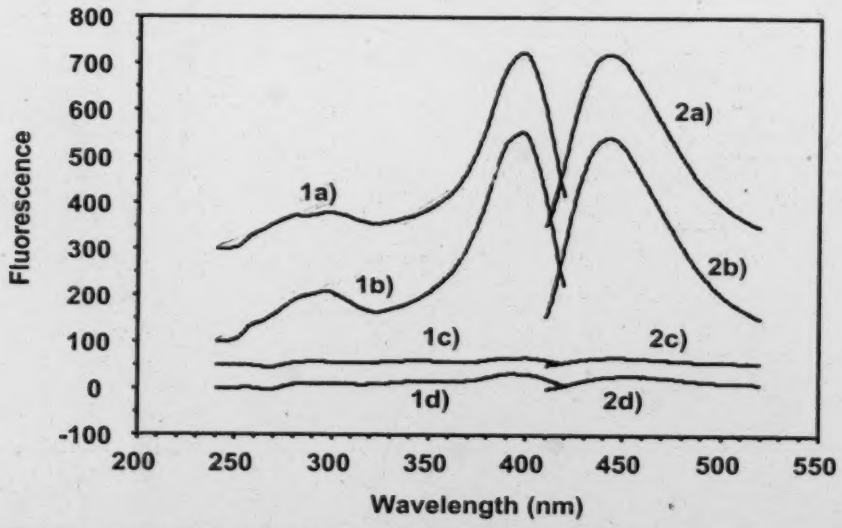

Fig 3.6 Fluorescence excitation (1), and emission (2), spectra on the crude membranes from HB101 cells expressing either a) DmsABC grown in 15 μM NaMo; b) DmsA^{C75S}BC grown in 15 μM NaMo, c) DmsABC grown in 100 μM NaW d) DmsA^{C75S}BC grown in 100 μM NaW. Spectra from negative control membranes was subtracted from the data in all cases. Data is representative of three separate trials.

HOQNO binding assays show levels of DmsC decrease in the membranes of cells expressing DmsA^{C75S}BC when grown in the presence of excess tungstate

DmsC is the membrane anchor subunit of DMSO Reductase. When all of the subunits of the enzyme are folded and assembled into the enzyme complex it can be targeted to the inner membrane. DmsC contains a menaquinol-binding site, which binds to the analogue HOQNO. This property can be utilized as an assay not only to analyze the

quinol-binding properties of the enzyme but also to detect levels of enzyme in a sample as described in the methods section. The concentration of DmsC in a sample can be calculated as the moles of HOQNO titrated into the sample at the point when the fluorescence begins to rise. It was observed that only when the DmsA^{C75S}BC enzyme was grown in the presence of excess tungstate was the level of DmsC in the membrane reduced to zero. The mutant grown in the presence of molybdenum as well as the wild-type grown with either molybdenum or tungstate showed similar DmsC levels. HOQNO titrations allow for the quantification of enzyme expression where gels and blots are more qualitative. Because there is only one quinol binding site per DmsC subunit, the concentration of HOQNO when the fluorescence begins to rise is the concentration of enzyme in the cuvette, which can be put in terms of enzyme concentration per mg of total protein in the original sample.

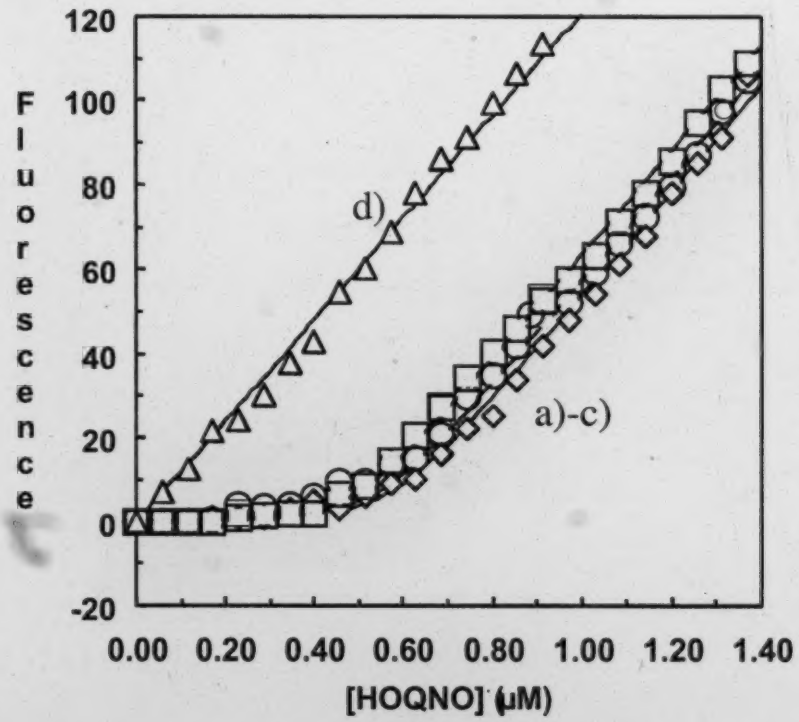

Fig 3.7 Fluorescence quench titrations of crude membrane preparations from HB101 cells with HOQNO to assay the amount of DmsC present in cells expressing either DmsABC or DmsA^{C75S}BC and grown on minimal media containing either 15 μM of Mo or 100 μM of W. The florescence of the membrane solution (Y) is plotted as a function of the concentration of HOQNO in the membrane solution. (a) membranes from cells expressing DmsABC grown in 15 μM Mo, (b) expressing DmsABC grown with 100 μM W, (c) expressing DmsA^{C75S}BC grown in 15 μM Mo and (d) expressing DmsA^{C75S}BC grown in 100 μM W.

In this case, wild-type enzyme expressed with or without cofactor and the C75S mutant expressed with cofactor appear to have similar enzyme concentrations (0.49μM/mg), in agreement with the blot of HB101 cells, and this concentration is approximately 0.52nmols DmsABC/mg protein. This data is supporting evidence for the C75 residue of DmsA being very important for enzyme stability when there is no molybdenum cofactor present. It is also evidence for the requirement of coordinated assembly of all three subunits of the enzyme for membrane stability. A destabilized DmsA subunit results in a loss of DmsC from the membrane.

EPR spectra of the iron sulfur region of the DmsA C75S BC mutant

The C75S mutant was further analyzed by EPR spectroscopy. Enriched membranes of HB101 cells expressing only chromosomally derived *DmsABC* (a negative control), wild-type DMSO reductase from pDMS160 (a positive control), and the $DmsA^{C75S}BC$ mutant enzyme were analyzed. Membranes from cells grown in media containing molybdenum or excess tungstate were also analyzed, to observe the effect of elimination of the Mo-bisMGD cofactor on the 4Fe-4S cluster signals in all of the membranes characterized. Fig. 3.8A shows the inner membranes from the negative control HB101 cells. When grown either with W or Mo, a peak trough at g=2.02 and 1.96 is observed characteristic of the 2Fe-2S cluster of the background enzyme FrdABCD. In Fig. 3.8A a signal with a small upward feature at g=2.03 crossing the base line at g=2.01 is observed at temperatures below 30K. This is characteristic of a 3Fe-4S cluster and is from fumarate reductase, the only known FeS cluster binding protein known to be in the membranes of HB101. Mo-bisMGD appears to have no effect on this signal as cells grown with either Mo or excess tungstate show the same EPR signal in this region. In Fig. 3.8B a very obvious 4Fe-4S signal characteristic of DMSO reductase is observed (Fig. 2.4B). At temperatures below 40K a broad and complex feature centered around g=1.94 is observed. Here the same signal is observed in cells grown with either Mo or excess W indicating that the attenuation of Mo-bisMGD cofactor has no effect on the EPR visible 4Fe-4S cluster signal in these

membranes. The EPR spectra of the membranes from the C75S mutants (fig. 3.8C) show a reduction in the 4Fe-4S cluster EPR signal, but the features of the signal including the location of signal peaks and troughs are still representative of the characteristic 4Fe-4S signal at this temperature. The reduction of the signal intensity is due to a decrease in 4Fe4S cluster levels. These signals are significantly reduced in the membranes of cells expressing the C75S mutant and grown in the presence of

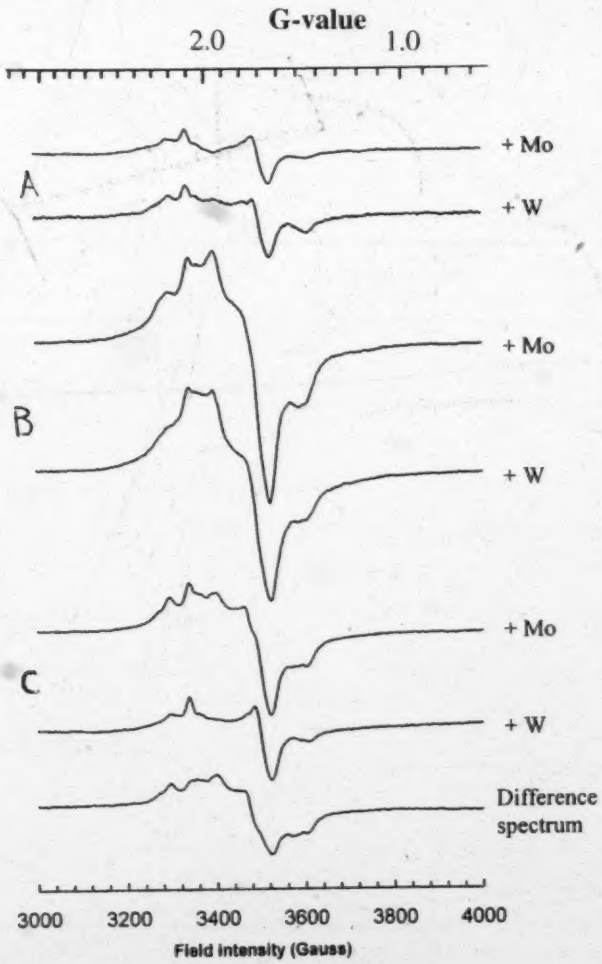

***Fig 3.8** EPR spectra of enriched membranes expressing the C75S mutant of DmsABC.* **A.** Dithionite-reduced enriched membranes from HB101 cells harbouring pBR322 and grown with either Mo or W in the growth media. **B.** Dithionite-reduced membranes from HB101 cells harbouring pDMS160 and grown with either Mo or W in the growth media. **C.** Dithionite-reduced membranes from HB101 cells harbouring pDMS160F ($DmsA^{C75S}BC$ mutant enzyme) and grown with either Mo or W in the growth media. Samples were at pH= 7.0 and spectra were recorded at 12K, $10G_{pp}$ modulation amplitude, but 100mW microwave power.

tungstate. This can be observed by looking at the difference spectra (*Fig 3.8C*). The attenuation of 4Fe-4S cluster signal in these membranes suggests that less DMSO reductase is accumulating in the membranes without the cofactor. This result is consistent with the observation that the C75S mutant of DmsA is unstable in the membrane when the cofactor is unavailable as observed in western blot analysis. The reduction in 4Fe4S cluster signal for the mutant grown with molybdenum is inconsistent with HOQNO titrations that show roughly equivalent levels of wild-type and mutant enzyme in the membrane. This could be interpreted to mean that there is less 4Fe4S cluster assembled in the C75S mutant or that some of the cluster was lost during the redox poising of the membrane sample.

3.3 Conclusions

In this experiment, a simple amino acid substitution of cysteine 75 to serine seems to render the stability of DMSO reductase Mo-bisMGD dependent. Characterization by several methods show that the mutant enzyme is unable to fold and associate with the membrane only when expressed under conditions which eliminate the cofactor from the cell. When the cofactor is available, the enzyme is stably expressed at the plasma membrane. This differs from the wild-type enzyme, which is expressed with or without Mo-bisMGD cofactor. Cysteine and serine are very similar amino acid residues. Both are similar sizes and both are residues with uncharged polar side chains, cysteine an SH group, and serine an OH group. It is surprising that this mutation has an effect on the enzymes' stability given this similarity. Importantly, serine is almost never involved in the coordination of an iron sulfur cluster (Rothery RA, personal communication). This is strong supporting evidence for a role for cysteine in the coordination of a 4Fe-4S cluster in *E. coli* DmsA. Replacement of the cysteine with a serine would disrupt the coordination of the 4Fe-4S cluster causing significant structural alterations in the enzyme resulting in a destabilization of the

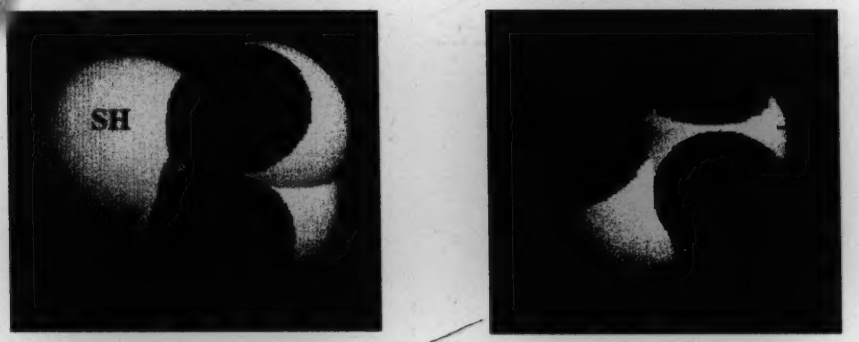

Fig 3.9 Rasmol illustration of a cysteine residue that is replaced by a serine residue in DmsA C75S BC. The residues are extremely similar in physical and biochemical properties. Both have uncharged polar side chains. SH groups are very similar to OH groups. In homologous enzymes such as *E. coli* FdhN, the S of the cysteine is coordinated to an Fe of a 4Fe-4S cluster.

enzyme without cofactor. That is to say, it is more likely that disruption of FeS cluster assembly would have more structural repercussions on the enzyme than would the substitution of one amino acid side chain with another very similar in biochemical properties. SH groups are more reactive than OH groups and the sulfur electron orbitals are larger. This difference in atomic size and reactivity would change the FeS cluster binding properties of the group. The destabilization of the mutant in the absence of cofactor makes the most sense in this model. If the cysteine is not involved in the coordination of an iron sulfur cluster then destabilization of the enzyme in the absence of molybdopterin cofactor is not totally unreasonable if the residue is in close proximity to the cofactor and makes important contacts in this area. The homologous cysteine of *E. coli* FdhN comes within 7Å of the molybdopterin cofactor as seen in Fig. 3.10.

Results of these experiments suggest that cysteine 75 is a residue that is important for the structural integrity of the protein and that it likely makes contact with the molybdopterin cofactor. This contact does not seem to be vital to the structural integrity of the protein except when cofactor availability is attenuated. Alternately this residue could play an important role in coordinating a redox factor such as an iron sulfur cluster. If cluster coordination is altered, it is easy to imagine that the entire

protein might become unstable. At the same time, if this residue is important in coordinating an FeS cluster one would also expect that substituting this residue would result in a loss of activity in the protein as a result of losing an important component of the electron transfer pathway; this was not observed. My results would thus suggest that the serine mutation only results in a loss of FeS cluster coordination when the MGD cofactor is not present, resulting in a completely destabilized enzyme. EPR analysis has failed to identify an FeS cluster in DmsA however initially, EPR also failed to observe the FeS cluster in NarG, another Type II enzyme (Rothery et al, personal communication). The FeS cluster of NarG was visualized by X-ray crystallography.

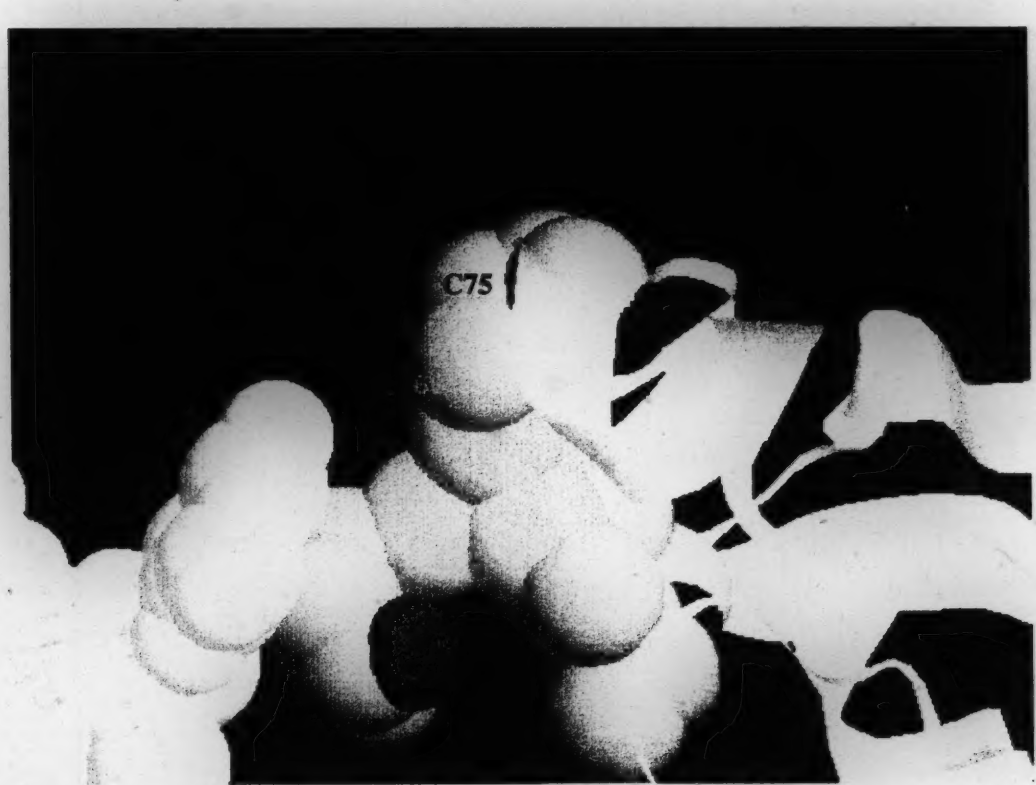

Fig 3.10 Rasmol depiction showing how the sulfhydryl group of cysteine 75 makes contact with an Iron of the 4Fe4S cluster of the DmsA subunit from E. coli FdhN. This amino acid side chain is also located in fairly close proximity to the Mo-bisMGD cofactor. Other residues highlighted are the other cysteine involved in the coordination of the 4Fe-4S cluster.

4.0 N-TERMINAL CYSTEINE CLUSTER MUTANTS OF DmsA

4.1 Introduction

In situations where the crystal structure for a protein is unavailable, site directed mutagenesis based on sequence alignments and the identification of conserved amino acid residues is an effective way of elucidating structural and functional information about an enzyme. DmsA has been fairly well characterized. A remaining interest is the role of a highly conserved ferredoxin-like, iron sulfur cluster binding, cysteine motif located close to the N-terminus of the protein.

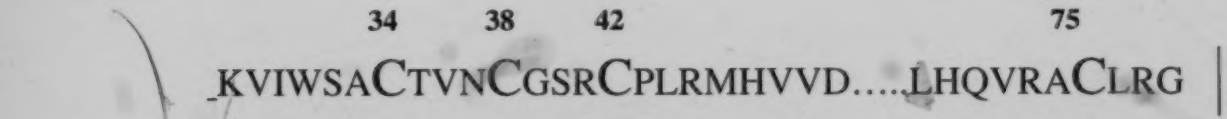

Fig 4.1 The N-terminal region of DmsA. This region is very similar to a ferredoxin 4Fe-4S cluster binding motif and has four highly conserved cysteine residues.

Ferredoxins and other proteins that contain 4Fe-4S clusters usually coordinate these clusters via motifs of conserved residues that contain four cysteines. The spacing of the Cys residues within these Cys motifs is typically as follows: the first two are separated by two amino acids, while the spacing between the second, third and fourth Cys residues is somewhat variable. The iron sulfur clusters play a role in electron transfer through the protein with the metal centers conducting electrons in the direction of more negative to more positive redox potential. Homologs of DmsA were divided into three basic types based on the characteristics of the N-terminal region. The type I enzymes contain a highly conserved ferredoxin-like cysteine cluster involved in the binding of a 4Fe-4S cluster. The Type II enzymes contain a similar conserved cluster although here the spacing between the first two cysteines is different. There are three rather than two amino acids and the first cysteine can be replaced with a histidine. The Type III enzymes lack this region altogether, see Fig.

1.32. Until recently only the crystal structure of a few of the type I enzymes had been solved (FdhF, FdnG, NapA). These enzymes were all shown to bind 4Fe-4S clusters by their N-terminal cysteine motifs [71] [72] [16]. Based on this information it was believed that all of the Type I enzymes were capable of binding 4Fe-4S clusters. Conversely, spectroscopic evidence was lacking for a similar cluster in the type II enzymes. It was assumed that the spacing between the first two cysteines was critical for cluster assembly. EPR analysis on DMSO reductase from *E. coli* as well as on nitrate reductase from *E. coli,* both type II enzymes, suggested that the catalytic enzymes did not bind 4Fe-4S clusters. The function of this vestigial cluster in the type II enzymes remains uncertain but it may be involved in electron transfer to the active site of DmsA. Perhaps in the case of the type II enzymes, the conserved Cys motif is involved in the binding of some unknown redox center such as a metal ion; which might aid in electron transport. Another possibility could be the cysteine residues act directly in electron transfer. To confuse the matter further the recent solution of the X-ray crystal structure of periplasmic nitrate reductase from *E. coli* has shown that this particular type II enzyme does bind a 4Fe-4S cluster in its catalytic subunit which had not been observed by EPR. Perhaps this is also the case for *E. coli* DMSO reductase.

Chapter 3 described the affect of mutating Cys 75 to Ser. This chapter describes the creation and characterization of 5 mutant DmsA proteins altered to encourage the assembly of a 4Fe-4S cluster into the subunit or to perhaps alter an already existing cluster to render it more spectroscopically visible. The objective was to alter the N-terminal cysteine consensus sequence to more closely resemble that of the type I enzymes. Changes in the N-terminal consensus sequence ranged from minimal to drastic in hopes of identifying the essential requirements for cluster assembly. The smallest change was the substitution of a conserved arginine 77 in the type II enzymes with a lysine, which is conserved in the Type I enzymes **(Mutant C, R77K)**. Another mutant was created which altered the spacing and conserved the amino acids between

	34 38 42 75
DmsA *E. coli*	KVIWSACTVNCGSR CPLRMHVVD.....LHQVRACLRG
A (CS1)	KVIWSACTY - CGVGCGLRMHVVD.....LHQVRACLRG
B (CS2)	KVIWSACTY- CGSR CPLRMHVVD.....LHQVRACLRG
C (R77K)	KVIWSACTVNCGSR C PLRMHVVD.....LHQVRACLKG
D (CS1+R77K)	KVIWSACTY - CGVGCGLRMHVVD.....LHQVRACLKG
E (CS2+R77K)	KVIWSACTY- CGSR CPLRMHVVD.....LHQVRACLKG
FdhN *E. coli*	KEIRNTCTY - CSVG CLLMYSLGD.....VSRGALCP KG

Fig 4.2 Five mutants of the DmsA conserved N-terminal cysteine motif. The first sequence is the conserved N-terminal cysteine motif from *E. coli* DmsA. **(A-E)** are the mutants in this region created using mutagenic primers, polymerase chain reaction and molecular cloning techniques. The last sequence is from FdhN from *E. coli*, a typical type I enzyme.

the first two cysteines to be more representative of the type I enzymes **(Mutant B, CS2)**. Another mutant more drastically altered the cysteine region of the sequence, changing specific amino acid residues in addition to the spacing between the first two cysteines to maximize its similarity to the type I enzyme sequence, (see ***Fig. 1.32*** and ***Fig. 4.2***), **(Mutant A, CS1)**. Double mutants of A and C and of B and C were also created, **(Mutant D, CS1+R77K)** and **(Mutant E, CS2+R77K)** respectively.

The mutants were characterized by assaying for assembly into the plasma membrane, activity, and for the presence of molybdenum cofactor. The metal centers were identified by EPR (electron paramagnetic resonance).

The following results suggest that in all the mutants created except for mutant C, alteration of the conserved N-terminal sequence altered the enzymes in such a way as to render them inactive and inhibit the assembly of molybdenum cofactor to some

extent. No FeS clusters in the catalytic subunit could be identified in any of the mutants characterized by EPR analysis.

4.2 Results and Discussion

Growth experiments

HB101 or DSS301 cells were transformed with pDMS160, the mutant plasmids, and a negative control pBR322 as discussed in the Materials and Methods section. Growth experiments were performed by inoculating overnight cultures of cells expressing the enzymes into Klett flasks containing either Glycerol-fumarate or Glycerol-DMSO minimal media and antibiotics for plasmid and cell selection. Flasks were incubated anaerobically for 48 hours with stirring in a 37°C water bath. Readings were taken over the course of the experiment to monitor cell density and growth curves obtained. When the cells are grown on glycerol-fumarate media, DMSO reductase is not necessary for cellular respiration, as an alternative respiratory chain which uses fumarate as a terminal electron acceptor for electrons derived from glycerol can be expressed by either strain. When cells are grown on glycerol-DMSO minimal media, DMSO reductase is required to complete the *E. coli* respiratory chain. This would suggest cells overexpressing an active DMSO reductase enzyme will grow faster than cells expressing a normal amount of the enzyme. Cells without any DMSO reductase or expressing a nonfunctional enzyme will not grow. In ***Fig. 4.3*** and ***4.4*** we observe no significant difference in the growth rates when the mutants are compared with the wild-type enzyme or the pBR322 negative control. In ***figs 4.5*** and ***4.6*** we observe a definite difference in growth rates between cells expressing the different enzymes. In ***Fig 4.5*** the enzymes are expressed in DSS301 cells and we observe growth in only cells expressing the wild type enzyme or mutant C (R77K). The negative control

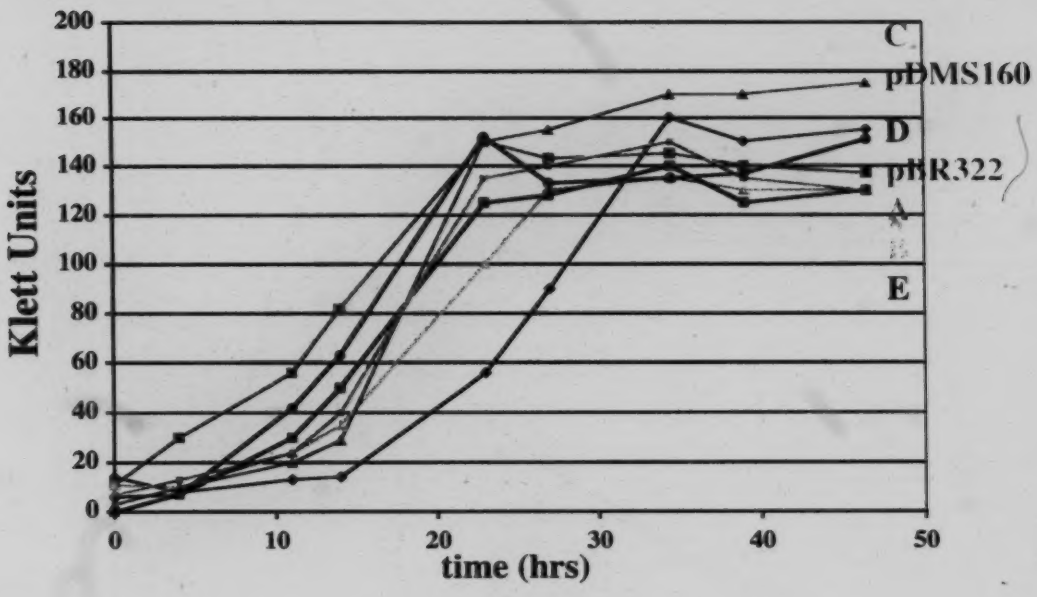

Fig 4.3 pDMS160, pBR322 and five DmsA mutants expressed in DSS301 cells and grown on glycerol-fumarate minimal media. Curves are the average of three trials from one experiment that was representative of three separate experiments.

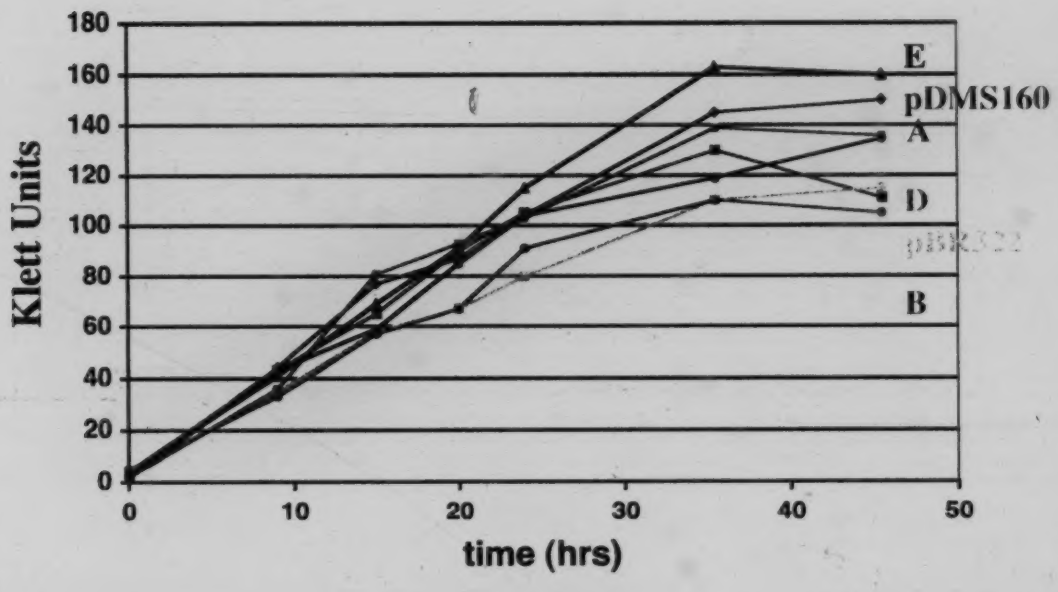

Fig 4.4 pDMS160, pBR322 and five DmsA mutants expressed in HB101 and grown on glycerol-fumarate minimal media at 37° C. Curves are the average of three trials from one experiment that was representative of three separate experiments.

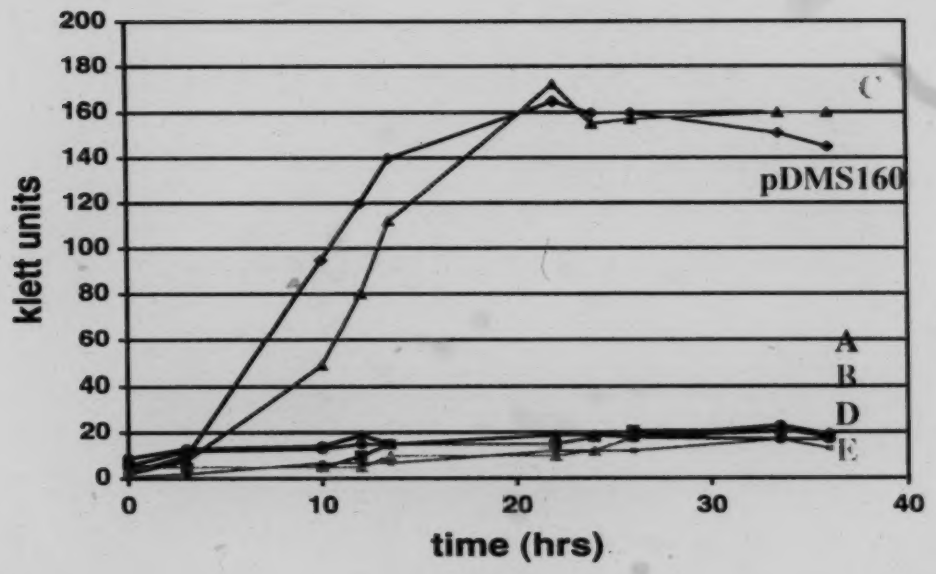

Fig 4.5 pDMS160, pBR322 and five DmsA mutants expressed in DSS301 cells and grown on glycerol-fumarate minimal media at 37°C. Curves are the average of three trials from one experiment that was representative of three separate experiments.

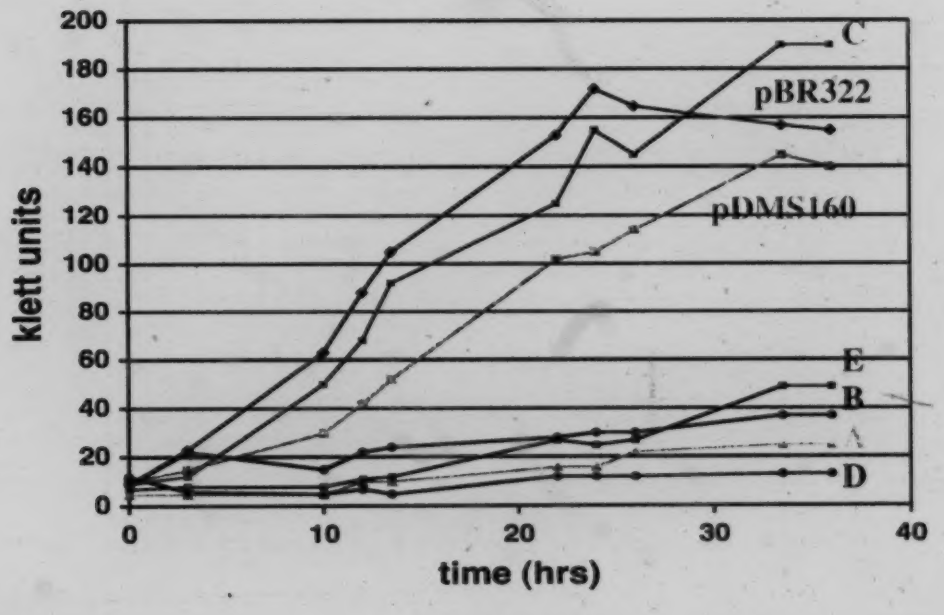

Fig 4.6 pDMS160, pBR322 and five DmsA mutants expressed in HB101 cells and grown on glycerol-fumarate minimal media at 37°C. Curves are the average of three trials from one experiment that was representative of three separate experiments.

Shows no growth because there is no chromosomal copy of DMSO reductase in this strain, and the others show no growth because they are likely expressing non-functional mutants (or perhaps are not expressing anything at all.) In HB101 cells, similar trends were observed (***Fig 4.6***), except cells transformed with pBR322 show growth rates comparable to cells transformed with pDMS160 or Mutant C. This is because HB101 cells have a chromosomal copy of DMSO reductase which is expressed allowing growth on GD minimal media. The fact that Mutants A, B, D and E do not grow at all is evidence for these enzymes being expressed and nonfunctional as opposed to not expressed at all. If they were not expressed one might expect growth comparable to that of cells transformed with pBR322. However the fact that no growth is observed suggests that non-functional enzymes are expressed to high enough levels that they compete out the functional reductase in terms of targeting to the inner membrane. This phenomenon is often termed negative dominance.

All mutants are stably expressed in the inner membrane of E. coli by western blot and HOQNO titration analysis

Large batches of cells expressing the different enzymes were grown up and harvested by using a membrane filtration system and low speed centrifugation. The cells were then lysed by the French pressure method and separated into membrane and soluble fractions. Finally the inner membrane fraction was enriched by high speed centrifugation using a sucrose cushion as described in the Materials and Methods section.

The levels of expression of the various enzymes was measured by first quantifying the amount of protein in the various fractions by the Lowry method and then by western blot analysis using anti-DmsA or anti-DmsB antibodies. All mutants expressed well in both DSS301 and HB101. Figure 4.7 shows enriched membrane fractions from HB101 cells expressing the mutants A-E.

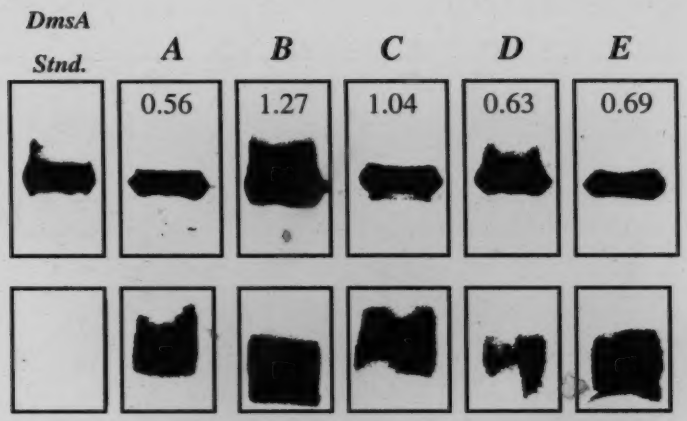

Fig 4.7 Western blot analysis of the enriched membranes from HB101 cells expressing mutant enzymes A,B,C,D,E and a DMSO Reductase standard in the first lane. Numerical values are concentrations of enzyme in the membrane sample as determined by HOQNO titration analysis (DmsC as an indirect measurement of A and B) and are in units of μM/mg protein. Blot is representative of several independent gels.

Fluorescence quench titrations using the inhibitor HOQNO were carried out on the enriched HB101 membranes to complement western blot analysis and to more quantitatively compare the expression levels of enzyme in the membrane. Results from these experiments suggest that all mutants were expressed well and to similar levels. Actual numerical values for the amount of enzyme present in the membranes were derived from the concentration of HOQNO which saturates the fluorescence quenching properties of the sample. At this point all of the DmsC quinol binding sites (of which there is only one per enzyme) are saturated with HOQNO. Enzymes concentrations were calculated to be; Mutant A: 0.56 μmol/mg Mutant B: 1.27 μmol/mg, Mutant C: 1.04 μmol/mg, Mutant D: 0.63 μmol/mg, Mutant E; 0.69μmol/mg. These amounts are also shown in Fig. 4.7.

Benzyl viologen TMAO and lapachol assays suggest Mutant C is the only enzyme with activity levels comparable to wild-type DMSO reductase

Enriched membranes were used in benzyl viologen-TMAO or Lapachol activity assays as described in the Materials and Methods (Table 1). The TMAO assays show high

	DSS301		HB101	
	Membrane	Soluble	Membrane	Soluble
pDMS160	108.2	9.1	130.8	9.1
pBR322	0	0	9.2	0
A	3.8	0.3	2.4	0.3
B	1.4	0	4.6	0
C	83.8	9.1	140.5	4.8
D	1.4	0	2.2	0
E	0	0	3.8	0

Table 4.1 Enzyme activity of the enriched membrane and soluble fractions from either DSS301 or HB101 cells expressing the different enzymes. Activities are in U/mg and were calculated as described in the Methods section. Values are an average of three trials done in each experiment and are representative of the values obtained in three experiments.

levels of activity for wild-type enzyme and for mutant C in both DSS301 and HB101 cells. Low levels of activity seen in other mutants are due to non-specific activity in the case of DSS301 cells. In HB101 cells the low levels of activity observed in the negative control and in the non-functional mutants results from chromosomally expressed enzyme. The levels are lower in the mutants than in the negative control supporting the idea that nonfunctional enzyme is targeted to the membrane competing out the chromosomally derived reductase.

The lapachol assay is a more physiologically relevant assay, in which electrons are donated to DMSO reductase via the quinol binding site in DmsC as opposed to the nonspecific reduction of DMSO reductases in the benzyl viologen assay. Similar results were observed. Mutant C showed levels of activity comparable to that of the wild-type enzyme, while all other mutants and a negative control show no activity.

Form A fluorescence assays show that the molybdenum cofactor levels are attenuated in mutants A, B, D and E

In order to assay for the assembly of molybdenum cofactor into the mutant enzymes, a Form A florescence assay was performed. In this assay enriched membrane samples from HB101 cells expressing the various enzymes were oxidized with iodine to create a degradation product of the molybdenum cofactor which has spectroscopic qualities and can be quantified. Figure 4.8 depicts the emission and excitation spectra of cofactor isolated from wild-type membranes and membranes of the five mutants. In all cases the spectra of negative control membranes have been subtracted to eliminate background effects. It was observed that only Mutant C, the R77K mutant, showed molybdenum cofactor levels comparable to that of the wild-type enzyme. All other mutants, although stably expressed at the plasma membrane, showed attenuated Mo cofactor levels. These levels are fairly significant with Mutants A,B,D and E showing approximately 40%, 25%, 60% and 40% of wild-type levels, respectively, after normalizing the data for enzyme concentration based on numbers derived from HOQNO titration information. This is an interesting result given that the activity of all of these mutants was totally knocked out. There are two possible explanations for these results: (1) There are two populations of enzyme, one of which contains Mo-bisMGD, and one which does not, and the mutations are simply changing the ratio between these. A loss of activity in these mutants must be the result of structural or functional alterations that disrupt electron transfer to the cofactor, because if the loss was due to the attenuation of cofactor assembly alone then the activity would not have been completely eliminated in mutants A,B,D and E; (2) The mutations are affecting the insertion of MGD-P to a much greater extent than MGD-Q, resulting in there being about 50% of cofactor present. That is, only the unobstructed half of the cofactor binding site assembles a pterin molecule and the other half does not presumably because the mutation affects the conformataion of the site in a way that makes pterin assembly unlikely. This result would explain the complete lack of activity observed in these enzymes. The presence of a single MGD would also explain this result. In this

situation only half of the cofactor is assembled into the enzyme (a Mo-MGD). Perhaps the mutations cause structural alterations that don't allow assembly into the proximal pterin binding site and only the distal pterin binding space is filled. If this were the case we should see roughly 50% of the levels of Form A in these membranes. After normalizing the spectra for enzyme concentration, Mutants A,D and E show close to this value. Obviously, catalysis cannot take place without the molybdenum cofactor active site. It seems that the minimal alteration of the N-terminal consensus sequence cysteine spacing could be enough to modify the structure of the subunit in such a way that the cofactor is not assembled into the protein. Perhaps this small change allows the mutant enzymes to assemble a 4Fe-4S cluster which greatly alters the protein structure so that the cofactor cannot be assembled. Or perhaps the mutations result in the loss of, or substitution of, an already existing cluster with another which has a structural effect resulting in the disruption of cofactor assembly.

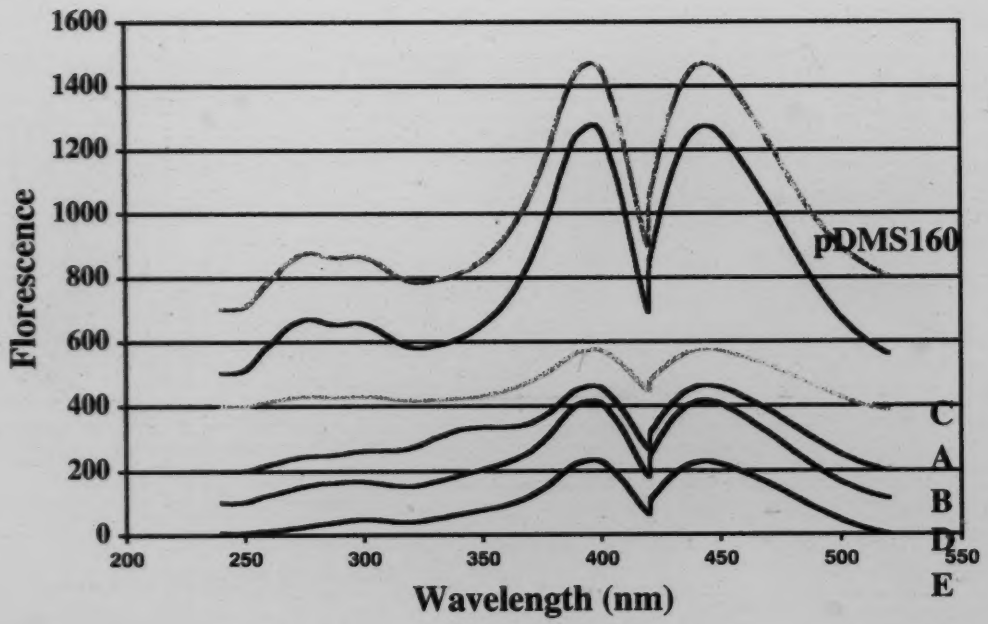

Fig 4.8 Form A fluorescence emission and excitation spectra from the enriched membranes of HB101 *E. coli* cells expressing mutants A,B,C,D and E as well as the wild-type enzyme. In all cases the pBR322 negative control was subtracted from the results. Data is representative of three independent experiments.

These are not unreasonable possibilities given the proximity of the 4Fe-4S cluster to the molybdenum cofactor in homologous proteins whose crystal structures are known. Also at least one of the cysteines, (C75) in this conserved sequence is important for cofactor assembly as discussed in the previous chapter.

EPR analysis of N-terminal cysteine mutants

Figure 4.9A shows the EPR spectra of enriched membranes from HB101 cells expressing Mutant A (CS1) at various redox potentials. This is the mutation which greatly alters the cysteine cluster sequence in the N-terminal conserved part of DmsA and includes altering the spacing between the first two amino acids from 3 to 2. Samples were poised at a range of potentials, 297 to -437mV. At high potentials, the spectrum resembles that of the [3Fe-4S] cluster of fumarate reductase (FrdABCD), with a peak at g=2.02 followed by a broad peak-trough immediately upfield. At lower potentials, features attributable to the four [4Fe-4S] clusters of DmsB appear, centered around a peak-trough at approximately g=1.94. No evidence was found in these spectra for an additional [4Fe-4S] cluster coordinated by the N-terminal Cys group of DmsA. If this mutant had picked up a new 4Fe-4S cluster in the DmsA subunit, we might expect to see an alteration in the low potential EPR line shape due to the magnetic coupling of the new cluster with the other redox centers.

Fig 4.10 shows the oxidized and reduced spectra of the remaining mutants. The spectra of Mutant C (R77K), is identical to the wild-type enzyme and consistent with all of the other data for this mutant which suggests that in all respects, mutating Arg77 to Lys has no effect on the enzyme. When the R77K mutation was incorporated into the CS1 mutant (*Fig. 4.10*), the reduced spectra was identical to the wild-type enzyme but the oxidized spectra is slightly different with exaggerated peak/troughs in the same locations as the wild-type enzyme. This is indicative of a small amount of [3Fe-4S] cluster being assembled into this mutant and mirrors the spectra seen for the CS1 mutant. Modifying this mutant by changing R77K appears to have no additional

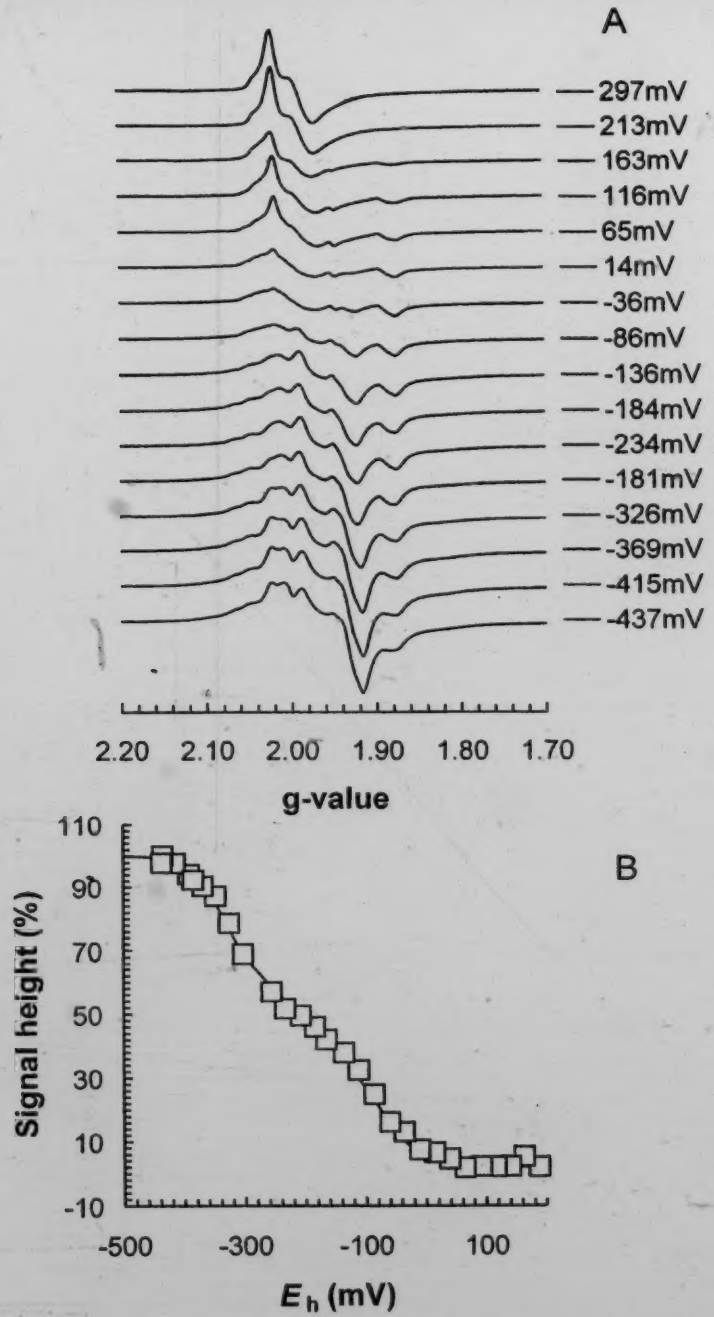

***Fig. 4.10** Redox titration data for the CS1 mutant of DmsABC.* **A** Redox-poised samples at pH=7.0 of membranes enriched in the CS1 mutant. Spectra were recorded at 12K, $10G_{pp}$ modulation amplitude, but 100mW microwave power. The potentials at which the samples were poised are indicated to the right of the individual spectra. **B** Plot of the intensity of the g=1.94 peak-trough *versus* potential. Data were fit to four midpoint potentials with E_m values of -50 (20%), -120 (22%), -230 (18%), and -337mV (38%).

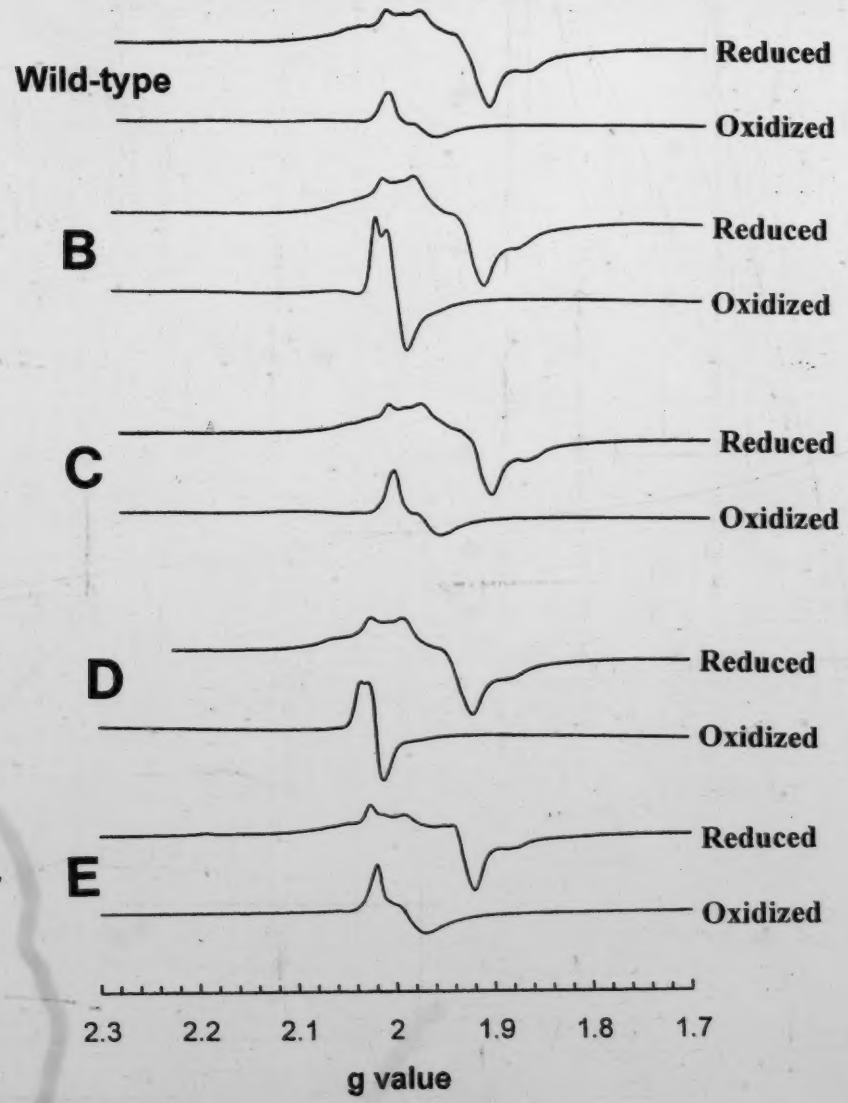

Fig 4.10 Oxidized and reduced redox-poised samples at pH=7.0 Spectra were recorded at 12K, $10G_{pp}$ modulation amplitude, but 100mW microwave power.

effect. Reduced spectra of the Mutant B membranes are typical of wild-type DMSO reductase but as with the A and D mutant, the oxidized spectra show a more exaggerated peak/trough at 2.02/1.98 g. This suggests that a small amount of [3Fe-4S] cluster is assembled into this mutant. The final spectra of Mutant E shows oxidized and reduced spectra similar to that of wild-type and so suggests that there has been no change in the iron sulfur cluster binding properties of this region.

suggests that there has been no change in the iron sulfur cluster binding properties of this region.

4.3 Conclusions

In this study, five mutants of the DmsA cysteine motif were created. Mutants were designed to alter the conserved motif to more closely resemble that of the type I enzymes. Changes ranged from single amino acid residue substitution to complex multiple residue substitutions and deletions. All mutants were relatively well expressed in both HB101 and DSS301 cells as determined by western blot analysis and HOQNO titration enzyme quantification. Activities for all of the enzymes analyzed, except for the R77K mutant, showed a complete lack of function as determined by inability to grow on DMSO-minimal media as well as activity assays. Form A fluorescence data, which analyzes the molybdopterin content of cell membranes showed that cofactor assembly, normal for the R77K mutant, was attenuated but not completely eliminated in the membranes of cells expressing all of the mutants. This suggests structural alterations in the N-terminal cysteine binding region of these mutants disrupts electron transport or causes structural changes which cause a complete loss of MGD in the MGD binding region proximal to this cysteine motif. This does not necessarily mean the loss of cofactor in the distal MGD binding region. Either of these results would explain the complete loss of activity in these mutants. It seems that the minimal alteration of the N-terminal cysteine consensus sequence, changing the spacing between the first two cysteines, disrupts the enzyme so that molybdenum cofactor assembly is attenuated. The overall stability of the enzymes is unaffected. All mutants which show a lack of cofactor have had the spacing between the first two cysteines of the ferredoxin like cluster changed from 3 to 2 as a minimal alteration. This amino acid loss could be the reason for the loss in cofactor assembly. Perhaps the structural modifications are more indirectly a result of the change in cysteine spacing. For example, the change in spacing could result in altered iron sulfur cluster binding properties, allowing the mutant to assemble a novel

iron sulfur cluster or modify an existing cluster resulting in the loss of cofactor. Either option is a possibility as the crystal structure of homologous enzymes places the cysteine cluster in very close proximity to the molybdopterin cofactor (*Fig. 4.11*). EPR analysis of the mutants created in this chapter shows some interesting results. Fresh inner membrane preparations were used here as an inordinate amount of protein is required for this method (10ml of 30mgs/ml). Mutant C (R77K), shows no difference in either oxidized or reduced EPR spectra compared with the wild-type enzyme. This compliments all of the other findings which show that this mutation alone has no effect on the enzyme. Both the CS1 and CS2 mutants appear to assemble a small amount of 3Fe-4S cluster, suggested by the similarity of the high potential spectra to the 3Fe-4S signal characteristic of fumarate reductase. Likely the minimal change of altering the cysteine spacing between the first two conserved cysteines is responsible for this modification in cluster assembly. Interestingly, the CS1 mutation in combination with a R77K mutation shows the same spectra as the CS1 mutation alone but the CS2 mutation in combination with the R77K mutation looks more like the wild-type spectra for the oxidized and reduced membranes. Here the reduced spectra of the 4Fe-4S cluster signal region appears to be attenuated likely due to lower enzyme levels in this membrane preparation. These results could be interpreted to mean one of two possible things; 1) Perhaps changing the spacing between the first two cysteines of the N-terminal sequence has the effect of allowing a small amount of 3Fe-4S cluster to assemble into this region of DmsA; 2) Perhaps the wild-type enzyme assembles a 4Fe-4S cluster and this cluster cannot be observed in the g=2 region as is the case with the type II enzyme nitrate reductase. If this were the case perhaps the appearance of a 3Fe-4S signal in the CS1, CS1+R77K and CS2, (Mutants A, B and D) is the result of a conversion of a population of the pre-existing 4Fe-4S cluster to a 3Fe-4S cluster, rather than the assembly of a novel cluster into DmsA. It is difficult to imagine why the CS2+R77 (Mutant E) enzyme does not show a spectra which more closely resembles that of mutants A, B and D. If anything, this mutant looks most similar to the wild-type enzyme. This is supporting evidence to suggest that the wild type enzyme likely already assembles a 4Fe-4S cluster. This is because Mutant E so closely resembles a Type I sequence that it is difficult to imagine a 4Fe-

not bound by this subunit yet the spectra is very similar to the wild-type DMSO reductase previously interpreted to suggest there is no cluster bound here. The EPR analysis of the Type II enzyme nitrate reductase from *E. coli* was interpreted to mean that there was no 4Fe-4S cluster bound by the catalytic subunit, which was later proved wrong after the solving of its 3-dimensional structure by X-ray crystallography.

Fig 4.11 Rasmol depiction of the cysteines of the N-terminal cluster binding a 4Fe-4S cluster in the DmsA homologue *E. coli* fumarate reductase. Cysteines are labeled as they would be in *E. coli* DmsA

5.0 CONCLUSIONS AND FUTURE DIRECTIONS

In Chapter 3, a simple amino acid substitution of cysteine 75 to serine seems to render the stability of DMSO reductase Mo-bisMGD dependent. Characterization of the mutant shows that the enzyme is unable to fold and associate with the membrane only when expressed under conditions which eliminate the cofactor from the cell. This differs from the wild-type enzyme, which is expressed with or without Mo-bisMGD cofactor. Cysteine and serine are very similar amino acid residues with polar sidechains very similar in biochemical properties so it is interesting that this mutation has an effect on the enzyme's stability. This is strong evidence for the involvement of cysteine 75 in the coordination of a redox cofactor, because it is more likely the enzyme is destabilized as a result of structural changes caused by a loss of iron sulfur cluster assembly than by the simple exchange of one amino acid side chain with another almost identical in biochemical properties. This would contradict EPR analysis which has shown that DMSO reductase from *E. coli* does not bind an iron sulfur cluster in the DmsA subunit. It is important to keep in mind however that EPR incorrectly suggested that there was no FeS cluster in the catalytic subunit of *E. coli* nitrate reductase, another type II enzyme. It was later shown that this enzyme binds a 4Fe-4S cluster within the cysteine binding motif by X-ray crystallography.

In the second experiment, five mutants of the DmsA cysteine motif were created. Mutants were designed to alter the conserved motif to more closely resemble that of the Type I enzymes which are known to bind a 4Fe-4S cluster by four conserved cysteines which conserve a very specific spacing in these enzymes. Changes ranged from basic, (single amino acid residue substitution), to complex, (multiple residue substitutions and deletions). All were stably expressed but inactive enzymes except for the R77K mutant. Form A fluorescence data showed that cofactor assembly was attenuated but not completely eliminated in the membranes of cells expressing all of the mutants except for the R77K mutant. This suggests structural alterations in the N-terminal cysteine binding region of these mutants which disrupts electron transport or results in the loss of MGD from the MGD binding region proximal to this cysteine

motif but not from the distal MGD binding region (which would explain the presence of approximately 50% of the Form A fluorescence). All mutants which show a lack of cofactor have had the spacing between the first two cysteines of the ferredoxin-like cluster changed from 3 to 2 as a minimal alteration. This amino acid loss could be the reason for the loss in cofactor assembly. Perhaps the structural modifications are more indirectly a result of the change in cysteine spacing. For example, the change in spacing could result in the loss of iron sulfur cluster coordination. EPR analysis confirms at least an alteration in the iron sulfur cluster coordinating properties of the mutants by a difference in the oxidized and reduced spectra. Specifically, the change in cysteine spacing from three to two residues results in the assembly of a 3Fe-4S cluster typical of fumarate reductase. This could mean that; 1) The mutation causes the conversion of a population of a pre-existing cluster to a 3Fe-4S cluster; 2) The mutations cause the assembly of a novel cluster. EPR analysis of the 4Fe-4S cluster spectra of the mutants and comparison with the wild type would suggest the latter possibility as this spectra has been interpreted to suggest the presence of four 4Fe-4S clusters in the DmsB subunit in the wild-type and mutant enzymes. Experimental results from the C75S mutant point to the first option as being likely if the EPR spectra analysis was unable to detect the 4Fe-4S cluster as was the case for *E. coli* nitrate reductase, another Type II enzyme. Nitrate reductase has a 4Fe-4S cluster bound by its catalytic subunit by X-ray crystallography.

It seems unlikely that further mutations of the N-terminal cysteine cluster binding motif of DmsA would shed any more light on the role of this sequence in the DmsA subunit. Experiments outlined in this thesis have utilized mutations in this region ranging from relatively insignificant to drastic, completing the objective of changing the region from a type II sequence to a type I 4Fe-4S cluster binding sequence. These experiments complement previous experiments which involved mutation of highly conserved amino acid residues in this region including the four conserved cysteines of this cluster. A large number of DmsA N-terminal conserved cysteine cluster motif amino acid residues have been mutated to date. Some of these have been substituted to more than one different residue and some have been mutated in different

combinations with other mutations. Details about these mutations were presented in this thesis as well as in references [59] and [16].

One way to solve the issue of iron sulfur cluster assembly in the DmsA subunit of DMSO reductase is through the use of AAS or EXAFS. The best way to conclusively solve the issue of iron sulfur cluster assembly in the DmsA subunit of DMSO reductase is to purify, crystallize, and solve the 3-dimensional structure of the enzyme by X-ray crystallography. This may prove to be a difficult task as membrane proteins are inherently very difficult to crystallize. Protocols have been developed for the purification of a number of *E. coli* proteins possessing integral membrane anchor subunits which were then successfully crystallized. Examples include *E. coli* nitrate reductase and formate dehydrogenase. The protocols for purification and crystallization could be used for DMSO reductase and modified as needed to suit this purification of this particular enzyme. In the recently solved crystal structure of nitrate reductase [66], Bertero *et al* (2003) overexpressed the enzyme in *E. coli* and after membrane purification and detergent extraction using thesit, purified the enzyme using two anion exchange steps. Gel filtration experiments were carried out to determine the best detergent and detergent concentrations for producing optimally diffracting crystals. Crystals of native and selenomethionine-substituted NarGHI in 0.7mM thesit were obtained by vapour diffusion with sitting drops equilibrated against a resevoir solution. Formate dehydrogenase-N was purified from anaerobically grown *E. coli* cells by Jormakka *et al* (2002) [72]. Membranes were prepared and the proteins solubilized by the addition of 1% n-Dodecyl-β-D-maltoside (DDM). Lipid and debris were removed by centrifugation and the Fdh-N purified in three steps. The first was purification on a sepharose FF column and the active fraction was applied to a Highprep Sepharose S-300 gel filtration column. Finally the active fraction was run on an anion-exchange column. The Fdh-N fractions were then pooled, concentrated, and crystallized using the hanging drop vapour diffusion technique. Clearly these two protocols are very similar and could likely be adapted to the purification of DMSO reductase from *E. coli*. Presently a high copy number expression vector exists which allows for overexpression of DMSO reductase in *E. coli* by its natural promoter,

meaning it will be expressed when cells are grown anaerobically on glycerol-fumarate minimal media. Proteins from the membrane preparations of these cells could then be solubilized using detergent and column purified by optimizing the conditions outlined in Jormakka or Bertero et al for the DMSO reductase enzyme. The enzyme could then be concentrated and crystallized for X-ray analysis to solve the three dimensional structure of the enzyme.

References

1. McMaster J, Enemark JH, *The Active Sites of Molybdenum and Tungsten Containing Enzymes*. Current Opinion in Chemical Biology, 1998. Apr;2(2): p201-207.

2. Weiner JH et al., *Purification and Properties of Escherichia coli Dimethyl Sulfoxide Reductase, an Iron-sulfur Molybdoenzyme with Broad Substrate Specificity*. Journal of Bacteriology, 1988 Apr; 170(4): p1505-1510

3. Cammack R, Weiner JH. *Electron Paramagnetic Resonance Spectroscopic Characterization of Dimethyl Sulfoxide Reductase of Escherichia coli.* Biochemistry, 1990. Sept 11;29(36): p. 8410-6

4. Unden G, Bongaerts J, *Alternative Respiratory Pathways of Escherichia coli: Energetics and Transcriptional Regulation in Response to Electron Acceptors*. Biochemica et Biophysica Acta, 1997 Jul 4; 1320(3): p217-234.

5. Raitsimring AM et al, *Pulsed EPR Studies of the Exchangable Proton at the Molybdenum Center of Dimethyl Sulfoxide Reductase*. Journal of Biological Chemistry, 2003. Jan; 8(1-2): p95-104.

6. Rivers SL et al, *Molecular Genetic Analysis of the Moa Operon of Escherichia coli K-12 Required for Molybdenum cofactor Biosynthesis*. Molecular Microbiology, 1993 Jun8(6): p1071-81

7. Kebir MO, Kendall DA, *SecA Specificity for Different Signal Peptides*. Biochemistry, 2002 Apr30;41(17): p5573-80.

8. Johnson KE, Rajagopalan KA, *An Active Site Tyrosine Influences the Ability of the Dimethyl Sulfoxide Reductase Family of Molybdopterin Enzymes to Reduce S-Oxides*. Journal of Biological Chemistry, 2001 276(16) Apr20: p13178-13185.

9. Kail B et al, *Synthesis, Characterization, Elecrochemistry, Electronic Structure, and Isomerization of Mononuclear Oxo-Molybdenum(V) Complexes: The serine Gate Hypothesis in the Function of DMSO Reductases*. Inorganic Chemistry, 2002. Mar11;41(5): p1281-1291.

10. Robinson C, Bolhuis A, *Protein Targeting by the Twin-Arginie Translocation Pathway*. Nature Reviews, Molecular Structural Biology, 2001. May2(5): p350-356

11. Berks BC, Palmer T, *Assembly of Membrane-Bound Repiratory Complexes by the Tat Protein-Transport System*. Archives of Microbiology 2002 Aug; 178(2): p77-84

12. Heffron K et al, *Determination of an Optimal Potential Window for Catalysis by E. coli Dimethyl Sulfoxide Reductase and Hypothesis on the Role of Mo(V) in the Reaction Pathway.* Biochemistry, 2001. 40: p3117-3126.

13. Weiner JH et al, *Molecular Analysis of Dimethylsulfoxide Reductase: a Complex Iron-sulfur Molybdoenzyme of Escherichia coli.* Biochemica et Biophysica Acta, 1992 Aug 28; 1102(1): p1-18.

14. Bilous PT et al, *Purification and Properties of Escherichia coli dimethyl sulfoxide reductase, an Iron-Sulfur Molybdoenzyme with Broad Substrate Specificity* Journal of Bacteriology 1988 Apr; 170(4): p1505-10

15. Schindelin H et al, *Crystal Structure of DMSO Reductase: Redox-linked Changes in Molybdopterin Coordination.* Science, 1996. 272(5268): p1615-1621.

16. Trieber CA et al, *Engineering a Novel Iron-Sulfur Cluster into the Catalytic Subunit of Escherichia coli Dimethyl Sulfoxide Reductase.* Journal of Biological Chemistry, 1996. 271 Mar 1: p4620-4626.

17. Rothery RA et al, *Association of Molybdopterin Guanine Dinucleotide with Escherichia coli Dimethyl Sulfoxide Reductase: Effects of Tungstate and a mob Mutation.* Journal of Bacteriology (Apr 95): p. 2634.

18. Jormakka M et al, *Molecular Basis of Proton Motive Force Generation: Structure of Formate Dehydrogenase-N.* Science, 2002. 295: p1863-1868.

19. Weiner JH et al, *the Topology of the Anchor Subunit of Dimethyl Sulfoxide Reductase of Eschericia coli.* Journal of Biological Chemistry, 1993. 268: p3238-3244.

20. Unden G et al, *Oxygen Related Gene Expression in Facultatively Anaerobic Bacteria.* Antinie Van Leeuwenhoek, 1994. 66(1-3): p. 3-22.

21. McDevitt CA et al, *Molecular Analysis of Dimethyl Sulphide Dehydrogenase from Rhodovulum Sulfidophilum: Its Place in the Dimethyl Sulphoxide Reductase Family of Microbial Molybdopterin-containing Enzymes.* Molecular Microbiology, 2002: p1575-1587.

22. Mitchell P, *A General Theory of Membrane Transport From Studies of Bacteria.* Nature 1957 Jul 20;180(4577): p134-6

23. Neidhardt FC, Curtis R, *Escherichia coli and Salmonella typhimurium.* 1996.

24. Richardson D, Sawers G, *PMF Through the Redox Loop.* Science, 2002. 295: p1842-1843.

25. Jormakka M et al, *Molecular Basis of Proton Motive Force Generation: Structure of Formate Dehydrogenase-N.* Science, 2002. 295: p1863-1868.

26. Bilous PT et al, *Proton Translocation Coupled to Dimethyl Sulfoxide Reduction in Anaerobically Grown Escherichia coli HB101.* Journal of Bacteriology, 1985 (Jul;163(1)): p369-75.

27, Wallace BJ, Young IG, *Aerobic Respiration in Mutants of Escherichia coli Accumulating Quinone Analogues of Ubiquinone.* Biochemica et Biophysica Acta., 1977 (Jul 7: 461(1)): p75-83

28. Wissenbach U et al, *An Escherichia coli Mutant Containing only Dimethylmenaquinone, but no Menaquinone: Effects on Fumarate, Dimethylsulfoxide, Trimethylamine N-oxide and Nitrate Respiration.* Archives of Microbiology, 1990. 158(1): p68-73.

29. Spiro SG, Guest JR. *Adaptive Responses to Oxygen Limitation in Escherichia coli.* Trends in Biochemical Science, 1991 Aug 16(8): p310-4

30. Gunsalus RP. *Control of Electron Flow in Escherichia coli: Coordinated Transcription of Respiratory Pathways.* Journal of Bacteriology, 1992 (Nov;174(22)): p7069-74.

31. Iuchi S et al. *Adaptation of Escherichia coli to Respiratory Conditions: Regulation of Gene Expression.* Cell, 1991(Jul 12;66(1)): p5-7.

32. Uden G et al. *O_2-sensing and O_2-dependent gene Regulation in Facultative Anaerobic Bacteria.* Archives of Microbiology, 1995(Aug 164(2)): p81-90.

33. Calhoun MW et al. *Energetic Efficiency of Escherichia coli: Effects of Mutations in Components of the Aerobic Respiratory Chain.* Journal of Bacteriology, 1993(May;175(10)): p3020-5.

34. Spiro S, Guest JR, *Adaptive Responses to Oxygen Limitation in Escherichia coli,* Trends in Biochemical Science 1993 Aug16(8): p310-4.

35. Stouthamer AH et al. *Daltons Comprehensive Biotechnology.* 1985: p215-238.

36. Barrett EL, Kwan H. *Bacterial Reduction of Trimethylamine Oxide.* Annual Review of Microbiology, 1985. 39: p131-49.

37. Zinder SH, Brock TD, *Dimethyl Sulphoxide Reduction by Micro-organisms.* Journal of Genetic Microbiology, 1978(Apr;105(2)): p335-42.

38. Kiene RP et al, *Biological Removal of Dimethyl Sulphide from Sea Water*, Nature 1990. 345: p702-704.

39. Lovelock JE et al, *Air Pollution and Climate Change*, Nature, 1972. 237: p452-453.

40. Kellogg WW et al, *The Sulfur Cycle*. Science, 1972. Feb 11;175(22): p587-596.

41. Bilous PT et al, *Proton Translocation Coupled to DMSO Sulfoxide Reduction in Anaerobically Grown Escherichia coli HB101*. Journal of Bacteriology, 1985. 163(July): p369-375.

42. Mouncey NJ, Kaplan S, *Cascade Regulation of Dimethyl Sulfoxide Reductase (dor) Gene Expression in the Facultative Phototroph Rhodobacter sphaeroides*, Journal of Bacteriology, 1998: p2924-2930.

43. Iuchi S, Lin EC, *Molybdenum Effector of Fumarate Reductase Repression and Nitrate Reductase Induction in Escherichia Coli*, Journal of Bacteriology, 1987 169: p3720-3725.

44. Pascel M et al, *Regulation of the Nitrate Reductase Operon: Effect of Mutations in chlA, B, D and E Genes*. Molecular Genetic Genomics, 1982. 188: p103-106.

45. McNicholas P et al, *Oxygen Nitrate and Molybdenum Regulation of dmsABC Gene Expression in Escherichia Coli*, Journal of Bacteriology, 1989. 171: p3817-3823.

46. McNicholas P et al, *Anaerobic Regulation of the Escherichia Coli dmsABC Operon Requires the Molybdate-responsive Regulator ModE*. Molecular Microbiology, 1998. 27: p197-208.

47. Turner RJ et al, *Expression and Epitope Tagging of the Membrane Anchor Subunit (DmsC) of Escherichia coli Dimethyl Sulfoxide Reductase*. Protein Engineering, 1997. 10(3): p285-290.

48. Weiner JH et al, *Molecular Analysis of Dimethylsulfoxide Reductase; A Complex Iron-sulfur Molybdoenzyme of E. coli*. Biochem Biophys Acta, 1992. 1102(1): p1-18.

49. Rothery RA et al, *Topological Characterization of Escherichia coli DMSO Reductase by Electron Paramagnetic Resonance Spectroscopy of an Engineered [3Fe-4S] Cluster*. Biochemistry, 1993. 32: p5855-5861.

50. Weiner JH et al, *A Novel and Ubiquitious System for Membrane Targeting and Secretion of Cofactor-Containing Proteins.* Cell, 1998: p93-101

51. Wu LF et al, *Bacterial Twin-arginine Siganl Peptide-dependent Protein Translocation Pathway: Evolution and Mechanism.* Journal of Molecular Microbiology and Biotechnology, 2000. 2(2)(Apr): p179-89.

52. Voordouw G, *A Universal System for the Transport of Redox Proteins: Early Roots and Latest Developments.* Biophysical Chemistry, 2000. 86(2-3)(Aug 30): p131-40.

53. Driessen AJM et al, *The Structural Basis of Protein Targeting and Translocation in Bacteria.* Nature Structural Biology, 2001. 8(6): p492-498.

54. Zhongwei Z et al, *Interaction of 2-n-Heptyl-4-Hydroxyquinoline-N-Oxide with Dimethyl sulfoxide Reductase of Escherichia coli.* Journal of Biological Chemistry, 1998. 273(Aug 14): p20758-20763.

55. Cecchini G et al, *Succinate Dehydrogenase and Fumarate Reductase from Escherichia coli.* Biochem Biophys Acta., 2002. Jan 17: p140-57.

56. Stewart V et al, *Periplasmic Nitrate Reductase (NapABC Enzyme) Supports Anaerobic Respiration by Escherichia coli K-12.* Journal of Bacteriology, 2002. March 2002: p1314-1323.

57. Rothery RA et al, *Hydroxylated Napthoquinones as Substrates for Escherichia coli Anaerobic Reductases.* Biochemical Journal, 1998. 332: p35-41.

58. Rothery RA Weiner JH, *Interaction of an Engineered [3Fe-4S] cluster with a Menaquinol Binding site of Escherichia coli DMSO Reductase.* Biochemistry, 1996. 35: p3247-3257.

59. Trieber CA et al, *Multiple Pathways of Electron Transfer in Dimethyl Sulfoxide Reductase of Escherichia coli.* The Journal of Biological Chemistry, 1994. 269(10): p7103-7109.

60. Stewart LJ et al, *Dimethylsulfoxide Reductase: An enzyme Capable of Catalysis with Either Molybdenum or Tungsten at the Active site.* Journal of Molecular Biology, 2000. 299: p593-600.

61. McAlpine AS et al, *The High Resolution Crystal Structure of DMSO Reductase in Complex with DMSO. Consequences of Removal of a Molybdenum Ligand DmsSer176 of Escherichia coli Dimethylsulfoxide Reductase in Complex with DMSO.* Journal of Molecular Biology, 1998. 275: p 613-623

62. Trieber CA et al, *Consequences of Removal of a Molybdenum Ligand DmsSer176 of Escherichia coli Dimethylsulfoxide Reductase*. Journal of Biological Chemistry, 1996. 271(Nov1): p27339-27345.

63. Simala-Grant JL et al, *Modulation of the Substrate Specificity of Escherichia coli Dimethylsulfoxide Reductase*. European Journal of Biochemistry, 1998(Jan 15(25)): p510-5.

64. Dias JM et al, *Crystal Structure of the First Dissimilatory Nitrate Reductase at 1.9A Solved by MAD Method*. Structure Folding and Design, 1999. 7(1): p65-79.

65. Gladyshev VN et al, *Characterization of Crystalline Formate Dehydrogenase H from Escherichia coli. Stabilization, EPR Spectroscopy, and Preliminary Crystalographic Analysis*. Journal of Biological Chemistry, 1996. 271(14): p8095-8100.

66. Bertero MG et al, *Insights into the Respiratory Electron Transfer Structure of Nitrate Reductase A*. Nature Structure Biology, 2003. 10(9): p681-687.

67. Rothery RA et al, *Interactions Between the Molybdenum Cofactor and Iron Sulfer Clusters of Escherichia coli Dimethylsulfoxide Reductase*. Journal of Biological Chemistry, 1999. 274: p13002-13009.

68. Rajagopalan KV et al, *The Pterin Component of the Molybdenum Cofactor, Structural Characterization of the Two Fluorescent Derivatives*. The Journal of Biological Chemistry, 1984. 259(May 10): p5414-5422

69. Cammack R et al, *Electron Paramagnetic Resonance Spectroscopic Characterization of Dimethyl Sulfoxide Reductase of Escherichia coli*. Biochemistry, 1990. Sept 11;29(36): p8410-6.

70. Cammack R et al, *Evidence that center 2 in Escherichia coli Fumarate Reductase is a [4Fe-4S] Cluster*. Biochimica et Biophysica Acta., 1986. 870: p545-551.

71. Rothery RA et al, *Association of Molybdopterin Guanine Dinucleotide with Escherichia coli Dimethyl Sulfoxide Reductase: Effect of Tungstate and a mob Mutation*. Journal of Bacteriology, 1995. Apr;177(8): p2057-63

72. Boyington JC et al, *Crystal Structure of Formate Dehydrogenase H: Catalysis Involving Mo, Molybdoppterin, Selenocysteine and an Fe4S4 Cluster*. Science, 1997. 275(5304): p1305-8.

73. Jormakka M, et al., *Molecular Basis of Proton Motive Force Generation: Structure of Formate Dehydrogenase-N.* Science, 2002. 295: p1863-1868.

74. Rupp et al, *Electron Spin Relaxation of Iron-Sulphur Proteins Studied by Microwave Power Saturation.* Biochemica et Biophysica Acta. 1978 Dec20;537(2): p225-60

Appendices

A. BV Activity Assay (DMSO/TMAO as Substrate)

The reaction solution was prepared by adding all of the required reagents to a 3ml cuvette and the reaction was initiated by adding the catalyst enzyme DMSO reductase. The reaction solution contained the following;

- 2.5ml 50mM MOPS pH 7.0 (degassed)
- 100 μl BV
- 88 μl NaDTH in MOPS
- 0.2 ml Nafumarate 0.5M pH=7.0
- 100 μl 2M TMAO or DMSO in H_2O

The cuvette was covered over with parafilm and inverted three times to mix the reagents. Diluted enzyme was added using a Hamilton syringe and the cuvette was again covered and inverted three times. The cuvette was then placed in a varion spectrophotometer which measured the change in absorbance which was recorded on paper using a chart recorder. The specrometer was set at; A_{570nm} with the absorbance set to 2.2. The recorder was run at 0.5 mm/sec at 50mV. As the reaction proceeds a slope is recorded onto the chart paper which can be converted into a rate of reaction in mM/sec. The activities from a minimum of three trials were averaged.

B. EPR Analysis of Enriched Membrane Samples

Preparation of EPR samples included poising highly concentrated enriched membrane preparations (30mg/ml) from HB101 cells at a variety of defined redox potentials (as described by Cammack et al, 1990). Samples were placed in an anaerobic chamber under argon, in 0.1 MOPS buffer, pH 7.0. A variety of reducing agents were used in the appropriate regions of potential and the redox potential was measured with a platinum and calomel electrode, at 25 degrees C. The reducing agents used include the following mediators: Quinhydrone, 2,6-dichloroindophenol, 1,2-naphtoquinone, toluylene blue, phenazine methosulfate, thionine, duroquinone, methylene blue and resorufin. The potential was adjusted with small additions of 0.1M dithionite and 0.2M ferrecynanide solutions. After an equilibrium time, at least 2 minutes, samples were transferred with a microlitre syringe through an anaerobic chamber into quartz tubes and frozen in liquid nitrogen. Potentials are recorded relative to the standard hydrogen electrode.

EPR spectra were recorded on a Bruker ESP300 spectrometer equipped with an Oxford Instruments ESR900 helium cryostat. Integrations were performed by double integration with Cu(II)-EDTA as standard. The magnetic field was calibrated relative to diphenylpicrylhydrazyl and manganese in SrO standards. Microwave power saturation data were plotted and fitted to an empirical equation (as described by Rupp et al., 1978).

Spin quantifications were carried out by double integrations of spectra from redox titrations (microwave power, 2 milliwatts; temperature, 12K). The presence of background signals (primarily fumarate reductase) in the membranes was partly compensated for by subtracting the base line intensity (at approximately 0mV) from the fully oxidized and reduced intensities.

C. *Form A Fluorescence Assay*

This assay is based on the work of Rajagopalan et al., 1984. 10mg of membrane protein solution must be pelleted by spining at 95K for 25minutes using a TL100 ultracentrifuge and Ti100.3 rotor. (Add appropriate volume to the tubes, and then make up to about 3ml using buffer to balance them). Drain the pellet and shake to remove excess buffer. Add 300μl of distilled water, resuspend carefully with a teflon homogenizer. Transfer the membranes to 1.5ml Eppendorf tubes. Add 200μl 6N Hcl and vortex. Add 800μl I_2/KI (2%/4% w/v) an vortex. Put a small needle hole in the lid and place in a boiling water bath for 25minutes. Cool the solution on ice for 2 minutes. Centrifuge for 15minutes. Transfer 0.8ml of supernatant into new tube. Use 200μl of supernatant to record fluorescence spectra. Add to 3.5mL 1M ammonium hydroxide in fluorescence cuvette. Record the spectra using the following parameters (initially):

Excitation: 240-420nm (emission at 442nm)
Emmision: 410-520nm (Excitiation at 395nm)

Use initial spectra of positive control to optimize wavelengths and slit widths.

D. *HOQNO Fluorescence Quench Titrations*

HOQNO (2-n-heptyl-4-hydroxyquinoline-N-oxide) was obtained from Sigma. The concentration of HOQNO was determined spectrophotometrically after diluting an ethanolic stock solution in 1mM sodium hydroxide using an extinction coefficient of $9450^{-1}M^{-1}$-1cm at 346nm. Fluorescence measurements were carried out using a Perkin-Elmer LS-50B luminescence spectrometer. The fluorescence emission spectrum of HOQNO in 100mM MOPS and 5mM EDTA (pH 7.0) exhibits a maximum at 479nm with the excitation at 341nm.

In fluorescence titration experiments, aliquots of a 50μM HOQNO stock solution were added to a cuvette containing the protein (1mg/ml) in 100mM MOPS and 5mM EDTA (pH 7.0) buffer solution using a Hamilton syringe (2μl increments). Fluorescence emissions were measured at 479nm (with excitation at 341nm). The background fluorescence of the protein sample in the absence of HOQNO was subtracted from the fluorescence of the sample in the presence of HOQNO. The fluorescence from the cuvette was measured after addition of HOQNO and establishment of a stable equilibrium. Plots of fluorescence versus HOQNO concentration were then created for analysis of the DmsC quinol binding site concentration.

E. Lapachol Activity Assays

Assays were carried out in N_2-saturated 100 mM Mops/KOH/5 mM EDTA, pH 7.0, using 4 ml acryl cuvettes (Sarstedt 67.738) with machined Teflon stoppers constructed in the Faculty of Medicine's Biomedical Workshop (University of Alberta). These had an 11 mm plugs that inserted into the acryl cuvettes, creating an effective seal against oxygen diffusion. Holes suitable for insertion of Hamilton syringe needles were bored through the stoppers. The combination of the acryl cuvettes and the Teflon stoppers maintained stable anaerobic conditions during the kinetics experiments described here. Mixing of the cuvette contents was achieved by inserting a micro stir bar (2 mmÅ~7 mm; Fisher 14511-67) and inversion. Assays were carried out as follows: Reduced quinol was prepared by exposing an acidified (to a final concentration of 0.18 M HCl) 20 mM stock solution in ethanol to metallic zinc powder in a 2 ml glass HPLC vial with a septum and cap. For DmsABC assays, the buffer (100 mM Mops/KOH/5 mM EDTA, pH 7.0) was supplemented 70 mM trimethylamine *N*-oxide (TMAO). After transfer of the N2-saturated buffer to the cuvette (3.31 ml volume), the stopper was inserted, and quinol was added at a range of concentrations up to approx. 0.3 mM. No gas phase was present above the reaction solution in the cuvette. The reaction was initiated by addition of enzyme and followed at 481 nm. These wavelengths allowed the formation of LPC (i.e. the oxidized forms) to be followed.

LPC shows a well-resolved absorbance at 481 nm, and an intense absorbance at 275 nm, which has some overlap with the absorbance of the reduced form. The 275 nm absorbance also potentially overlaps with the absorbance of protein at approximately 280 nm, suggesting that the 481 nm absorbance of LPC is the most suitable for studying the enzymic oxidation of LPCH2. (Rothery RA et al., 1998)

F. *Electrocompetent Cell Preparation and Plasmid Transformation*

Preperation of electrocompetant cells;

Innoculate 5mls SOB without magnesium and grow overnight at 37° C with shaking. In the morning dilute 50μl into 50ml SOB without magnesium and grow at 37° C with shaking to OD_{550} = 0.8 [2-3hrs]. Harvest the cells by spinning @ 5K for 10minutes. Resuspend the cells in 50ml 10% glycerol (ice cold). Spin @ 5K for 15 minutes and drain carefully. Again resuspend in 50ml of 10% glycerol and spin @5K for 15 minutes and then drain. Resuspend the cells in the 10% glycerol left in the centrifuge tube and flash freeze in dry ice and dry ice and stored @ -70° C.

Electroporation

Take 20μl of cells and add 1μl DNA and place inside an electroporation cell. Place the cell in "Single Safe" and "Zap" on the medium setting. Remove the cells and grow in 1ml SOC @ 37° C. Place the cells on an appropriate antibiotic and grow overnight at 37°C on a rich media.

G. *Gel Electrophoresis*

SDS-PAGE Gel (Separate proteins based on size)

Whole Cell Preperation (if applicable)

1. Add 1.5ml of an overnight culture of cells grown on a rich media to an eppendorf tube and spin @ 13K for 5 minutes. Use the entire 10ml overnight culture (approximately 6 tubes/sample).
2. Resuspend the cells from each 1 ml tube in 50mM MOPS and spin @ 13K for 5 minutes.
3. Combine all tubes and resuspend in 600μl 50mM MOPS.
4. For gel loading add equal amounts of LSB (200μl sample + 200μl LSB) and boil for 3-5 minutes with the lid punctured.

Lowery Protein Assay

For whole cell preperations, use 2μl, 5 μl, 10 μl, and 25 μl volumes of each sample.

SDS PAGE Gel

Prepare resolving gel in 50ml sidearm flask with a small stirbar

	10%	
	1X	2X
H_2O	4.02ml	8.04ml
1.5M tris pH 8.8	2.5ml	5ml
10% SDS	0.1ml	0.2ml
30%Acy:0.8%Bis	3.33ml	6.66ml

Degas the solution for @ least 10 minutes. Assemble glass plates separated by two spacers and a card. Put them in front of a holder to line up the plates so there is a slight overhang (screws facing in) and tighten the screws. Snap in place in the holder (screws facing out) and test for leaks with water.

To degassed resolving gel add:

	10%	
	1X	2X
10% NH4/sulfate	4.02ml	8.04ml
TEMED	2.5ml	5ml

Swirl to mix. Using a pasteur pipette, dispense the resolving gel between glass plates (2/3-3/4 full). Leave some gel in the pipette so as to know when gel is hard. Add one squirt of butanol to get rid of the bubbles and to make the gel flat. Leave the gel to harden (20minutes).

Prepare the stacking gel:

H2O	3.05 ml
1.5M tris pH 8.8	1.25ml
10% SDS	50μl
30%Acy:0.8%Bis	0.65 ml

Degass @ least 10 minutes

Once the resolving gel is hard, pour out remaining butanol and rinse with water.

To the degassed stacking gel add:

10% NH4/sulfate	25μl
TEMED	5μl

Swirl to mix. Put long wide combs in place with equal space between the edges of the glass plates. Using a pasteur pipette, dispense the stacking gel slowly to avoid bubbles between wells of combs up to the top of the short plate. Push the combs down to the top of the wells. Once the stacking gel is hard, slowly remove the combs and rinse the wells with water. Put assembled glass plates in the holder used to run the gel in and place into running apparatus containing 800ml of running buffer (10X dilution of Tris-Glycine buffer + 10ml 10% SDS). Load the samples (20-40μg) and 5μl of Low molecular wieght standard.

Run the gel for 45 minutes @ 200V or until the dye front is at the bottom of the glass plates.

Western Blot

Prepare 2l transfer buffer (10X dilution of Tris-glycine buffer + 400ml Methanol). Soak 2 filter pads/gel, 2 pieces of filter paper/gel, and 1 piece of nitrocellulose/gel, cut to the size of a small glass plate. Make sure there is a Bio-Ice cooling unit in the -70° C freezer.

Remove the gel holder from the running apparatus. Unscrew knobs and remove plates from the holder. Use spacers to push gels into the transfer buffer and soak for at least 15 minutes.

1. Assemble the blotting components on blotting apparatus.
1. clear plastic
2. white filter pad
3. filter paper
4. nitrocellulose
5. gel
6. filter paper
7. white filter pad
8. black plastic

Place the blotting apparatus (black plastic facing black side of holder) into the running tank (with the blotting holder in it). Add a small stirbar and a cooling unit. Fill the tank with transfer buffer and run for 1 hour @ 100V, 250mA (run on volts).
Remove the nitrocellulose paper and put it into a tupperware dish. Add a small volume of Ponceau's stain and rock back and forth until red bands appear. Rinse with water until there is no red run off. Incubate the nitrocellulose for 8 hours or overnight in 50ml TBS/azide/10% milk to block the membrane. These solutions contain the following:

10X TBS = 40ml 5M NaCl + 50ml 1M TrisHCL pH 7.5 + 10ml water
TBS/azide = 100μl 20% azide/50ml TBS
TBST = 250μl 10% Tween 20/50ml TBS

Prepare 25ml/membrane of TBST/Azide/1% milk powder with 1° antibody (5μl-lactamase Ab) for 1 hour. Wash the blot 2 times for 5 minutes each with 50ml TBS. Then wash the blot 2 times for 5 minutes each with 50ml TBST. Incubate the blot in 25ml TBST with 2μl secondary antibody, HRP (horse raddish peroxidase) for 1 hour. Wash blot 2 times for 5 minutes each with 50ml TBS then wash the blot 2 times for 5 minutes each with 50ml TBST. Mix a 1:1 ratio (2ml each) of ECL reagents (photographing activating reagents for visualization of the secondary antibody). Disperse this onto the blot for 10-20 seconds. Shake off the paper and place between two slices of saran wrap and use to expose photographic paper in a dark room. Develop the paper to observe the relative amounts of DmsA or B loaded into each lane.

DNA Gel (separate DNA based on size)

TAE or TBE gels

TAE- can use DNA again for cloning
TBE- can run gel faster
-1% Gel for 1000-5000 bps
-1 x TAE in 100ml so 2ml 50x in 98 mL H_2O

Spoon 1g of powdered agarose into a dilution bottle with 100ml of water and microwave until the agarose is dissolved. Pour the gel onto a plate after allowing to cool with a lane comb in place. Allow the gel to harden and remove the lane comb. Place the hardend gel into a running tank containing running buffer (TAE/TBE). In the first lane run 10ul of λ marker. Load the samples in the other lanes. Run the gel at 110V for 40 minutes.

H. *Growth Media*

Preparation and Growth of 19 L Glycerol-fumerate Batch Cultures of Escherichia Coli

Each batch contains the following ingredients added to a 19L carboy before autoclaving:

SALTS	g/19L
KH_2PO_4	103.36
K_2HPO_4	199.31
$(NH_4)SO_4$	38.00
NaOH	71.25
Fumeric Acid	88.16

Add a large stir bar, approximately 10L of distilled water, and tape tin foil over the top. Autoclave the carboy for at least 90 minutes. Autoclave some extra carboys full of only distilled water for 90 minutes and cool to room temperature (enough to top up the media containing carboys). Rubber stoppers for the carboys and funnels for pouring in the extra water wrapped in tin foil should also be sterilized by autoclaving. The following sterile solutions were prepared to make the 19L batch of media.

	ml/19 L
metal mix	19
50% w/v Glycerol	190
20% w/v peptone	95
20mM Ammonium molybdate	1.9
1% w/v vitamin B1	57
1% w/v Pro/Leu (if required)	57

Innoculate 250ml of LB media containing the appropriate antibiotics with 2.5 ml of an overnight culture saturated with the appropriate DMSO cell stock and grow overnight @ 37°C with shaking. The next morning, filter sterilize antibiotic solution(s) for batch culures. To the carboys containing the autoclaved water and salts, add the autoclaved solutions, antibiotics, and 250ml cultures. Fill the carboy with autoclaved water using a sterile funnel. Stopper, and tape down with packing tape. Grow @ 37 ° C on a stir plate with for 24hrs (DSS301) or 48 hrs (HB101).

Terrific Broth

Tryptone	12g
Yeast Extract	24g
Glycerol	4ml
Vitamin B1	0.3g
Distilled water	to 1L

Mix well until all the ingredients are dissolved. Split into 4x250ml batches in 1L baffled flasks. Make up the following phosphate solution in 100ml of distilled water:

KH_2PO_4	2.31g
K_2HPO_4	12.54g

This is 0.17M KH_2PO_4 and 0.72M K_2HPO_4 solution. Autoclave the above: Add 25ml of the phosphate solution to the 250ml baffle flasks before innoculation with a 5ml overnight culture of the required DMSO cell stock and appropriate antibiotics.

S.O.B. Media (w/out Mg)

Bacto-tryptone	20.0g
Bacto-yeast extract	5.0g
NaCl	0.584g

KCl	0.186g
Distilled water	to 1L

Mix components, adjust pH to 7.0 with NaOH using a pH meter, and autoclave.

S.O.C. Media

Mg++ stock

$MgCl_2_6H_2O$	20.33g
$MgSO_4_7H_2O$	24.65g
Distilled water	to 100ml

Autoclave or filter sterilize

2 M Glucose

glucose	36.04g
distilled water	to 100ml

filter-sterilize

add 1 ml of 2M Mg^{++} stock and 1ml of 2M glucose to 98ml of S.O.B. medium

50x TE buffer

Tris base	12.11g
Na_2EDTA	3.72g

Dissolve tris and EDTA in 100ml of water. Titrate with HCl to pH 7.4. Bring the volume to 200ml with distilled water. Filter sterilize or autoclave. For 0.5x TE buffer, add 1ml of 50x TE to 99ml of distilled water, and filter-sterilize.

I. *Lyse and Separate Cells into Soluble, Crude and Enriched Innermembrane Fractions*

To a 250mL tube of thawed cells add 50mL of 100mM MOPS/5mM EDTA and approximately 0.2mM PMSF (protease inhibitor) and resuspend. Use the French Pressure method to lyse the cells. For this large volume of cells the large pressure cell is appropriate. Place the cooled cell on the stand with the piston inserted and attach tubing to both the intake and outputs. Place the input tube in the cell solution and the output tube into an empty 250ml centrifuge tube. Open the intake valve and keep the output valve containing a nylon ball closed. Fix the top of the piston to the motorized arm using a metal brace by means of a rubber mallet. Turn the pump on allowing the piston to be drawn up allowing the cell solution to be drawn through the input tubing into the pressure cell. When the piston can be no longer pulled out of the cell. Turn off the motor and switch the setting on the machine to high (only for the large cell). Close the intake valve and leave the output valve shut. Turn the pump back on but now the piston will be inserted into the pressure cell. Allow the pressure in the cell to build up to 1000psi, then slowly begin opening the output valve being careful not to let the pressure fall below 500psi. The cell solution will be passed over the nylon ball ripping the cells open and pass through the tubing into the empty centrifuge bottle. Keep the solution cold by keeping the centrifuge bottles on ice. Repeat this procedure until the entire solution has been run through the cell at least twice. Dilute the sample with MOPS/EDTA buffer and do a low speed spin at 8000 RPM for 15 minutes. Recover the supernatant and transfer to 25ml ultracentrifuge tubes. Spin at 40K for 1.5 hours. The supernatant is the soluble fraction. Resuspend the membrane pellet in MOPS/EDTA buffer with a teflon homogenizer. Add 5 mls to a 20ml 55% sucrose solution w/v (weight/volume) in MOPS/EDTA in a 25ml ultracentrifuge tube. Spin at 40K for 1.5 hours. The suspended band is enriched in inner membrane and the pellet is other cell membrane. Remove the bands, consolidate and dilute them in MOPS/EDTA buffer. Then transfer to ultracentrifuge tubes and spin at 40K for 1.5 hours. The pellet is enriched membrane. Resuspend and freeze in liquid nitrogen.

J. *Lowery Protein Assay*

The assay requires the following reagents which can be made up in bulk beforehand and stored at room temperature.

Solution A

20g sodium carbonate

0.5g sodium potassium tartrate

4g sodium hydroxide

10g SDS

Made up to 1L

Solution B

0.1g copper sulphate

Made up to 100ml

Protein Standard

Use the protein standard purchased from Biorad

Protocol

For typical membrane preparations and soluble protein samples, dilute protein to be assayed 1:10 with distilled water. Set up disposable glass test tubes for assay, at least 6 are needed for the standard curve and at least two are required for each protein concentration to be determined. Mix 9 parts of Solution A with 1 part of Solution B. Note: Each assay incubation requires a total of 3ml of the A/B mixture. Next add 3ml of the A/B mixture to each assay tube. Add a protein standard to 5 standard tubes (typically 0,10,20,30,40, and 50ul of the standard protein solution) To the assay tubes add the protein solution being determined (typically 10 and 20μl of a 1:10 dilution of the protein solution) and vortex. Add 0.3ml of a 1:1 dilution in water of Folin and Ciocalteus's Phenol reagent, vortex, and incubate for 35 minutes to allow colour development. Read the absorbance of each tube at 750nm. Plot out a calibration graph and interpolate using the sample OD_{750}'s.